

The postcranial skeleton of *Cerrejonisuchus improcerus* (Crocodyliformes: Dyrosauridae) and the unusual anatomy of dyrosaurids (#50652)

1

First submission

Guidance from your Editor

Please submit by **30 Nov 2020** for the benefit of the authors (and your \$200 publishing discount) .



Structure and Criteria

Please read the 'Structure and Criteria' page for general guidance.



Raw data check

Review the raw data.



Image check

Check that figures and images have not been inappropriately manipulated.

Privacy reminder: If uploading an annotated PDF, remove identifiable information to remain anonymous.

Files

Download and review all files from the [materials page](#).

10 Figure file(s)
22 Latex file(s)
1 Table file(s)
2 Raw data file(s)
1 Other file(s)



Structure and Criteria

Structure your review

The review form is divided into 5 sections. Please consider these when composing your review:

1. BASIC REPORTING
2. EXPERIMENTAL DESIGN
3. VALIDITY OF THE FINDINGS
4. General comments
5. Confidential notes to the editor

You can also annotate this PDF and upload it as part of your review

When ready [submit online](#).

Editorial Criteria

Use these criteria points to structure your review. The full detailed editorial criteria is on your [guidance page](#).

BASIC REPORTING

- Clear, unambiguous, professional English language used throughout.
- Intro & background to show context. Literature well referenced & relevant.
- Structure conforms to [Peerj standards](#), discipline norm, or improved for clarity.
- Figures are relevant, high quality, well labelled & described.
- Raw data supplied (see [Peerj policy](#)).

EXPERIMENTAL DESIGN

- Original primary research within [Scope of the journal](#).
- Research question well defined, relevant & meaningful. It is stated how the research fills an identified knowledge gap.
- Rigorous investigation performed to a high technical & ethical standard.
- Methods described with sufficient detail & information to replicate.

VALIDITY OF THE FINDINGS

- Impact and novelty not assessed. Negative/inconclusive results accepted. *Meaningful* replication encouraged where rationale & benefit to literature is clearly stated.
- All underlying data have been provided; they are robust, statistically sound, & controlled.
- Speculation is welcome, but should be identified as such.
- Conclusions are well stated, linked to original research question & limited to supporting results.



The best reviewers use these techniques

Tip

Example

Support criticisms with evidence from the text or from other sources

Smith et al (J of Methodology, 2005, V3, pp 123) have shown that the analysis you use in Lines 241-250 is not the most appropriate for this situation. Please explain why you used this method.

Give specific suggestions on how to improve the manuscript

Your introduction needs more detail. I suggest that you improve the description at lines 57- 86 to provide more justification for your study (specifically, you should expand upon the knowledge gap being filled).

Comment on language and grammar issues

The English language should be improved to ensure that an international audience can clearly understand your text. Some examples where the language could be improved include lines 23, 77, 121, 128 - the current phrasing makes comprehension difficult.

Organize by importance of the issues, and number your points

1. Your most important issue
2. The next most important item
3. ...
4. The least important points

Please provide constructive criticism, and avoid personal opinions

I thank you for providing the raw data, however your supplemental files need more descriptive metadata identifiers to be useful to future readers. Although your results are compelling, the data analysis should be improved in the following ways: AA, BB, CC

Comment on strengths (as well as weaknesses) of the manuscript

I commend the authors for their extensive data set, compiled over many years of detailed fieldwork. In addition, the manuscript is clearly written in professional, unambiguous language. If there is a weakness, it is in the statistical analysis (as I have noted above) which should be improved upon before Acceptance.

The postcranial skeleton of *Cerrejonisuchus improcerus* (Crocodyliformes: Dyrosauridae) and the unusual anatomy of dyrosaurids

Isaure Scavezzoni^{Corresp., 1}, Valentin Fischer¹

¹ Evolution and Diversity Dynamics Lab, University of Liège, Liège, Belgium

Corresponding Author: Isaure Scavezzoni
Email address: isaure.scavezzoni@doct.uliege.be

Dyrosauridae is a clade of neosuchian crocodyliforms that diversified in terrestrial and aquatic environments across the Cretaceous–Paleogene transition. The postcranial anatomy of dyrosaurids has long been overlooked, obscuring both their disparity and their locomotive adaptations. Here we thoroughly describe of the postcranial remains of an unusually small dyrosaurid, *Cerrejonisuchus improcerus*, from the middle-late Paleocene Cerrejón Formation of Colombia, and we provide a wealth of new data concerning the postcranial anatomy of the key dyrosaurids: *Congosaurus bequaerti* and *Hyposaurus rogersii*. We identify a series of postcranial autapomorphies in *Cerrejonisuchus improcerus* (an elliptic-shaped odontoid laterally wide, a ulna possessing a double concavity, a fibula bearing a widely flattened proximal end, a pubis showing a large non-triangular distal surface) as well as functionally-important traits such as a relatively long ulna (85% of the humerus' length), short forelimb (83% of hindlimb's length), or thoracic vertebra bearing comparatively large lateral process (with widened parapophysis and diapophysis) along with strongly arched thoracic ribs allowing a more sturdy and cylindrical rib cage. These indicate a more terrestrial lifestyle for *Cerrejonisuchus* compared to the derived members of the clade. We also built a dataset of 187 traits on 27 taxa, that extensively samples the cranial and postcranial architectures of exemplar crocodyliforms. We analyze these data via Principal Coordinate Analysis (PCoA) to visualize the postcranial morphospace occupation of Dyrosauridae, Thalattosuchia, and Crocodylia. Our data reveal the existence of a distinctive postcranial anatomy for Dyrosauridae that is markedly distinct from that of crocodylians. As a result, modern crocodylians do not prove to be a good analogy for extinct groups, and it also appears necessary to include more and more postcranial data in future Crocodyliformes analyses.

The postcranial skeleton of *Cerrejonisuchus improcerus* (Crocodyliformes: Dyrosauridae) and the unusual anatomy of dyrosaurids

Isaure Scavezzoni¹ and Valentin Fischer²

¹ULiège

Corresponding author:

Isaure Scavezzoni¹

Email address: isaure.scavezzoni@uliege.be

ABSTRACT

Dyrosauridae is a clade of neosuchian crocodyliforms that diversified in terrestrial and aquatic environments across the Cretaceous-Paleogene transition. The postcranial anatomy of dyrosaurids has long been overlooked, obscuring both their disparity and their locomotive adaptations. Here we thoroughly describe of the postcranial remains of an unusually small dyrosaurid, *Cerrejonisuchus improcerus*, from the middle-late Paleocene Cerrejón Formation of Colombia, and we provide a wealth of new data concerning the postcranial anatomy of the key dyrosaurids: *Congosaurus bequaerti* and *Hyposaurus rogersii*. We identify a series of postcranial autapomorphies in *Cerrejonisuchus improcerus* (an elliptic-shaped odontoid laterally wide, a ulna possessing a double concavity, a fibula bearing a widely flattened proximal end, a pubis showing a large non-triangular distal surface) as well as functionally-important traits such as a relatively long ulna (85% of the humerus' length), short forelimb (83% of hindlimb's length), or thoracic vertebra bearing comparatively large lateral process (with widened parapophysis and diapophysis) along with strongly arched thoracic ribs allowing a more sturdy and cylindrical rib cage. These indicate a more terrestrial lifestyle for *Cerrejonisuchus* compared to the derived members of the clade.

We also built a dataset of 187 traits on 27 taxa, that extensively samples the cranial and postcranial architectures of exemplar crocodyliforms. We analyze these data in via Principal Coordinate Analysis (PCoA) to visualize the postcranial morphospace occupation of Dyrosauridae, Thalattosuchia, and Crocodylia. Our data reveal the existence of a distinctive postcranial anatomy for Dyrosauridae that is markedly distinct from that of crocodylians. As a result, modern crocodylians do not prove to be a good analogy for extinct groups, and it also appears necessary to include more and more postcranial data in future Crocodyliformes analyses.

1 INTRODUCTION

Dyrosauridae is an extinct family of marine and fresh-water neosuchian crocodyliforms that is first recorded in the Campanian-Maastrichtian Shendi Formation of Sudan [Salih et al., 2015]. Dyrosaurids survived the Cretaceous-Paleogene mass extinction [Bronzati et al., 2012, 2015, Hastings et al., 2014, Wilberg et al., 2019, Jouve and Jalil, 2020], and disappeared during the Eocene (presumably at the Ypresian-Lutecian boundary) [Buffetaut, 1978c, Jouve et al., 2006, Jouve, 2007, Martin et al., 2019]. Dyrosaurids have a long history of detailed craniodental studies [Denton et al., 1997, Jouve, 2007, Barbosa et al., 2008, Hastings et al., 2010, Martin et al., 2019]. ~~On the contrary,~~ their postcrania was believed to be undiagnostic [Buffetaut, 1976, 1978b, Parris, 1986, Storrs, 1986, Norell and Storrs, 1989, Denton et al., 1997], and thus often overlooked in anatomical descriptions and diagnoses [Langston, 1995, Godoy et al., 2016, de Souza et al., 2019]. This, in turn, hampers a thorough assessment of the ecological diversity of the group as a whole, which likely colonized several niches ~~colonized~~ (*i.e.* marine, freshwater, terrestrial) [Hastings et al., 2014, Wilberg et al., 2019].

46
47 More recently, postcranial remains have started to show their importance [Langston, 1995, Jouve
48 and Schwarz, 2004, Schwarz et al., 2006, 2009, Martin et al., 2019, de Souza et al., 2019]. Here,
49 we thoroughly describe the postcranial anatomy of the early dyrosaurid *Cerrejonisuchus improcerus*
50 [Hastings et al., 2010] the middle-late Paleocene of Colombia and provide a series of novel anatomical
51 observations on *Congosaurus bequaerti* and *Hyposaurus rogersii*. We also build a morphological dataset
52 containing 187 traits that describe the cranial and postcranial anatomy of 27 selected taxa in Dyrosauridae,
53 Thalattosuchia, and Crocodylia. Our multivariate analyses of this dataset reveal that dyrosaurids have a
54 distinctive postcranial anatomy and that the morphological signal in craniodental and postcranial regions
55 are concordant, urging that postcranial characters should make their way in phylogenetical analyses.

56 2 ABBREVIATIONS

57 **AMNH** New York: American Museum of Natural History, USA;
58 **ANSP** Philadelphia: Academy of Natural Sciences Drexel University, USA;
59 **DGM** Brazil: Divisão de Geologia e Mineralogia, Departamento Nacional da Produção Mineral, Brazil;
60 **MRAC** Tervuren: Musée Royal de l'Afrique Centrale, Belgium;
61 **NHM** London: Natural History Museum, England;
62 **NJSM** Trenton: New Jersey State Museum, USA;
63 **NMI** Dublin: Natural History Museum of Ireland, Republic of Ireland;
64 **RBINS** Brussels: Royal Belgian Institute of Natural Sciences, Belgium;
65 **SMNS** Stuttgart: Staatliches Museum für Naturkunde, Germany;
66 **UF/IGM** Gainesville: **UF**, Florida Museum of Natural History, University of Florida, USA / **IGM**, Museo
67 Geológico, at the Instituto Nacional de Investigaciones en Geociencias, Minería y Química, Bogotá,
68 Colombia;
69 **YPM** New Haven: Yale Peabody Museum, USA.

70 3 MATERIALS AND METHODS

71 *Cerrejonisuchus improcerus* Hastings et al. [2010] is a dyrosaurid crocodyliform, ranging from the
72 middle-late Paleocene of Colombia. Phylogenetic analyses placed *Cerrejonisuchus improcerus* as a rather
73 primitive dyrosaurid along with *Anthracosuchus balrogus*, where both are intermediate taxa between
74 the more basal *Phosphatosaurus-Sokotosuchus* clade and [Young et al., 2016, Wilberg et al., 2019],
75 *Arambourgisuchus* [Young et al., 2016].

76
77 *Cerrejonisuchus improcerus* was recovered from the Cerrejón Formation, Colombia, at the La Puente
78 Pit within the Cerrejón Coal Mine (underclay of Coal Seam 90, see Hastings et al. [2010]). The en-
79 vironment within which the Cerrejón Formation deposited corresponds to a tropical rainforest of the
80 middle-late Paleocene [Wing et al., 2009].

81
82 *Cerrejonisuchus improcerus* comprises of four different individuals bearing distinct inventory numbers,
83 which are stored at the Florida Museum of Natural History, University of Florida (**UF**) [Hastings et al.,
84 2010]:


- 85 • **UF/IGM 29**, the *holotype*, it is a nearly complete skull;
- 86 • **UF/IGM 30**, a *referred specimen*, it is a lower jaw (dentaries, splenials and 11 teeth);
- 87 • **UF/IGM 31**, a *referred specimen*, it comprises a nearly complete skull and several postcranial
88 elements (**humerus, ulna, left femur, fibula, tibia, left and right pubi, 17 vertebrae, 1 rib,**
89 **8 osteoderms**);
- 90 • **UF/IGM 32**, a *referred specimen*, it is a partial skull (complete snout up to **beginning** of orbital
91 region).

92 The specimen **UF/IGM 31** is the most interesting one as it is the only one possessing postcranial
93 material. The skull of this specimen will not be redescribed here has the skull of the holotype (UF/IGM

94 29) has already been given an extensive description in Hastings et al. [2010].

95
96 Dyrosaurid phylogeny overrelies on cranial and mandibular characters [Langston, 1995, Jouve, 2007,
97 Bronzati et al., 2012, Hastings et al., 2014, Wilberg et al., 2019, de Souza et al., 2019]: the dyrosaurid
98 matrices used in the past 15 years have a proportion of 98.78% (81/82 in Hastings et al. [2010, 2011,
99 2014] to 100% (30/30 in Jouve et al. [2005]) of cranial characters compared to 82% in Wilberg et al.
100 [2019] for Crocodylomorpha, 73.26%-72.112% in Johnson et al. [2019, 2020] for Crocodylomorpha,
101 47-62% for neoiichthyosaurs (42/88 – 84/134) [Fischer et al., 2016, Zverkov and Jacobs, 2020], 52% in
102 plesiosaurians (140/270) [Benson and Druckenmiller, 2014], 53% in turtles (187/355) [Evers et al., 2019],
103 26% (125/477) for sauropod dinosaurs [Tschoop et al., 2015], and 9.6% (20/208) for hesperornithiform
104 birds [Bell and Chiappe, 2015]. In our analyses, we used a dataset employing 15% of cranial characters
105 (10/65); postcranial data should be used alongside cranial data in phylogenetic analyses in order to help
106 resolving relationships.

107
108 We used a digital caliper to record most of the measurements (approximate error of 0.1mm) on several
109 relatively complete crocodyliforms (see Supplementary Information for the lists of individuals). We also
110 used laser (Creaform Handyscan 300) and white light (Artec Eva) surface scanners to acquire additional
111 measurements on 3D models, using the software GOM Inspect 2019. We laser scanned all the elements of
112 the holotype of *Congosaurus bequaerti* (MRAC 1741-1743, 1745, 1796, 1797, 1799, 1802, 1803, 1806,
113 1809-11, 1813-1819, 1822-1832 (A, B & C), 1835 (A, B & C)-1841, 1844-1846, 1848-1858, 1860-1874,
114 1876, 1877, 1879, 1882-1884, 1887-1896), at resolution ranging from 0.3 to 0.5 mm, depending on the
115 size of the element. We surface scanned *Hyposaurus rogersii* (NJSM 23368) using structured white
116 light with error down to 0.5 mm and this scan was complemented by digital caliper measurements of
117 the cast replica of both femora and humeri (thanks to Rodrigo Pellegrini for the realization) and from
118 measurements gathered prior the mounting of the specimen (W. Callahan pers. comm. 14 August 2019).

119
120 We build an SQLite database to manage measurement data. We used our measurements to create
121 a morphological dataset containing 187 features as dimensionless ratios (113 length ratios and 74 area
122 ratios), scored for 27 taxa (see supplementary information). All analyses were then conducted in the
123 R statistical environment (v 3.5.1) using the following packages: APE [Paradis et al., 2004], VEGAN
124 [Oksanen et al., 2019], PSYCH [Revelle, 2019], DENDEXTEND [Galili, 2015], GGDENDRO [de Vries,
125 2016], PVCLUST [Suzuki and Shimodaira, 2006], DBI [Wickham and Müller, 2019] (with RSQLite),
126 and GGLOT2 [Wickham et al., 2020]. The morphological dataset of 187 characters (ratios, of which
127 9.83% are skull ratios) and 27 specimens (taxa) initially contained 70.17% missing data. This value is
128 reduced to 33.44 % after the application of a completeness threshold of 40% for specimens and 30% for
129 morphological features. These thresholds ensure the establishment of a complete distance matrix and
130 hence prevents non-comparability issues and morphospace distortion by highly incomplete specimens. At
131 this stage, the proportion of skull ratios reaches 15.15% of the whole dataset (10 out of 65 characters in
132 total). We then scaled the data so that each morphological feature has a variance of 1 and a mean of 0
133 (z-transform). This scaled dataset was then used to compute distance matrix using Euclidean distances.
134 The codes are available in the Supplementary Information .

135
136 We subjected this distance matrix to two ordination methods: cluster dendrograms and a principal
137 coordinate analyses (PCoA) (see fig. 15 in section 8). For the cluster dendrograms, we employed the
138 pvclust function from the PVCLUST package from Suzuki and Shimodaira [2006], which is hierarchical
139 agglomerative approach of the cluster analysis. For the clustering criterion located within the hclust
140 function, we chose the argument 'ward.D'. The pvclust function uses columns from the dataset (here our
141 distance matrix) to form a hierarchical cluster, and provides p-values to show the degree of support from
142 the data each cluster possesses (so high p-values indicate highly supported branches). This hierarchical
143 clustering works with multiscale bootstrap resampling, here we chose to keep the default value of 1000 for
144 the replication number (within nboot) of bootstraps per subset. Indeed, this clustering approach constitutes
145 several subsets differing in size from the original dataset; we chose the interval 0.5 until 10 times the size
146 of our original dataset with the incremental value of 0.5.


147
148 We assessed the morphological differences between dyrosaurids, crocodylians and thalattosuchians



149 using PERMANOVA (Permutational multivariate analysis of variance, non-parametric) [Anderson, 2001].
 150 The distance matrix was set as the dependent variable, and taxonomy served as the independent variable.
 151 We also assessed the existence of significant differences between the different ecomorphological groups.
 152 For this, the distance matrix was again set as the dependent variable, while the three main morphological
 153 clusters served as the independent variable. In each case, we set the number of permutations to 1000. The
 154 p-value we obtained for both results was significant ($p < 0.01$). The distance matrix was then subjected to
 155 a PCoA (APE package) to analyze patterns of morphospace occupation. We used the 'cailliez' correction
 156 for negative eigenvalues; this correction method simply adds a constant to each value of the distance
 157 matrix (except the diagonal ones).


158
 159 We also visualized the strength of the ties between cranial and postcranial characters using the
 160 tanglegram function from the DENDXEXTEND R package. The tanglegram was drawn over the clusters
 161 obtained from cranial and postcranial limited matrices (respectively possessing 25 and 170 columns of
 162 characters initially). The datasets were both subjected to a slightly less stringent completeness threshold
 163 of 20% for their characters and 30% for their specimens, thus reducing the amount of missing data to 28%
 164 for the skull dataset and 43% for the postcranial dataset.





165 4 AXIAL SKELETON ANATOMY

166 4.1 General information

167 The referred specimen of *Cerrejonisuchus improcerus* (UF/IGM 31) s  a total of 18 vertebra plus an
 168 odontoid: 1 odontoid; 4 cervicals; 10 thoracics (one is actually flattened on the ventral side of the skull); 2
 169 lumbar; 2 sacrals; and 1 caudal.

170
 171 All of the vertebrae are weathered  We have labeled the cervical vertebra *C*, the thoracics *Th*, the
 172 lumbar *L*, the sacrals *S*, and the caudal  We have also numbered each vertebrae, but it does not reflect
 173 their relative nor absolute position in the vertebral column. All vertebral stiffness inferences are based on
 174 the works of Molnar et al. [2014, 2015], and also Schwarz et al. [2009].

175 The centrum width has been chosen as the reference measurement for the centrum. The length
 176 (anteroposteriorly) of the centrum is subject to change too significantly  along the axial region (as for other
 177 crocodyliforms such as *Dakosaurus maximus*, *Cricosaurus suevicus* [Fraas, 1902], *Steneosaurus leedsi*
 178 [Andrews, 1913], or any modern crocodylian [Grigg and Kirshner, 2015]). The height of the centrum is
 179 also varying a lot for this specimen, whereas the width remains more constant.

180
 181 Hyposaurine dyrosaurids possess at least 22 pre-sacral vertebra [Langston, 1995, Schwarz et al.,
 182 2009], but there are evidence from *Rhabdognothrus* [Storrs, 1986, Langston, 1995] and *Dyrosaurus*
 183 *maghribensis* [Jouve et al., 2006] that s  dyrosaurids had at least 25 pre-sacrals. Modern crocodylians
 184 possess 8 to 9 cervicals and 15 to 16 d  s [Mook, 1921, Grigg and Kirshner, 2015, de Souza, 2018],
 185 while crocodylomorphs are considered to possess 9 cervical vertebra [Steel, 1973]. Jouve et al. [2006]
 186 interpreted that *Dyrosaurus maghribensis* possess 9 cervicals  (including the atlas-axis complex as two
 187 separate vertebra). By observing several partial and less  al dyrosaurid skeletons (*e.g.* *Dyrosaurus*
 188 *maghribensis* NHM VP R36759, *Hyposaurus rogersii* NJSM 23368, *Congosaurus bequaerti* MRAC
 189 1839, 1870, 1840, 1868, 1850, 1871, 1869, 1872, 1873, 1849), we confirm that dyrosaurid possessed 7 post
 190 atlas-axis cervicals like in the hyposaurine skeletal reconstruction of Schwarz et al. [2006]. Indeed,
 191 some anterior thoracic vertebra are sometimes mistaken for cervicals due to the shifting position of
 192 the parapophysis in this area (*e.g.* as in Jouve and Schwarz [2004], Callahan et al. [2015]). A great
 193 particularity of dyrosaurids is the presence of large hypapophyses among the anterior thoracic vertebra
 194 [Owen, 1849, Langston, 1995], just like *Hyposaurus rogersii* [Owen, 1849].

195
 196 • **The cervical region** is composed of 5 vertebra: there are 4 cervicals and an odontoid preserved.
 197 *Hyposaurus rogersii* (NJSM 23368) possessed 7 cervicals (comprising the atlas and axis-odontoid as CI
 198 and CII respectively) while modern crocodylians reach 8 or 9 cervicals [Mook, 1921, Grigg and Kirshner,
 199 2015, de Souza, 2018]. The odontoid bears a shape that is similar to other crocodyliform groups like
 200 *Thalattosuchia* and *Crocodylia*, but is significantly wider laterally. The other cervicals were identified
 201 following the presence of a parapophysis and a diapophysis on the lateral sides of the centrum, or the
 202 presence of a cervical rib as it is the case for modern crocodylians [Grenard, 1999, Grigg and Kirshner,

203 2015, de Souza, 2018].

204

205 • **The dorsal region** is composed of 12 vertebra: 10 thoracics and 2 lumbar are preserved.

206

207 These vertebra were identified as such using the shape and position of the lateral process: it is
 208 generally single (*i.e.* single base) and borne on the neural arch, just like crocodylians where it is often
 209 called 'the transverse process' [Romer, 1956, Grenard, 1999, Grigg and Kirshner, 2015, de Souza, 2018].
 210 Among thoracics, the lateral process splits into two processes distally which resemble two rami of a single
 211 structure: the parapophyseal process (anterior), and the diapophyseal process (posterior). Each process
 212 bears a distinct end, the parapophysis and diapophysis, corresponding to two different attachment sites on
 213 the thoracic rib just like modern crocodylians [Mook, 1921, Grigg and Kirshner, 2015, de Souza, 2018].
 214 We chose to follow the terminologies from de Souza [2018] because we found the definition transverse
 215 process of dorsals too ambiguous for this work on a more basal dyrosaurid; also we decided to use the
 216 general term of 'lateral process' for all bony structure of the vertebrae laterally emerging (either from the
 217 centrum or neural arch) instead of sporadically using 'transverse process' which has a restricted meaning
 218 among Crocodylia (and it is not always possible to meet with the necessary requirements with fossils to
 use this definition) [de Souza, 2018].

219

220 For each one of the thoracic of *Cerrejonisuchus* the lateral process is attached to the centrum, this
 221 indicating the relative maturity of the specimen [Hastings et al., 2010], even if dyrosaurids are known to
 222 possess weak neurocentral sutures [Buffetaut, 1978a]. The anterior portion of the lateral process, called
 223 the parapophyseal process, is always shorter than the posterior one, the diapophyseal process. Both
 224 processes are also distinguishable in parasagittal section (*i. e.* if the process is broken) as the diapophyseal
 225 process is dorsoventrally thicker than the parapophyseal process, with a constriction separating both. For
 226 these reasons, the two distinct portions of the lateral process will be called 'anterior' and 'posterior ramus'
 in the description of the material to remove any ambiguities.

227

228 Nevertheless, it is important to note the crushed state of all vertebra, which has influenced their
 229 thickness. Since dyrosaurid vertebra are amphicoelous [di Stefano, 1903, Buffetaut, 1976], both the lateral
 processes and the zygapophyses play a key role in orienting the vertebra anteroposteriorly.

230

231 One main difference we could observe is that dyrosaurids (*e.g.* *Congosaurus bequaerti* MRAC 1866
 232 or *Hyposaurus rogersii* NJSM 23368) do not tend to form a synapophysis (which is the fusion of both
 233 articular facets of the lateral process, or transverse process, into a single distal facet) on their last thoracics
 like crocodylians (*e.g.* *Mecistops cataphractus* RBINS 18374 or see de Souza [2018]).

234

235 The lumbar vertebrae also possesses two distal facets on its lateral process, but the parapophysis is less
 236 developed than the diapophysis. This is most probably because no actual ribs were born by the lumbar,
 237 which is part of the essence of being a lumbar vertebrae like in crocodylians [Grigg and Kirshner, 2015,
 de Souza, 2018].

238

239 Among the thoracic vertebra, five (UF/IGM 31 Th0, Th1, Th2, Th3, Th4 and Th5) belong to a more
 240 anterior portion of the thoracic region, two others (UF/IGM 31 Th6 and Th7) are certainly middle thoracic
 241 vertebra, and the two remaining ones (UF/IGM 31 Th8 and Th9) are more posterior ~~when compared~~
 242 ~~to the middle ones and are thus considered this way.~~ The actual number of vertebrae is unknown for
 243 *Cerrejonisuchus*, so we decided to order the thoracics relatively to one another. This classification is
 244 based on the evolution of several key features throughout the axial skeleton, which are: the parapophyseal
 245 and diapophyseal processes, the neural spine and the hypapophysis. The absolute length of the neural
 246 spine has been the most decisive character, and its importance is also apparent in its proportional length
 247 to the centrum. The next important traits are the dimensions of both rami (length, distal facet and
 248 base width), and mostly their proportions with regards to the centrum. Indeed, it is well known that
 249 the distal extremities (parapophysis and diapophysis) of thoracic lateral process encounter that of their
 250 corresponding thoracic rib, and also that a larger distal surface means a larger rib. Moreover, these larger
 251 ribs are ~~neither~~ anteriorly nor posteriorly found; they represent the stoutest part of the bracing system
 252 of the trunk, which gradually arise from cervical ribs and also gradually fades away, but more rapidly,
 253 towards the lumbar region [Schwarz et al., 2009]. Therefore, the evolution of the size of the parapophysis
 254 and diapophysis is an sorting feature vertebra.

255

256 We quantify the evolution of these traits in *C. improcerus* following different ratios, such as total
 257 length over centrum's width or total length over distal thickness, all of which are detailed underneath.
 The centrum width has been taken as the reference because it is more often preserved than the height of

258 the centrum. The absolute dimensions of the centrum and the different processes are considered. The
 259 tables below contain all of the measurements (see table 4, table 9), table 6 and ratios (see table 7) used for
 260 classifying and describing the thoracic vertebra.

261 The investigation of the skeletons of the hyposaurines *Congosaurus bequaerti* (holotype from MRAC
 262 Tervuren) and *Hyposaurus rogersii* (NJSM 23368; AMNH FARB 1416, 1421, 1432, 2389, 2390; YPM
 263 VP.000380, VP.000753, VP.000764, VP.000985; ANSP 8629-8669, 9631-9693, 13656), and the crocodyli-
 264 ans *Crocodylus porosus* (Aquarium-Museum Liège R.G.294), and *Mecistops cataphractus* (RBINS
 265 18374) helped elaborate the identification strategies for ordering the vertebra of *Cerrejonisuchus im-*
 266 *procerus*. The thorough investigation of the holotype of *Congosaurus bequaerti* (MRAC) and the
 267 reconstruction of the hyposaurine skeleton in Schwarz et al. [2009] revealed that the height of the neural
 268 spine was a good ordering trait for hyposaurine dyrosaurids. We then applied the same trend to *Cer-*
 269 *rejonisuchus* as we inferred it would be similar among early and late dyrosaurids. The neural spine of
 270 thalattosuchians and crocodylians does not vary much posteriorly, for this reason the extensive variation of
 271 the neural spine has been considered (yet hypothetically) a general dyrosaurid feature.

272
 273 • **The pelvic and caudal region** how many vertebra in total: 2 sacrals and 1 caudal. The
 274 sacrals of *Cerrejonisuchus* are fused together, and their lateral process facing each other make it
 275 easy to identify them. In Crocodylia, the existence of a single distal extremity on sacrals is due to
 276 the fusion of the diapophysis and parapophysis into the synapophysis [de Souza, 2018]. The single
 277 caudal of *Cerrejonisuchus* also bears distinctive features such as a long and narrow neural spine, small
 278 zygapophyses and the presence of prominent chevron facets. In Crocodylia, the lateral process of both
 279 sacral and caudal vertebra is to be called 'costal process' or 'rib' because its origin differs from that of
 280 the dorsals (thoracics and lumbar alike) according to de Souza [2018]. Here we decided to keep using
 281 'lateral process' because its broader and more basic meaning serve better the goals of this paper.

282 4.2 The cervical region

283 The odontoid (see fig. 1) presents the typical stretched-hexagonal shape as found in other crocodyliforms,
 284 notably among thalattosuchians (e.g. *Metriorhynchus moreli* SMNS 10116; pers. obs.), dyrosaurids
 285 (e.g. *Congosaurus bequaerti* holotype at MRAC ; *Hyposaurus rogersii* NJSM 23368 or AMNH FARB
 286 2390; pers. obs.) and crocodylians. Yet, the odontoid of *Cerrejonisuchus improcerus* (UF/IGM 31) is
 287 significantly wider laterally thus giving the impression of an ellipsoid (with its greatest axis laterally
 288 oriented) in anterior view; its height over width ratio is 0.61, while that of *Congosaurus bequaerti* (MRAC
 289 1839) is 0.78 and *Hyposaurus rogersii* (AMNH FARB 2390) is 0.82 (personal observations).

290 The anterior facet of the odontoid of *Cerrejonisuchus improcerus* is concave and is bordered laterally
 291 and posteroventral by two small protuberances (the lateral one being the largest). Posteriorly, the center
 292 and dorsal portion of the bone are protruding, leaving the lateral and ventral parts hollow. This hump is
 293 where the bone connects to the axis.

294
 295 Hyposaurine dyrosaurs (i.e. *Congosaurus bequaerti* and *Hyposaurus rogersii*, [Schwarz et al., 2009])
 296 possess rather long neural spines on their cervicals, which is a trait also observed on *Cerrejonisuchus*.
 297 Indeed, C4 (the only one preserved) displays a neural spine whose shape is not unlike that of the cervicals
 298 of the aforementioned i.e. *Congosaurus bequaerti* (holotype; pers. obs.) and *Hyposaurus rogersii* (NJSM
 299 23368; pers. obs.): among hyposaurine dyrosaurs anterior or middle cervicals possess slender or pointed
 300 neurals which become wider laterally around the thoracic transition. The neural spine of C4 measures
 301 66.9mm and accounts for 16% of the height of the anterior centrum, making it shorter than that of Th0.
 302 For these reasons, C4 must be at least a middle cervical vertebrae, i.e. it must have ranged from the
 303 position 3 to 5.

304
 305 The anterior facet of C2 displays a shield-like shape: its ventral surface is rounded while the dorsal
 306 surface is rather flat. In C4 both facets appear more round than shield-shaped. This variation is also
 307 found in *Hyposaurus rogersii* (YPM VP.000380, VP.000753; pers. obs.) where the anterior facet of a
 308 cervical is usually round or hexagonal but the posterior facet takes a shield-like shape. This difference is
 309 particularly marked in the anterior thoracics (i.e. CIII-CIV) of *Hyposaurus rogersii* (e.g. NJSM 23368;
 310 YPM VP.000380; pers. obs.) since the parapophyseal process and anterior facet are more or less joined,
 311 thus influencing the silhouette of the anterior facet's margin. Posteriorly, the size of the centrum increases

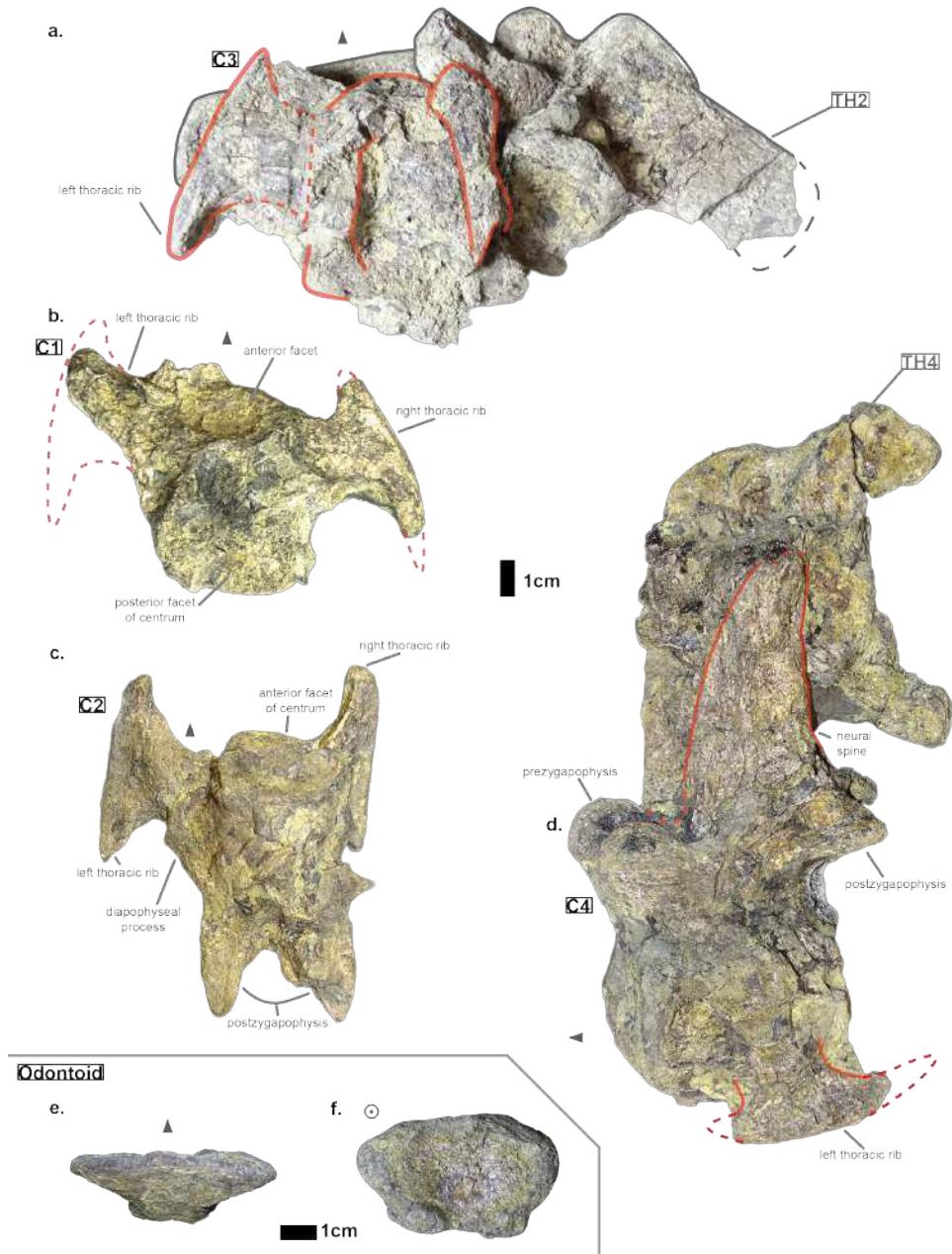


Figure 1. Cervicals of *Cerrejonisuchus improcerus* UF/IGM 31: **a.** Cervical C3 in dorsal view; **b.** Cervical C1 in dorsal view; **c.** Cervical C2 in dorsal view; **d.** Cervical C4 in lateral view (left); **f.** Odontoid in anterior view; **e.** Odontoid in dorsal view. Cervical C3 and C4 are respectively fused to Th2 and Th4. Scale bar represents 1cm. Grey arrow points towards anterior

	Aa	Ap	Ba	Bp	C	D	E	Hyp_height
UF/IGM 31 C1	-	29.03	-	27.76	38	-	-	-
UF/IGM 31 C2	24.01	-	29.35	29.59	36.34	-	-	-
UF/IGM 31 C3	-	-	-	43.95	55.38	-	-	-
UF/IGM 31 C4	40.29	40.58	-	-	50.45	72	66.89	-

Table 1. Table depicting each cervical vertebrae (ordered) and some measurements (part 1). 'A' represents the maximal height of the centrum (dorso-ventrally); 'B' represents the maximal width of the centrum (laterally); 'C' represents the anterior-posterior length of the centrum; 'D' represents the angle (whole number) that the neural forms with the horizontal. When the neural possesses a corner, the two angles are separated by a point; 'E' represents the height of the neural spine; and Hyp height represents the maximal height of the hypapophyse. The lower case letters 'a' and 'p' stand for 'anterior' and 'posterior' respectively

312 in width, height and length (the length of C3 may have been overestimated as its actual length is not easily
313 observable).

314

	Oa	Op	Pa	Pp	Ga	Gp
UF/IGM 31 C1	-	-	-	-	-	-
UF/IGM 31 C2	-	12.62	-	7.88	-	-
UF/IGM 31 C3	-	-	-	-	-	-
UF/IGM 31 C4	19.97	20.08	13.9	-	-	-

Table 2. Table depicting each cervical vertebrae (ordered) and some measurements (part 2). 'O' represents the longest axis of the elliptic surface of the corresponding pre- or postzygapophysis; 'P' represents the smallest axis of the elliptic surface of the corresponding pre- or postzygapophysis (and is usually perpendicular to the corresponding 'O'); 'G' refers to the angle (degree) between the horizontal plane (or coronal plane) and the corresponding pre- or postzygapophysis. The lower case letters 'a' and 'p' stand for 'anterior' and 'posterior' respectively.

315 In C1 and C2 the parapophyseal process is shorter than the diapophyseal process, which is a condition
316 also observed on the holotype of *Congosaurus bequaerti* (e.g. MRAC 1868; *pers. obs.*) and on *Hyposaurus*
317 *rogersii* (AMNH FARB 1421, 2389; NJSM 23368; *pers. obs.*), and which is also found in crocodylians
318 [Grigg and Kirshner, 2015]. However, in *Hyposaurus rogersii* AMNH FARB 2389 (*pers. obs.*), the
319 first cervical vertebrae directly posterior to the axis (*i.e.* CIII) shows a slightly longer parapophyseal
320 process, and in *H. rogersii* AMNH FARB 2390 both actually seem of relatively equal dimensions. In *C.*
321 *improcerus*, C2 has both its diapophyseal and parapophyseal processes centered on the lateral sides of the
322 centrum ~~which is like~~ the posterior cervicals (*i.e.* CVI and CVII) of *Hyposaurus rogersii* (NJSM 23368;
323 *pers. obs.*). Indeed, the diapophyseal and parapophyseal processes of the anterior and middle cervicals
324 (CIII-CV) of *Hyposaurus rogersii* (e.g. NJSM 23368; AMNH FARB 2389; YPM VP.000380; *pers. obs.*)
325 are anteriorly located, and migrate towards the center of the centrum posteriorly (so that the processes are
326 almost centered at CV).

327 The exact inclination angle of the diapophyseal and parapophyseal processes are lost, but C2 still
328 shows the remnants of their initial orientation: both were ventrally oriented with their distal facet (*i.e.*
329 diapophysis and parapophysis respectively) facing both anteriorly and laterally.

330

	E/Ba(%)	E/Aa(%)	Mp/Qp(%)	Ma/Qa(%)	Qa/Qp(%)	Qp/Ba(%)
UF/IGM 31 C1	-	-	-	-	-	-
UF/IGM 31 C2	-	-	-	-	-	-
UF/IGM 31 C3	-	-	-	-	-	-
UF/IGM 31 C4	-	166.02	-	-	-	-

Table 3. Table depicting different ratio from the cervical vertebra (ordered). 'A' represents the maximal height of the centrum (dorso-ventrally); 'B' represents the maximal width of the centrum (laterally); 'E' represents the height of the neural spine; 'M' stands for the greatest length of the surface (which may be tilted regarding the antero-posterior plane); 'Q' represents the proximal-distal length of the corresponding ramus (either the anterior or posterior one) of the lateral process. The lower case letters 'a' and 'p' stand for 'anterior' and 'posterior' respectively.

331 It is not possible to tell if *Cerrejonisuchus improcerus* possessed a posterior ventral keel on its anterior
332 or middle cervicals like *Hyposaurus rogersii* (e.g. NJSM 23368; YPM VP.000380; AMNH FARB 1416,
333 1432, 2389, 2390; ANSP 8649; *pers. obs.*) or *Congosaurus bequaerti* (MRAC holotype, e.g. MRAC
334 1840, 1868). This structure (*i.e.* ventral keel) differs from the hypapophysis as it is of less significant

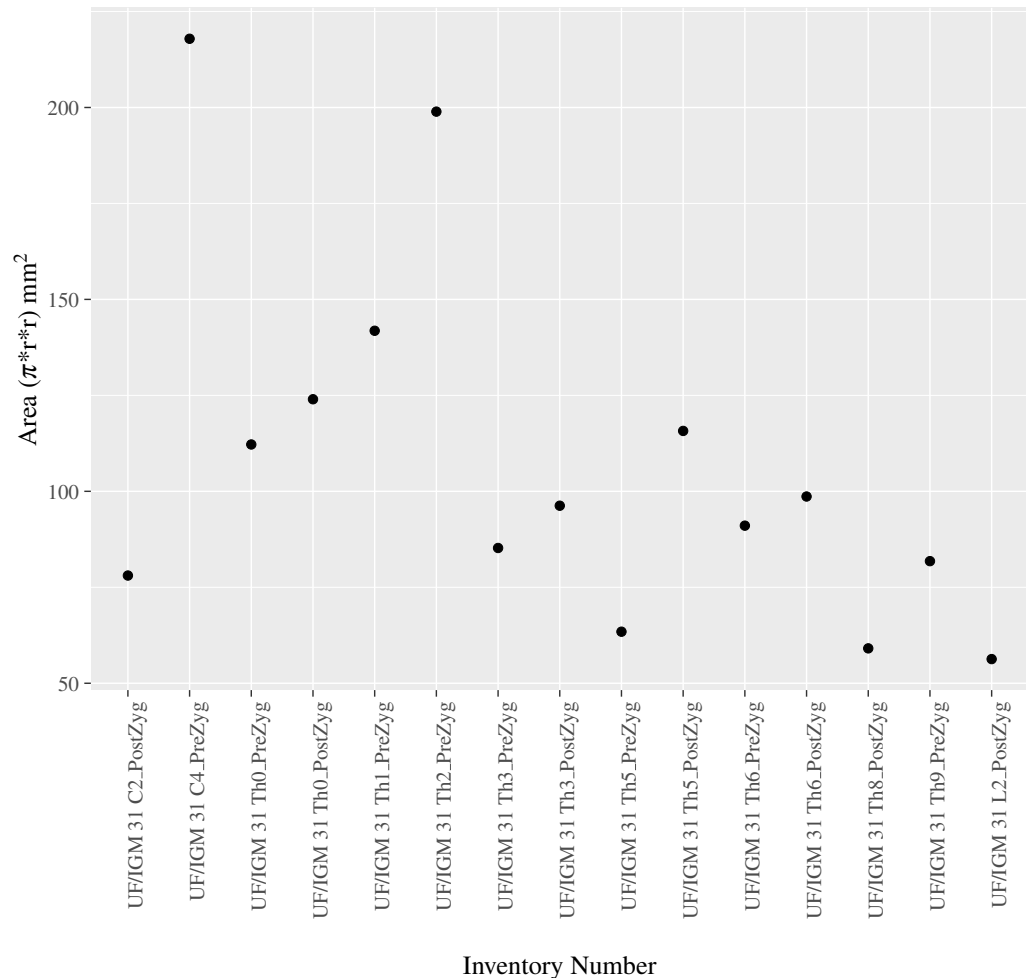
Pre- and postzygapophysis area of *C. improcerus* throughout the axial skeleton

Figure 2. Area in mm² of the preserved pre- and postzygapophysis of *Cerrejonisuchus improcerus* UF/IGM 31. There are two observable peaks and, unlike *Mecistops cataphractus* RBINS 18374, the three first anterior thoracics show an increasing trend. All the other remaining vertebrae show a gradual decrease in the total area of their zygapophysis.

335 height, and located posteriorly on the centrum as opposed to the anteriorly positioned hypapophysis of
 336 the last cervicals (e.g. *Hyposaurus rogersii* AMNH FARB 1421; *pers. obs.*) or anterior thoracics (e.g.
 337 thoracic numbered MRAC 1872 of *C. bequaerti*; *pers. obs.*).

338
 339 The pre- and postzygapophyses are already large in this portion of the skeleton compared to their
 340 centrum, see table 2 and table 1. Also, they are increasing in size posteriorly as they are getting closer to
 341 the thoracic region like, for example, the crocodylian *Mecistops cataphractus* (see fig. 3) or *Congosaurus*
 342 *bequaerti* (see fig. 4). However, in *Cerrejonisuchus improcerus*, the first thoracics are still following the
 343 increasing trend initiated among the cervicals and the decreasing trend occurs here more posteriorly (i.e.
 344 among the thoracics; see fig. 2) than in the crocodylian *M. cataphractus*. In *Congosaurus*, the anterior
 345 thoracics do not follow the same increasing trend as in *Cerrejonisuchus* but rather form a plateau before
 346 starting the decreasing slope posteriorly. Yet, both *Cerrejonisuchus* and *Congosaurus* show a peak among
 347 the anterior thoracics (see fig. 3 and fig. 4) which totally breaks from the other thoracics. This feature is
 348 not present in *Mecistops* (see fig. 3).

349 4.3 The anterior thoracic vertebra UF/IGM 31 Th0, Th1, Th2, Th3, Th4 and Th5:

350 The anterior-posterior sequence of anterior thoracic vertebra is as follow: UF/IGM 31 Th0, UF/IGM 31
 351 Th1, then UF/IGM 31 Th2 and UF/IGM 31 Th3, and finally UF/IGM 31 Th4. Classification details

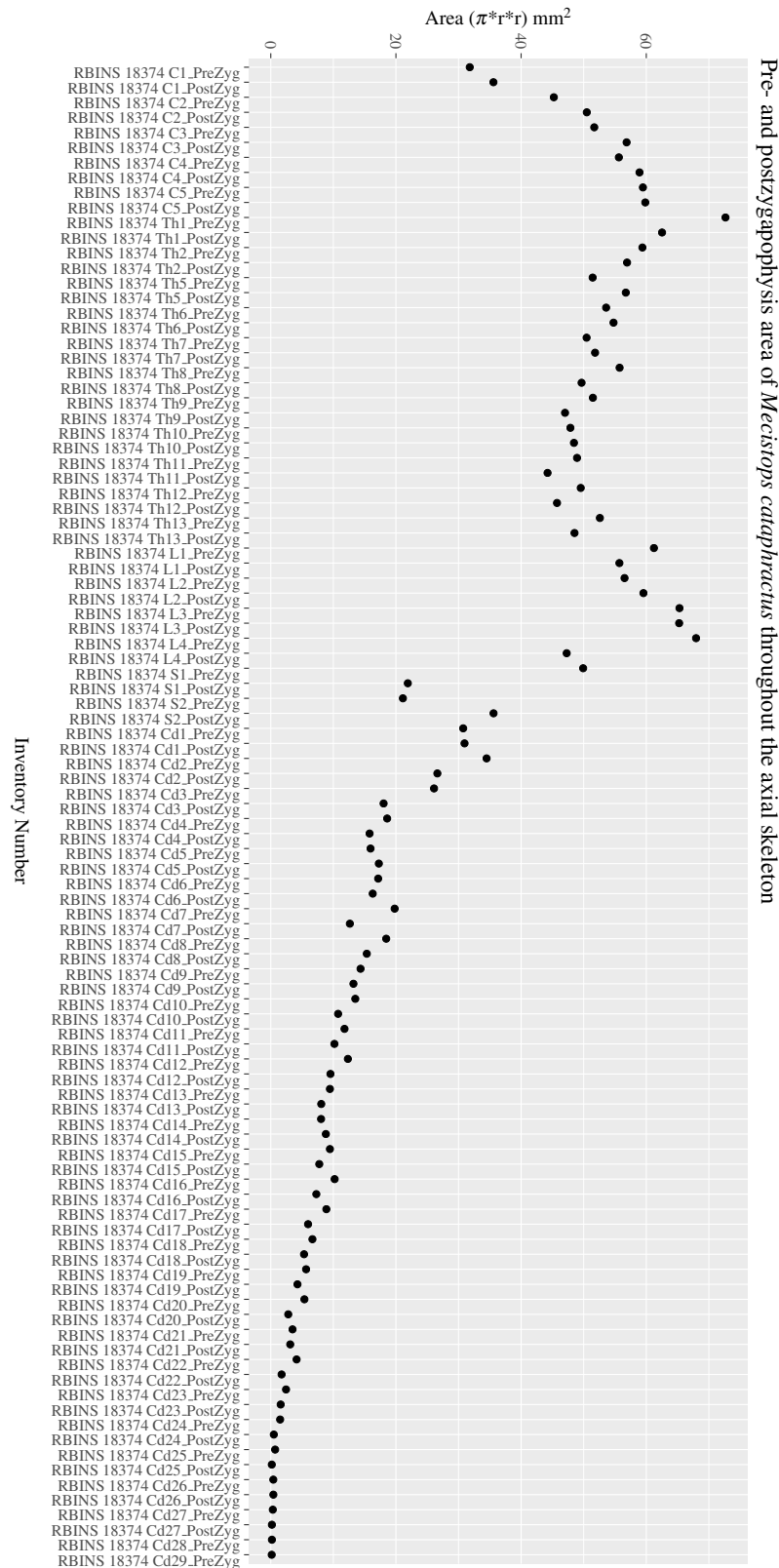


Figure 3. Evolution of the area in mm² of the pre- and postzygapophysis throughout the axial skeleton of *Mecistops cataphractus* RBINS 18374. Note the existence of two peaks indicating vertebral transition areas. Cervicals have an increasing trend while all the other parts, excluding the peaks, have a decreasing trend posteriorly.

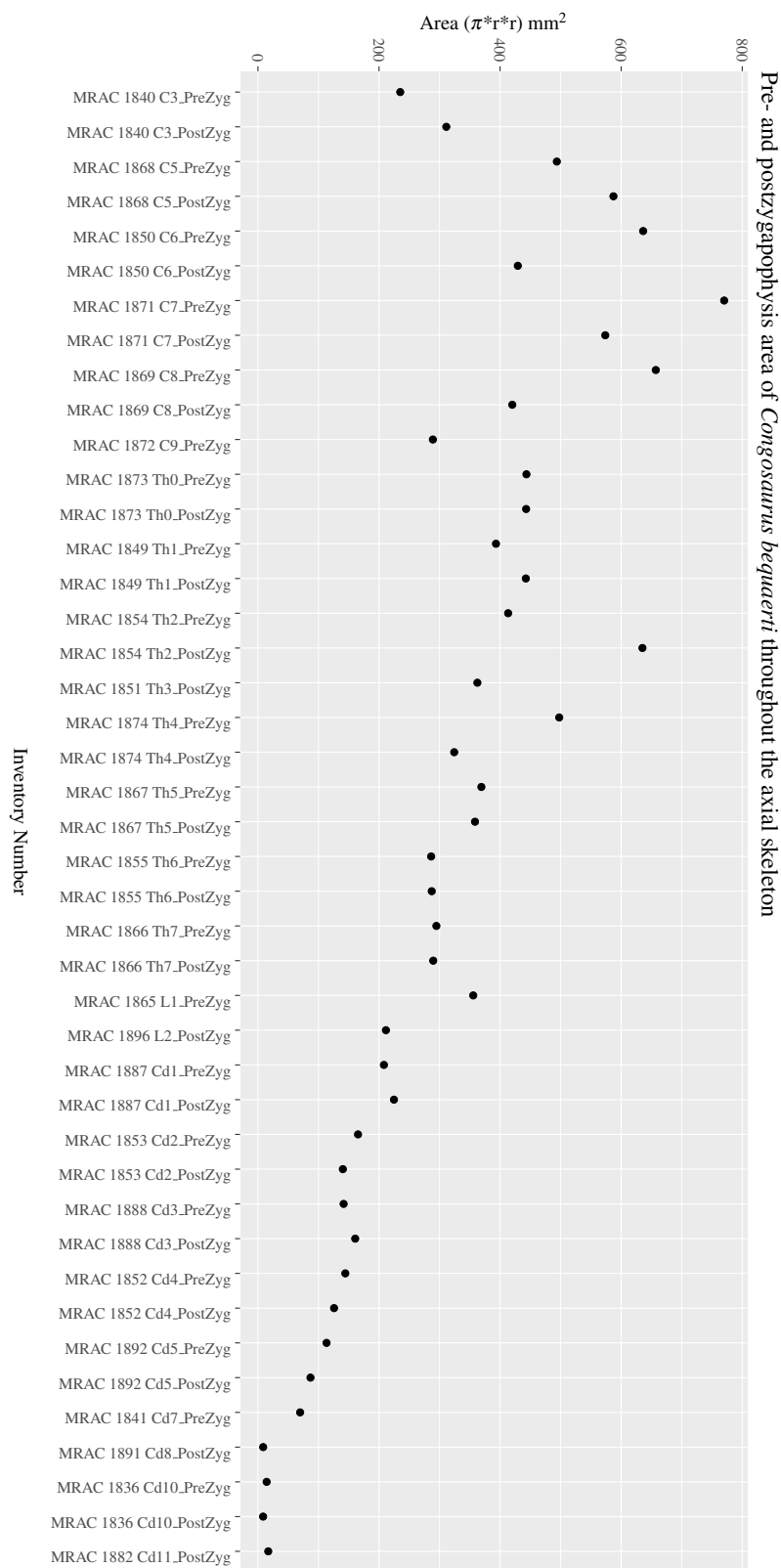


Figure 4. Evolution of the area in mm² of the pre- and postzygapophysis throughout the axial skeleton of *Congosaurus bequaerti*. Note the existence of two peaks: one at the mid-cervicals, and one at the anterior thoracics. Inventory number of each vertebrae listed on the abscissa axis.



352 are presented here below.


353

354 The anterior thoracic vertebra are recognizable thanks to the relatively short anterior ramus (or
355 parapophyseal process), plus the long neural as well as the presence of a hypapophysis. Indeed, middle
356 and posterior thoracics possess a longer anterior ramus (both absolute and relative) but, in contrast, a
357 shorter neural spine.

358 The parapophyseal and diapophyseal processes are borne on the neural arch but their orientation
359 remains unknown. Similarly, the orientation of the distal extremities of the processes (parapophysis and
360 diapophysis) has not been preserved. Anyhow, it is likely that both distal facets exhibited some sort of
361 oval shape before fossilization (*i. e.* longer anteroposteriorly than high). In the anterior-most thoracics (*i.e.*
362 Th0, Th1, and Th2), the parapophyseal process is close to the diapophyseal process so that both share the
363 same base (called the ‘lateral process’). Furthermore, the parapophyseal process (or ‘anterior ramus’) is
364 strictly ventral to the diapophyseal process (or ‘posterior ramus’) as it is the case for *Hyposaurus rogersii*
365 (NJSM 23368, *pers. obs.*). Yet another argument supporting the aforementioned classification of Th0,
366 Th1, and Th2. Unsurprisingly, the exact position of the lateral process as a whole is not certain but, from
367 what is apparent on lateral sides of Th2 and Th1, it appears to have been centered on the centrum like
368 *Congosaurus bequaerti* (holotype; *pers. obs.*) or *Hyposaurus rogersii* (NJSM 23368; YPM.VP000764;
369 *pers. obs.*) and unlike *Alligator mississippiensis* [Storrs, 1986] or *Mecistops cataphractus* (RBINS 18374;
370 *pers. obs.*) where they are more anteriorly located.

371

372 The neural spine is rather strait; both the anterior and posterior surfaces are parallel and tilted by more
373 or less 75 ° (in relation to the horizontal plane, see table 4). However, there is a portion at the base of
374 the anterior surface that is vertical  according to the presence of a flexion point along the surfaces. Hence
375 the neural spine displays a katana  shape, with the distal extremity being posteriorly pointed with a
376 smooth and convex anterior. The vertebra Th0, Th1 and Th2 greatly resemble one another both in the
377 shape of their neural spine and their lateral processes, meaning that they were probably closer together
378 than to the other anterior thoracics.

379 There is also the presence of a posterior notch which runs between half the total length of the neural
380 and almost all of it: on Th0 the notch appears restricted to the area between the postzygapophyses while,
381 on Th3 the notch stops at about 1/6th of the top. The notch separating the postzygapophyses ventrally
382 (visible in Th0, Th1, Th3 and Th4) shows the absence of a hyposphene and thus the non-existence of a
383 *hyposphene-hypantrum* articulation [Stefanic and Nesbitt, 2019]. Still, the existence of a notch along the
384 posterior surface of the neural conveys the thoracic vertebra’s capacity to interlock to a certain extent 
385 means that the vertebrae were probably quite close, *i.e.* the intervertebral disc was rather thin then th
386 The presence of a notch may express an attempt to enhance the column flexibility in the dorsal plane
387 by creating extra space for flexion. The original inclination of the neural spine is not preserved, but its
388 straight outline does not indicate any change of angle dorsally. Nevertheless, it seems the neural spine
389 was quite vertical (close to 80-90°).

390

391 Th2 has both the neural and hypapophysis (yet incomplete) preserved, and the length of both processes
392 (see table 1) place it as either the last cervical or one of the first thoracics. The wide and rounded tip of the
393 neural further support this hypothesis: indeed, among hyposaurine dyrosaurs (*i.e.* *Congosaurus bequaerti*,
394 holotype, and *Hyposaurus rogersii*, NJSM 23368), anterior or middle cervicals possess slender or pointed
395 neurals which become wider distally around the thoracic transition. Also, the outline of the neural of Th2
396 greatly resembles that of Th0 and Th1.


397 Both facets of the centrum are concave (amphicoelous), heart- or shield-shaped (larger dorsally
398 and pointed ventrally) and ventrally united by a process (the hypapophysis). Based on the preserved
399 dimensions, it seems that the posterior facet of the vertebrae is slightly taller than the anterior one (which
400 is a feature also found among some thalattosuchians, and on the holotype of *Congosaurus bequaerti*; *pers.*
401 *obs.*). Nevertheless, both facets are wider than tall, this feature being more emphasized for the anterior
402 facet. The hypapophysis starts from the anterior portion of the centrum, and is linked to the ventral margin
403 of the anterior facet. Its anterior surface is vertical while its posterior one is slightly concave since it
404 stretches out towards the posterior facet. Furthermore, the hypapophysis was long (unfortunately broken
405 in Th1) and exceeded the centrum’s height or width, at least in the anterior-most portion of the thoracic
406 region (see table 4). Where it is preserved the hypapophysis appears strait with no specific orientation,

407 which is a condition also observed in Hyposaurinae [Schwarz et al., 2006] like *H. rogersii* (NJSM 23368;
 408 *pers. obs.*) and *C. bequaerti* (MRAC holotype; *pers. obs.*) (while counter-example could be the condition
 409 observed in *Mecistops cataphractus* for instance; *pers. obs.*); its shape is of a rectangle with a possibly
 410 curved tip. The presence of the hypapophysis indicate that those vertebra were rather anteriorly positioned
 411 thoracics, and its decreasing length posteriorly (when preserved) helps ordering the vertebra.

412
 413 The prezygapophysis facet is mostly oriented dorsally, with an angle (taken from the horizontal plane)
 414 ranging from about 23° to roughly 40-45° (see table 6). The postzygapophysis appears to be facing mainly
 415 ventrally with an angle of about 40-45°. Yet the crushed condition of the vertebra makes it hard to secure
 416 the validity of these measurements. Nonetheless, the postzygapophysis value is plausible (when compared
 417 to the holotype of *C. bequaerti*; *pers. obs.*).

418 The pre- and postzygapophyses are quite large compared to the centrum (see tables 4 and 6), indeed if
 419 we take a look at the greater axis of these elliptic surfaces:

- 420 • **TH0** The prezygapophysis represents 42.1% of the width of the anterior facet, while the postzy-
 421 gapophysis accounts for 43.6%;
- 422 • **TH1** The maximal size of the articular facet of the prezygapophysis is quite important as it reaches
 423 45.75% of the anterior facet's width;
- 424 • **TH2** The prezygapophysis represents 51.3%, and the postzygapophysis reaches 52.4% of the width
 425 of the anterior facet;
- 426 • **TH3** The greater axis of the prezygapophysis accounts for 32.1% of the width of the anterior facet
 427 (and 35.1% of the posterior one). Also, the postzygapophysis reaches 30.2% of the width of the
 428 anterior facet (and 33% of the posterior one);
- 429 • **TH4** Only the postzygapophysis is present, and it represents 32.9% of the anterior facet's width.
- 430 • **TH5** Both the prezygapophysis and postzygapophysis are present. The prezygapophysis accounts
 431 for 26.9% of the anterior facet's width, while the postzygapophysis reaches 36.7%.

432
 433 The non-gradual evolution  between each of the anterior thoracic vertebra proves their non-adjacent
 434 state, but also helps positioning them relatively. These great differences are of course emphasized by the
 435 lack of transitional vertebra between them. Hence, the succession from anterior to posterior is likely to be:
 436 Th0, Th1, then Th3, and finally Th4. Let's now describe the whole trend and compare the two pairs of
 437 Th1-Th3 and Th3-Th4 to prove it.

438 The strongest evidence of classification is here going to be the size (both absolute and relative) of
 439 the neural spine since we are in the anterior-most part of the thoracic region (thanks to the holotype of
 440 *Congosaurus bequaerti*; *pers. obs.*). Indeed, the neural spine of each anterior thoracic is tall (± 98.8 mm
 441 for Th0, ± 86.4 mm for Th1; ± 58.8 mm for Th3, ± 57.9 mm for Th4 and ± 47.5 mm for Th5) and greatly
 442 exceeds the dimensions of their centrum, which confers them a unique identifiable look. When compared
 443 to the anterior width (or height for Th0) of their respective centrum (7): Th0 has by far the greatest ratio
 444 with $\pm 316\%$ (in relation to its height), Th1 equals almost three times its width with $\pm 277\%$, while Th3
 445 is worth $\pm 137.7\%$, Th4 reaches $\pm 137.5\%$ and Th5 about $\pm 122\%$. On the opposite, the hypapophysis
 446 shows a rather constant length of about 22mm among all of the thoracic vertebrae where it is preserved.
 447 Therefore its ratio with the respective centrum width is not relevant as it would only reflect the centrum's
 448 dimensions. Nevertheless, the hypapophysis of the posterior cervicals exceeds by far the length of that of
 449 the anterior-most thoracics, probably because their actual length is not preserved (*i.e.* the hypapophysis of
 450 Th0 and Th1 would be broken in that case).

451 Looking at Th0, Th1 and Th3, it appears clear from the absolute and relative height of the neural spine
 452 (see table 4 and table 7), doubled with the absolute width of their centrum (from table 4), that Th0 is the
 453 anterior-most thoracic and that Th1 is anterior to Th3 (rather than the opposite). Unfortunately, the lateral
 454 processes of Th0 and Th1 appear missing and cannot be used to further support this sorting. The neural
 455 spine of Th1 also suggests the existence of a posterior notch at about 1/3rd of its height. Th3 and Th5
 456 show the same structure but here it appears to run almost the full height of the neural. The information is
 457 not available on Th4.

458 The difference of size of the neural spine between Th3 and Th4 is here more stable (with $\pm 58.78\text{mm}$
 459 versus $\pm 57.9\text{mm}$ respectively, see table 4), which makes it less easier to understand. As it has been
 460 discussed in the section just above, there are also other important features which can corroborate this
 461 sorting: the relative length of the rami plus the size of their distal extremities (see table 4, table 9 and
 462 table 7). The proportional length of the anterior ramus (*i.e.* parapophyseal process) accounts for $\pm 19\%$
 463 of the posterior ramus (*i.e.* diapophyseal process) for Th3, and this number increases to $\pm 43\%$ for Th4.
 464 When compared to the width of their respective centrum, the posterior ramus of Th3 reaches up to $\pm 64\%$
 465 of the length while Th4 shows a greater proportion with $\pm 95\%$ (see table 7). If we look even further
 466 along the thoracic region, the length of the lateral process (*i.e.* parapophyseal and diapophyseal processes)
 467 shows an increasing trend posteriorly both proportionally to the corresponding centrum and absolutely.
 468 And not to mention that the extremity of both rami also increases from Th3 to Th4, with 8.84 mm for
 469 the length from the anterior ramus of Th3 versus 11.76 mm for that of Th4, and with 13.5mm for the
 470 length from the posterior ramus of Th3 versus 14.4mm for that of Th4 (see table 9). These last length
 471 measurements represent the greater extend of the distal surface, even if it is slightly tilted compared
 472 to the anteroposterior plane. Indeed, the length of the rami, and thus the overall attaching site of the
 473 ribs, considerably increases in size up to a certain point among the middle thoracics, where it starts to
 474 slowly shrink towards the lumbar (where the ribs finally disappear). As a consequence, the short rami
 475 (in both their lengths, and dimension of their distal facets) of Th3 must be placed anterior to that of Th4.
 476 Additionally, the shortness of the rami of UF/IGM 31 Th3 could imply a position of the vertebrae among
 477 the very first thoracics, probably from the third through fifth thoracic position as the first and second tho-
 478 racic would be expected to show resorbing parapophyseal processes like in *Crocodylia* and *Thalattosuchia*.

480 The neural spine can be used again to order Th4 and Th5 as their difference in size and shape is
 481 obvious. While the neural of Th4 is long ($\pm 57.9\text{mm}$) and blade-like, that of Th5 is shorter ($\pm 47.5\text{mm}$)
 482 and broader at its extremity. This posterior modification of the neural shape is not unlike *Hyposaurus*
 483 *rogersii* (NJSM 23368; *pers. obs.*), where the mid-thoracics and posterior thoracics show square-like
 484 neurals. The relative length of the parapophyseal process to the diapophyseal process in Th5 equals 45.6%,
 485 which is a small increase compared to Th4. Yet the parapophyseal process hasn't reached its maximum
 486 length at this point as it usually happens more posteriorly towards the lumbar region (like in *Hyposaurus*
 487 *rogersii* (NJSM 23368; *pers. obs.*) or *Congosaurus bequaerti* MRAC 1874). In overall, the articular
 488 facets of Th5 (*i.e.* parapophysis and diapophysis) are greater than those of Th4, which definitely resolves
 489 the ordering debate since the ribs are only getting bigger posteriorly at this stage (*i.e.* in the anterior
 490 portion of the thoracic region).

491 Generally, the anterior thoracics present an important decrease in the height of the neural spine
 492 posteriorly, while the hypapophysis remains quite stable. The centrum is also of equal dimensions
 493 throughout the anterior thoracic, with the height of Th1 being the sole exception. The postzygapophysis
 494 is slightly increasing posteriorly while the opposite trend strikes the prezygapophysis. The zygapophyses
 495 are also quite important in size compared to the centrum, but they are decreasing posteriorly. Lastly, the
 496 lateral process increases in length laterally as one goes posteriorly, so that both rami develop an increased
 497 articular facet (the diapophysis being the larger than the parapophysis) to hold even larger ribs. It seems the
 498 lateral process originated from the neural arch, however due to the crushed condition of each vertebrae, it
 499 is not possible to determine whether it was positioned at the base of the arch or on the same level as the
 500 neural canal. Likewise, assessing the orientation of the lateral process remains doubtful.

501 The size of the neural canal in Th4 is 9.87mm in height and 12.31mm in width, while that of Th1
 502 reaches 13mm in height and 12.38mm in width. The neural canal of Th3 is obstructed and cannot
 503 be measured. The neural canal of Th5 is 12.9mm high and 14.66mm wide. It is slightly wider than
 504 that of Th1, but is overall similar as it would be expected from two closely related thoracics among
 505 crocodyliforms (like for example in *Mecistops cataphractus* RBINS 18374 see the fig. 6).

506 On the scatter plot graph of *Congosaurus bequaerti* (see fig. 7), the evolution of the size of the neural
 507 canal reveals an overall decreasing trend posteriorly throughout the axial skeleton, which slightly differs
 508 from the cervicals of *Mecistops cataphractus* (see fig. 6). There is still a discernible increase occurring at
 509 the lumbar-caudal transition, highlighting the switch in vertebral regions.

510 4.4 The middle thoracic vertebra UF/IGM 31 Th6 and Th7:

511

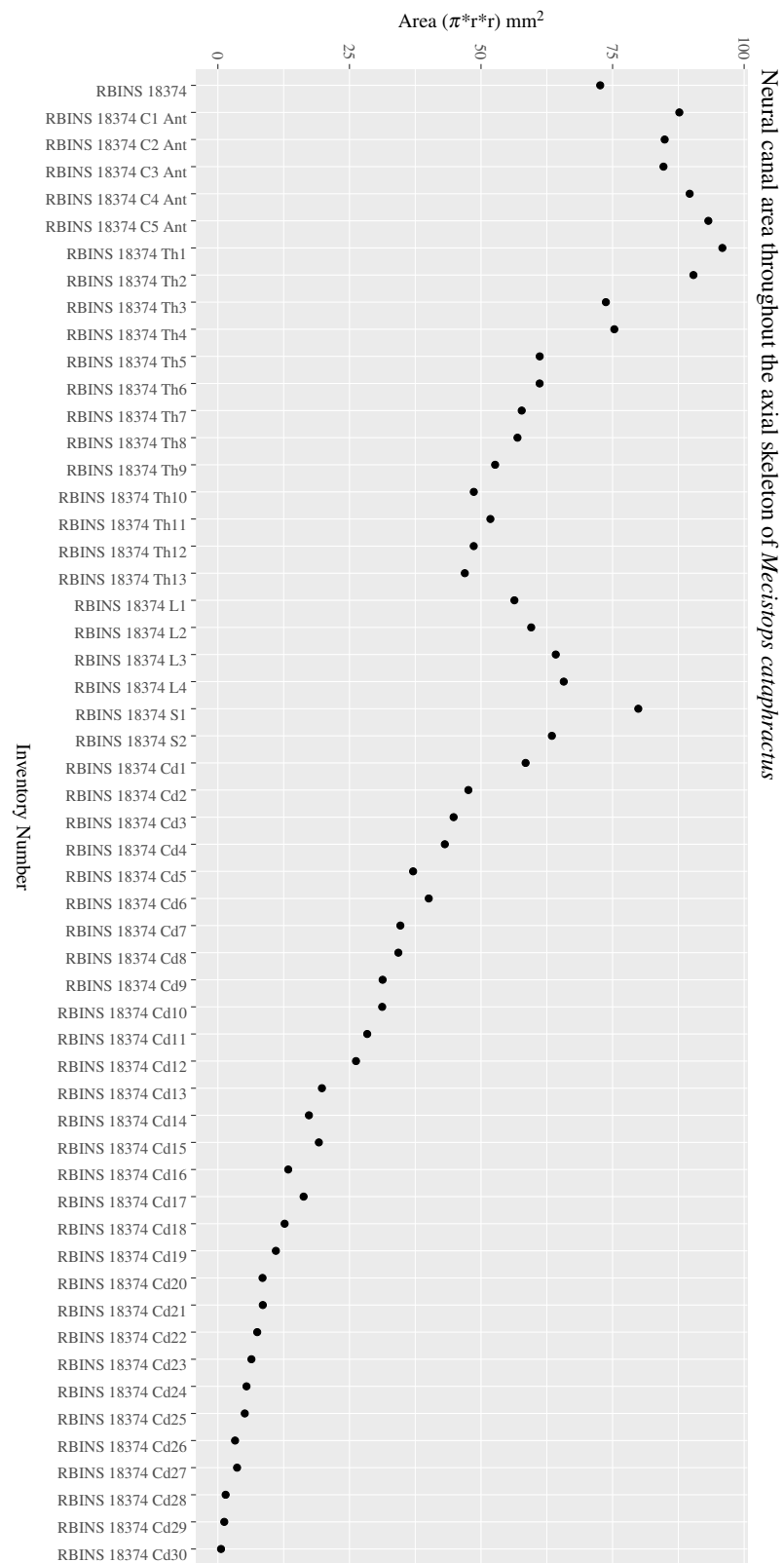


Figure 6. Scatter plot of the area variation of the neural canal throughout the axial skeleton of *Mecistops cataphractus* (RBNIS 18374).

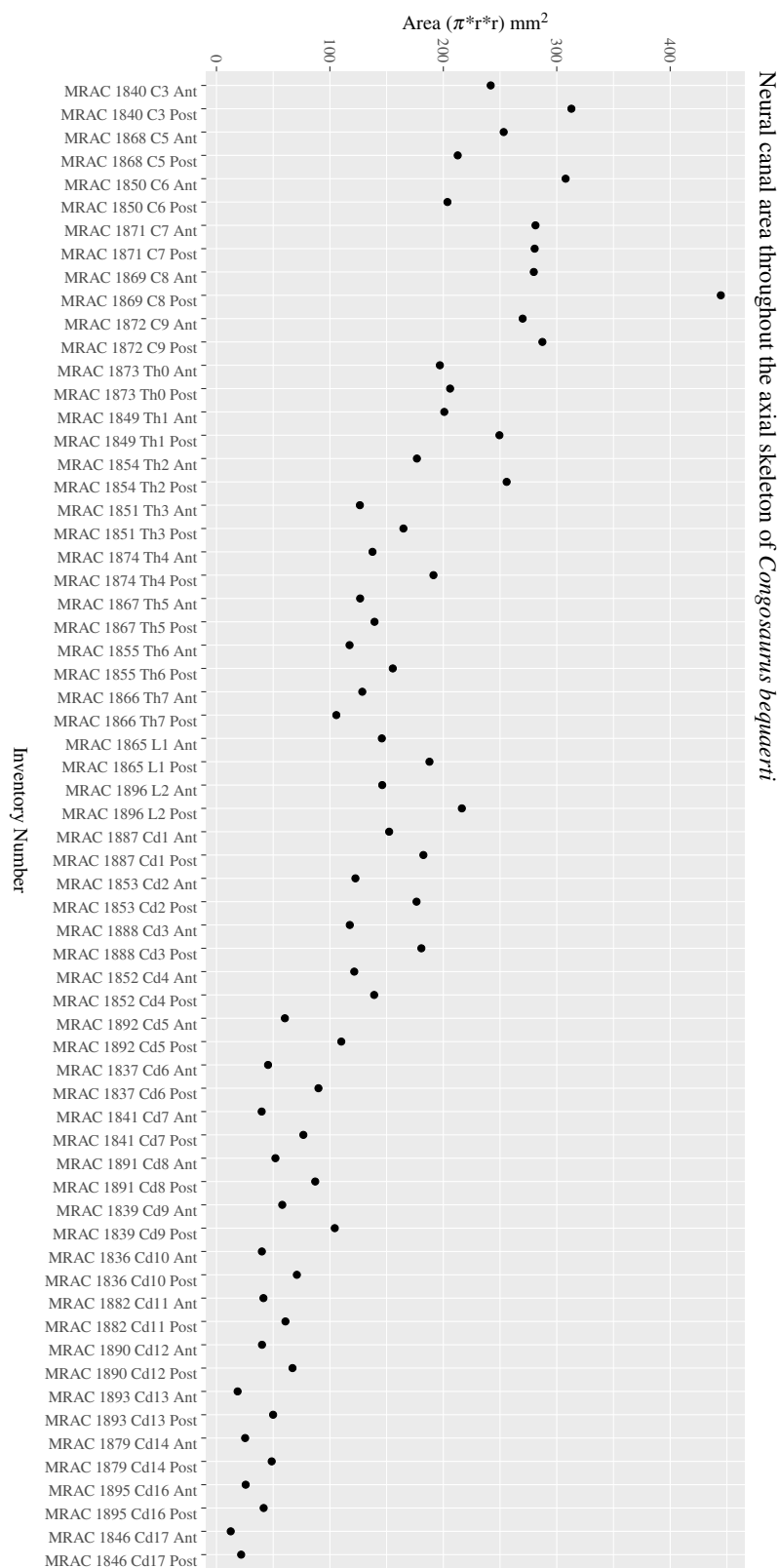


Figure 7. Scatter plot of the area variation of the neural canal throughout the axial skeleton of *Congosaurus bequaerti*. Inventory number of each vertebrae listed on the abscissa axis.

	Aa	Ap	Ba	Bp	C	D	E	Hyp.height
UF/IGM 31 Th0	31.23	31.36	-	32.3	32.53	90.77	98.82	-
UF/IGM 31 Th1	37.15	-	31.17	29.95	36.1	90.76	86.37	22.2
UF/IGM 31 Th2	-	36.05	-	35.25	39.45	90.61	78.8	42.78
UF/IGM 31 Th3	28.02	30.98	42.68	39.02	30.17	-	58.78	21.5
UF/IGM 31 Th4	29.62	-	42.09	-	-	-	57.9	23.61
UF/IGM 31 Th5	33.01	31.75	38.9	37.39	21.29	-	47.46	22.7
UF/IGM 31 Th6	37.24	39.64	43.65	44.02	-	-	44.71	-
UF/IGM 31 Th7	-	-	35.63	-	-	-	43.47	-
UF/IGM 31 Th8	36.33	34.74	35.02	33.92	35.39	84.58	33.34	-
UF/IGM 31 Th9	34.56	31.38	39.09	41.67	40.39	-	-	-

Table 4. Table depicting each thoracic vertebrae (ordered) and some measurements (part 1). 'A' represents the maximal height of the centrum (dorso-ventrally); 'B' represents the maximal width of the centrum (laterally); 'C' represents the anterior-posterior length of the centrum; 'D' represents the angle (whole number) that the neural forms with the horizontal. When the neural possesses a corner, the two angles are separated by a point; 'E' represents the height of the neural spine; and Hyp height represents the maximal height of the hypapophyse. The lower case letters 'a' and 'p' stand for 'anterior' and 'posterior' respectively

	J	K	La	Lp	Ma	Mp	Qa	Qp
UF/IGM 31 Th0	-	-	-	-	-	-	-	18.65
UF/IGM 31 Th1	-	-	-	-	-	-	-	-
UF/IGM 31 Th2	-	-	-	-	-	-	-	-
UF/IGM 31 Th3	26.61	7.65	4.72	5.62	8.84	13.5	8.19	31.17
UF/IGM 31 Th4	27.08	-	4.02	6.21	11.76	14.4	17.41	39.97
UF/IGM 31 Th5	23.27	8.94	5.76	7.23	9.57	17.74	20.82	45.61
UF/IGM 31 Th6	24.41	7.23	5.23	5.65	10.02	16.43	22.87	42.13
UF/IGM 31 Th7	27.76	7.39	7.84	6.49	10.56	18.46	29	47.61
UF/IGM 31 Th8	23.3	-	3.5	4.06	6.36	15.8	26.01	42.58
UF/IGM 31 Th9	25.05	8.39	-	3.64	-	13.2	-	44.07

Table 5. Table depicting each thoracic vertebrae (ordered) and some measurements (part 2). 'J' represents the base width (antero-posterior) of the lateral process; 'K' represents the base height (dorso-ventral) of the lateral process; 'L' represents the height of the distal surface of the lateral process and is taken perpendicular to 'M'; 'M' stands for the greatest length of the distal surface (which may be tilted regarding the antero-posterior plane) of the lateral process; 'Q' represents the proximal-distal length of the corresponding ramus (either the anterior or posterior one) of the lateral process; The lower case letters 'a' and 'p' stand for 'anterior' and 'posterior' respectively.

512 The anterior-posterior sequence of the middle thoracic vertebra is as follow: **UF/IGM 31 Th6** then
513 **UF/IGM 31 Th7**.

514

515 The middle thoracics have been ordered following the same process of classification than mentioned
516 in the previous section, which has furthermore been improved here using to the presence of a preserved
517 lateral process. Hence, the most important classifying features are (with the same degree of importance)
518 the dimensions of the centrum, the size of the neural spine and that of the parapophyseal and diapophyseal
519 processes (including the dimensions of the parapophysis and diapophysis).

520 In parallel, it is important to mention that both the anterior and posterior thoracic vertebra help
521 understand the organisation among the middle thoracics. Indeed, the anterior and posterior thoracics
522 being the easiest to identify and order, these were resolved in the first place. And their own characteristics
523 were used as a reference to classify those in between them (*i.e.* the middle thoracics).

524

525 The characteristics of the middle thoracics that stand out are: the widening of the lateral process
526 (which flares out anteroposteriorly from the neural arch to the distal ends), a further increase in the size
527 of the ribs attachment sites (*i.e.* area of the parapophysis and diapophysis) and finally a neural spine
528 decreasing in height posteriorly (which is therefore smaller than that of the anterior thoracics). All of
529 these traits were decisive in ordering the middle thoracics, using the global trend previously inferred from
530 the anterior and posterior thoracics.

531

532 The centrum is here heart-shaped since its maximal width is obtained more dorsally than ventrally
533 compared to the imaginary horizontal mid-line cutting the centrum. Still, like Th3, the centra are wider

	Oa	Op	Pa	Pp	Ga	Gp
UF/IGM 31 Th0	13.6	14.09	10.51	11.21	45	45
UF/IGM 31 Th1	14.26	-	12.67	-	45.9	-
UF/IGM 31 Th2	18.1	18.46	14	-	-	-
UF/IGM 31 Th3	13.71	12.88	7.92	9.52	22.9	41
UF/IGM 31 Th4	-	13.87	11.66	-	39.91	-
UF/IGM 31 Th5	10.48	14.3	7.71	10.31	45	45
UF/IGM 31 Th6	14.06	12.63	8.25	9.95	-	41.7
UF/IGM 31 Th7	-	-	-	-	-	-
UF/IGM 31 Th8	-	12.2	-	6.17	-	-
UF/IGM 31 Th9	11.04	-	9.44	-	15	-

Table 6. Table depicting each thoracic vertebrae (ordered) and some measurements (part 2). 'O' represents the longest axis of the elliptic surface of the corresponding pre- or postzygapophysis; 'P' represents the smallest axis of the elliptic surface of the corresponding pre- or postzygapophysis (and is usually perpendicular to the corresponding 'O'); 'G' refers to the angle (degree) between the horizontal plane (or coronal plane) and the corresponding pre- or postzygapophysis. The lower case letters 'a' and 'p' stand for 'anterior' and 'posterior' respectively.

	E/Ba(%)	E/Aa(%)	Mp/Qp(%)	Ma/Qa(%)	Qa/Qp(%)	Qp/Ba(%)
UF/IGM 31 Th0	-	316.43	-	-	-	-
UF/IGM 31 Th1	277.09	232.49	-	-	-	-
UF/IGM 31 Th2	-	-	-	-	-	-
UF/IGM 31 Th3	137.72	209.78	43.31	107.94	26.28	73.03
UF/IGM 31 Th4	137.56	195.48	36.03	67.55	43.56	94.96
UF/IGM 31 Th5	122.01	143.77	38.89	45.97	45.65	117.25
UF/IGM 31 Th6	102.43	120.06	39	43.81	54.28	96.52
UF/IGM 31 Th7	122	-	38.77	36.41	60.91	133.62
UF/IGM 31 Th8	95.2	91.77	37.11	24.45	61.09	121.59
UF/IGM 31 Th9	-	-	29.95	-	-	112.74

Table 7. Table depicting different ratio from the thoracic vertebra (ordered). 'A' represents the maximal height of the centrum (dorso-ventrally); 'B' represents the maximal width of the centrum (laterally); 'E' represents the height of the neural spine; 'M' stands for the greatest length of the surface (which may be tilted regarding the antero-posterior plane); 'Q' represents the proximal-distal length of the corresponding ramus (either the anterior or posterior one) of the lateral process. The lower case letters 'a' and 'p' stand for 'anterior' and 'posterior' respectively.

534 than tall. Also, the posterior facet is slightly more elongated dorsoventrally than the anterior one for
 535 an even width. Th6 presents a bigger centrum than Th5, indicating that the posteriorly increasing trend
 536 initiated with the anterior thoracics is still going. However, Th7 is drastically smaller than Th6, much
 537 like the posterior thoracics, which would mean that a downward trend has been taking place somewhere
 538 between the vertebrae Th6 and Th7 (which is also implying their non adjacent state).

539 The anteroposterior width of the centrum of Th6 could not be measured, but it seems that the hy-
 540 papophysis was uniting both facets. The length of the hypapophysis cannot be known as the process is
 541 broken in Th6. In Th7, the lower portion of the centrum is missing, thus making it impossible to assess
 542 the presence of a hypapophysis. It is interesting to note that the mid thoracics of *Cerrejonisuchus* still
 543 possessed a well-developed hypapophysis, which is not the case for *Congosaurus*.

544

545 Conversely, all lateral processes are preserved integrally among the middle thoracics and reflect the
 546 trend initiated in the anterior thoracics with the increase of the anterior ramus (*i.e.* parapophyseal process).
 547 Starting from Th6 the length of the anterior ramus greatly increases so that it represents 54.3% of the
 548 posterior ramus's length, and then it reaches up to 60.9% in Th7 (see table 7). In Th6, the posterior ramus
 549 is almost as long as the centrum is wide while the anterior branch is only equal to its half width. However,
 550 the posterior ramus is greater than the centrum's width for Th7. In overall, the articular facets of each
 551 rami (*i.e.* parapophysis and diapophysis) are the biggest in Th7 than any other thoracic indicating a peak
 552 in the robustness of the ribcage at this point. Before this turning point, distal facets are increasing in
 553 size, and afterwards (*i.e.* in the posterior thoracic part) they slowly begin to decrease. In lateral view, the
 554 parapophysis and diapophysis are oval (greater axis usually positioned in the anteroposterior plane, but
 555 this is not observable here), with the diapophysis showing a slender and slightly pointed posterior. Sadly,
 556 it is not possible to assess the original orientation and inclination of the lateral process as a whole or of

557 any of the rami.

558 Compared to *Congosaurus bequaerti* (MRAC 1855, 1874), the parapophyseal and diapophyseal
559 processes of *Cerrejonisuchus improcerus* (UF/IGM 31 Th5 and Th6) do not appear to arrange in tiers
560 vertically. Instead, the rami rather appear to have an anterior-posterior relationship. In *Hyposaurus*
561 *rogersii* (NJSM 23368), the relative position of each ramus evolves along the axial skeleton so that
562 their relationship is vertical anteriorly (reminiscent of the diapophyseal and parapophyseal processes
563 of the cervicals), and changes to horizontal posteriorly. These evolving arrangements are also reflected
564 on the proximal end of the thoracic ribs in *Hyposaurus rogersii* (NJSM 23368) and *Congosaurus bequaerti*.
565

566 The neural spine of both Th6 and Th7 are similar in size (Th6 may have a portion of the tip cut off),
567 and display the decreasing trend initiated in Th5 (see table 4). Their shape resembles that of the other
568 thoracics in being rather elongated, with the anterior portion of the tip being lower than the posterior part.
569 This looks like the extremity of a katana-blade. However, while the anterior thoracics did entirely look like
570 a blade due to their almost parallel anterior and posterior outlines, the middle thoracics show a rupture of
571 angle along the anterior outline. Indeed, at almost half of its total length, the anterior surface of the neural
572 presents a corner which gives a bent look to the neural. Unfortunately, the original orientation of the
573 neural cannot be assessed. The neural of Th6 also reveals the existence of a wide posterior notch running
574 along its full height (wider than the one suggested in Th1 but about the same as Th5). The existence of
575 such indentation most probably allowed some extended dorsoventral movement. The posterior notch is
576 wider, and was probably also deeper, just in between the postzygapophyses.
577

578 Th7 is extremely flattened dorsoventrally, with the ventral part of the centrum cut off. In Th6 the
579 prezygapophysis facets are mainly oriented dorsally but it seems that there is a small anterior component.
580 Their tilting angle of both prezygapophysis does not match due to conservation issue: the left one is tilted
581 at about 34° from the horizontal plane and the right one is steeper, with an angle of 42°. It would seem
582 that none of these values reflect the true angle of the prezygapophysis. The right postzygapophysis does
583 not bear any visible sign of deterioration, but its position has certainly been altered as well (even slightly).
584 Its facet is mainly oriented ventrally with a small posterior component; it shows an angle of more or less
585 41.7° with the horizontal plane. As opposed to Th3 and Th1, the dimension of the zygapophysis facets
586 are here small compared to the centrum: the greater axis of the prezygapophysis accounts for 37.75%
587 of the anterior height of the centrum (32.2% of the width) and that of the postzygapophysis makes up
588 31.86% of the posterior height of the centrum (28.7% of the width). The neural canal is partially visible
589 posteriorly and is wider than tall, almost twice as much with 10.78mm in height and 18.82 mm in width.
590 While Th3 and Th1 seemed to be rather close, this thoracic is probably situated quite a bit further from
591 them because of the zygapophyses. The neural spine and the hypapophysis would have helped resolving
592 such a case but are unfortunately missing.
593

594 **4.5 The posterior thoracic vertebra UF/IGM 31 Th8 and Th9**

595 The anterior-posterior sequence of the posterior thoracic vertebra is as follow: **UF/IGM 31 Th8** then
596 **UF/IGM 31 Th9**.

597
598 The shape and size of each vertebrae changes along the axial skeleton, and there are key features that
599 help identify them such as: the absolute and relative size of the lateral process, the shape and size of the
600 neural, and the absence of a hypapophysis (which characterized the more anterior portion of the axial
601 skeleton).

602 Focusing on the lateral process, the anterior ramus increases in length posteriorly so that it starts at
603 19% (Th3) and then reaches up to 61% (Th8) of the posterior ramus length. Hence, the absolute length of
604 both rami also differs for each vertebrae: both rami increase in length posteriorly up to a certain point
605 around the transition with the lumbar where their absolute dimensions are then reduced. Indeed, while
606 L1 shows the greatest ratio between the rami, both are also shorter than that of the directly surrounding
607 vertebra (*i.e.* the posterior and middle thoracics).

608 The size and shape of the neural spine, which is now a well known ordering character, is reduced
609 compared to the other thoracics. Indeed, the neural reaches 33.3mm for Th8, which represents 91.8%
610 of Th8 anterior facet's height (and 95.2% of its width) while these numbers were greater for the other

611 thoracics (see table 4 and table 7). Unfortunately, Th9 is missing its neural arch. Yet, the decreasing trend
 612 in the size of the neural spine is still going on posteriorly. The shape of the neural spine in Th8 mostly
 613 resembles the middle thoracics as its outline looks like a bent katana-blade: the anterior surface is firstly
 614 erected at angle of about 84° to the horizontal, then it decreases to 58°. The posterior surface shows
 615 nearly the same curve and also possesses a notch, but does not show any hypophene structure.

616
 617 In this portion of the axial skeleton, the centrum is not heart-shaped but has become rather round
 618 (*i.e.* shows similar height and width), with a slightly oval ventral extremity. The length of the centrum is
 619 increasing posteriorly from Th8 to Th9 (their crushed condition is different from the other thoracics and
 620 has here preserved the length).

621
 622 Based on the neural spine shape and size, and the absence of hypapophysis, Th8 resembles the thoracics
 623 of *Hyposaurus rogersii* (NSJM 23368) occupying the positions from 8 through 10. It is possible that Th8
 624 of *Cerrejonisuchus* occupied was of those positions as well. The last thoracic, Th9 seems to have been
 625 placed further posteriorly from Th8, and were not adjacent.

626
 627 To sum up, the transition from the middle to the posterior thoracics is achieved through a series of
 628 reductions, notably: the size of the neural and of the lateral process (both in length of the parapophyseal
 629 and diapophyseal processes, and in the dimensions of their articular facets).

630 4.6 The lumbar region

	Aa	Ap	Ba	Bp	C	D	E	Hyp_height
UF/IGM 31 L1	37.15	-	-	-	39.7	90.75	35.46	-
UF/IGM 31 L2	34.75	32.43	28.18	28.6	35.05	-	-	-

Table 8. Table depicting each thoracic vertebrae (ordered) and some measurements (part 1). 'A' represents the maximal height of the centrum (dorso-ventrally); 'B' represents the maximal width of the centrum (laterally); 'C' represents the anterior-posterior length of the centrum; 'D' represents the angle (whole number) that the neural forms with the horizontal. When the neural possesses a corner, the two angles are separated by a point; 'E' represents the height of the neural spine; and Hyp_height represents the maximal height of the hypapophyse. The lower case letters 'a' and 'p' stand for 'anterior' and 'posterior' respectively

	J	K	La	Lp	Ma	Mp	Qa	Qp
UF/IGM 31 L1	23.97	-	3.37	4.32	6.46	15.18	27.17	38.06
UF/IGM 31 L2	28.94	-	-	3.26	-	12.67	26.67	36.23

Table 9. Table depicting each lumbar vertebrae (ordered) and some measurements (part 2). 'J' represents the base width (antero-posterior) of the lateral process; 'K' represents the base height (dorso-ventral) of the lateral process; 'L' represents the height of the distal surface of the lateral process and is taken perpendicular to 'M'; 'M' stands for the greatest length of the distal surface (which may be tilted regarding the antero-posterior plane) of the lateral process; 'Q' represents the proximal-distal length of the corresponding ramus (either the anterior or posterior one) of the lateral process; The lower case letters 'a' and 'p' stand for 'anterior' and 'posterior' respectively.

	Oa	Op	Pa	Pp	Ga	Gp
UF/IGM 31 L1	-	10.5	-	6.83	-	-
UF/IGM 31 L2	-	-	-	-	-	-

Table 10. Table depicting each lumbar vertebrae (ordered) and some measurements (part 2). 'O' represents the longest axis of the elliptic surface of the corresponding pre- or postzygapophysis; 'P' represents the smallest axis of the elliptic surface of the corresponding pre- or postzygapophysis (and is usually perpendicular to the corresponding 'O'); 'G' refers to the angle (degree) between the horizontal plane (or coronal plane) and the corresponding pre- or postzygapophysis. The lower case letters 'a' and 'p' stand for 'anterior' and 'posterior' respectively.

631 The lumbar region is characterized by a series of traits: a short neural spine; overall short lateral
 632 process with great anterior ramus; existence of a ventral keel. Indeed, both L2 and L1 show locally a
 633 bump or a keel on the ventral side of the centrum. This feature was observed on *Hyposaurus rogersii*
 634 specimens (notably AMNH FARB 1416 & 2390, NJSM 12293, YPM VP.000380 & VP.000753; *pers.*
 635 *obs.*) and thus serves as an indicator of the lumbar region.

636
 637 The centrum has therefore changed slightly from the posterior thoracic region; the dorsal part of both
 638 facets is wider than the ventral part, which is in return pointed giving the impression of a shield. This

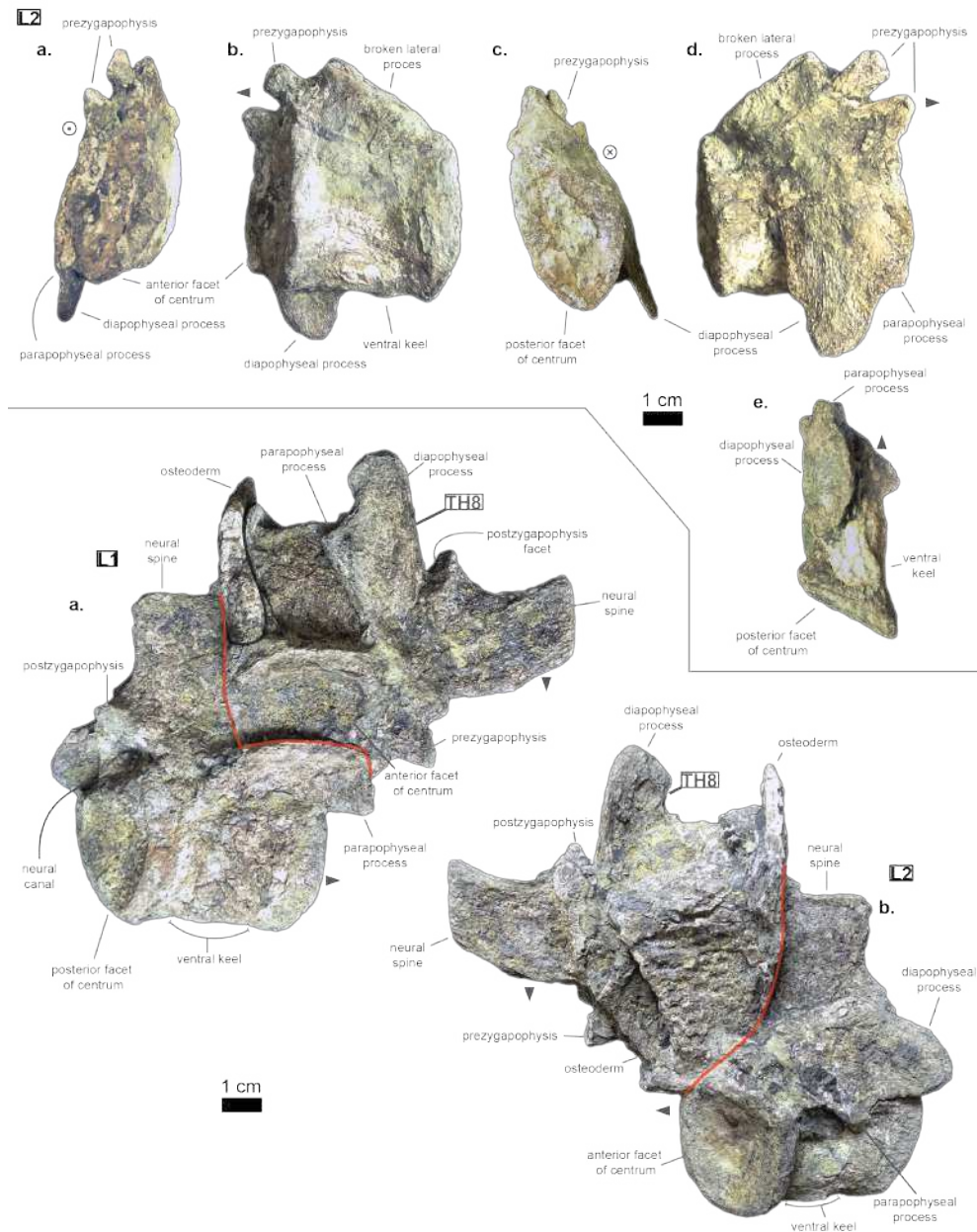


Figure 8. Lumbar of *Cerrejonisuchus improcerus* UF/IGM 31. **L1:** a. anterior view; b. left lateral view; c. posterior view; d. right lateral view. **L2:** a. right lateral view; b. left lateral view. Grey arrow points towards anterior.

	E/Ba(%)	E/Aa(%)	Mp/Qp(%)	Ma/Qa(%)	Qa/Qp(%)	Qp/Ba(%)
UF/IGM 31 L1	-	95.45	39.88	23.78	71.39	-
UF/IGM 31 L2	-	-	34.97	-	73.61	128.57

Table 11. Table depicting different ratio from the lumbar vertebra (ordered). ‘A’ represents the maximal height of the centrum (dorso-ventrally); ‘B’ represents the maximal width of the centrum (laterally); ‘E’ represents the height of the neural spine; ‘M’ stands for the greatest length of the surface (which may be tilted regarding the antero-posterior plane); ‘Q’ represents the proximal-distal length of the corresponding ramus (either the anterior or posterior one) of the lateral process. The lower case letters ‘a’ and ‘p’ stand for ‘anterior’ and ‘posterior’ respectively.

639 is probably influenced by the existence of a ventral keel. L2 is relatively smaller than L1 in the height
 640 of its facets and in the length of its centrum while it is not entirely certain that the length of L1 has not
 641 been increased by its crushed state. Due to its greater centrum, L1 was probably closer to the thoracic
 642 region (and Th9) than L2 was. Also, this ordering is supported by the size of the ventral keel which is
 643 more developed in L2 than in L1 (see fig. 8).

644 *Congosaurus bequaerti* (MRAC 1865 & 1896, holotype) and *Hyposaurus rogersii* (YPM VP.000380,
 645 YPM VP.000753 & YPM VP.000985) also bear ventral keels on their lumbar (and even the first sacral
 646 for YPM VP.000753 and YPM VP.000985), making it an important sorting feature. Yet, the middle
 647 thoracics of *Congosaurus bequaerti* (MRAC 1851 & 1874) possess a strong ventral ridge which is but a
 648 reminiscence of the hypapophysis.

650 As mentioned earlier, the neural spine is shorter in the lumbar region compared to the thoracic region.
 651 In L1 the neural spine accounts for 95.4% of the anterior facet’s height, and reaches 35.5mm in total (see
 652 tables 8 and 11). The posterior surface of L1 is clearly different from that of Th8, and its dorsal extremity
 653 is slightly broader which gives it a more squared look.

655 The anterior ramus is still following the increasing trend initiated in the thoracics: the length of the
 656 anterior ramus now reaches 71% of that of the posterior ramus in L1 while this number equals 73.6%
 657 in L2. However, their rami are reduced both in total length and size of their distal facets (especially the
 658 anterior one), which means that these were probably not able to support actual sturdy ribs like thoracics
 659 do. Yet these may have been connected to slender and short ribs, or some cartilaginous structure but it is
 660 currently unknown.

661 The overall reduction of the lateral process can be traced back to Th8. The distal extremities of the
 662 lateral processes of L2 and L1 take the shape of elongated ovals in the anteroposterior direction. The
 663 surface of those facets is no longer flat, but rather slightly convex.

664 The major difference between *Cerrejonisuchus* and modern crocodylians is that its lumbar are not
 665 fused into a synapophysis [de Souza, 2018] (e.g. *Mecistops cataphractus* RBINS 18374) but rather retain
 666 reduced but distinct distal facets.

668 The postzygapophysis is also smaller in this region of the skeleton compared to the thoracics (see ta-
 669 ble 9 and table 10). There are no evidence of a hypophene structure emanating from the postzygapophysis
 670 preserved in the lumbar [Stefanic and Nesbitt, 2019].

672 To sum up, the transition from the posterior thoracic vertebra to the lumbar region is easily identified
 673 thanks to the reduction in both the length and the thickness (dorsoventral) of the lateral process, plus in
 674 the size of their distal facets (which connect to the ribs). The overall shortening of the lateral process is
 675 proportionally less impressive than the two reductions just mentioned as it decreases more slowly.

677 4.7 The pelvic region

679 The sacral vertebra (see fig. 9) are typically bearing large but short lateral processes, each pointing
 680 towards each other in order to support the ilium. Indeed, the lateral process shows a sturdy base (see ‘J’
 681 and ‘K’ values in table 13, especially when compared to the centrum length) which flares out distally,
 682 forming again two distinct rami. In S1, the anterior ramus exceeds the posterior one and vice versa in
 683 S2 (see the ‘Q’ and ‘Qi’ values in table 14). The distal facets of the rami are clearly different from one

	Aa	Ap	Ba	Bp	C	D	E	Hyp_height
UF/IGM 31 S1	-	-	41.35	-	43.36	-	-	-
UF/IGM 31 S2	-	-	-	-	45.88	-	-	-

Table 12. Table depicting each sacral vertebrae (ordered) and some measurements (part 1). 'A' represents the maximal height of the centrum (dorso-ventrally); 'B' represents the maximal width of the centrum (laterally); 'C' represents the anterior-posterior length of the centrum; 'D' represents the angle (whole number) that the neural forms with the horizontal. When the neural possesses a corner, the two angles are separated by a point; 'E' represents the height of the neural spine; and Hyp height represents the maximal height of the hypapophyse. The lower case letters 'a' and 'p' stand for 'anterior' and 'posterior' respectively

684 another: the longest ramus (*i.e.* either the anterior one, here missing, in S1 or the posterior one in S2)
 685 is anteroposteriorly elongated but extremely flattened in the perpendicular direction; the shortest ramus
 686 takes the shape of an anteroposteriorly elongated triangle with a vertex pointing ventrally. These short
 687 rami are oriented towards the junction between S1 and S2 and were probably the main support for the
 688 ilium. The relatively short length of the lateral process compared to the centrum places the pelvic girdle
 689 closer to the axial skeleton than it is the case in metriorhynchids (*e. g. Metriorhynchus superciliosum*
 690 NMI F21731; *pers. obs.*).

691 The lateral process occupies almost the whole length of each centrum but it is not centered: the lateral
 692 process stems from the anteriormost portion of the centrum in S1 while it is located posteriorly in S2. The
 693 neural arch is missing on both sacrals, but it appears that the lateral process is entirely born by the centrum.
 694

695 The anterior facet of S1 slightly resembles the heart-shaped centrum of the anterior thoracics, it is
 696 however dorsoventrally flattened. Ventrally, a crest (or keel) is issued by the anterior facet but fades away
 697 before reaching the center of the centrum. S2, on the contrary, shows an oval-shaped posterior facet and
 698 does not bear any ventral keel.

	J	K	La	Lp	Ma	Mp	Q	Qi
UF/IGM 31 S1	30.51	14.38	-	16.53	-	21.13	-	30
UF/IGM 31 S2	32.39	-	11.49	-	19.44	17.13	51.68	27.63

Table 13. Table depicting each sacral vertebrae (ordered) and some measurements (part 2). 'J' represents the base width (antero-posterior) of the lateral process; 'K' represents the base height (dorso-ventral) of the lateral process; 'L' represents the height of the distal surface of the lateral process and is taken perpendicular to 'M'; 'M' stands for the greatest length of the distal surface (which may be tilted regarding the antero-posterior plane) of the lateral process; 'Q' represents the proximal-distal length of the greatest ramus, while 'Qi' concerns the shortest ramus of the lateral process; The lower case letters 'a' and 'p' stand for 'anterior' and 'posterior' respectively.

699

	E/Ba(%)	E/Aa(%)	Mp/Q(%)	Ma/Qi(%)	Q/Qi(%)	Q/Ba(%)
UF/IGM 31 S1	-	-	-	-	-	-
UF/IGM 31 S2	-	-	33.15	70.36	187.04	-

Table 14. Table depicting different ratio from the sacral vertebra (ordered). 'A' represents the maximal height of the centrum (dorso-ventrally); 'B' represents the maximal width of the centrum (laterally); 'E' represents the height of the neural spine; 'M' stands for the greatest length of the surface (which may be tilted regarding the antero-posterior plane); 'Q' represents the proximal-distal length of the greatest ramus, while 'Qi' concerns the shortest ramus of the lateral process. The lower case letters 'a' and 'p' stand for 'anterior' and 'posterior' respectively.

700

701 4.8 The caudal region

702 The sole caudal vertebrae retrieved, UF/IGM 31 Cd1 (see fig. 9), belongs to a rather anterior portion of
 703 the tail: its neural spine is long, vertical, and after a thick base, becomes rapidly finer distally; there are
 704 some evidence of a lateral process born on the neural arch; and the posterior facet has a ventral surface
 705 reserved for the haemapophysis.

706

707 Indeed, both *Hyposaurus rogersii* (NJSM 23368; *pers. obs.*) and *Congosaurus bequaerti* (Holotype,
 708 MRAC; *pers. obs.*) show an increase in the size of the neural spine in the anterior portion of the caudal
 709 region, which is even more emphasized as the sacrals and posterior caudals possess a shorter neural. Here,

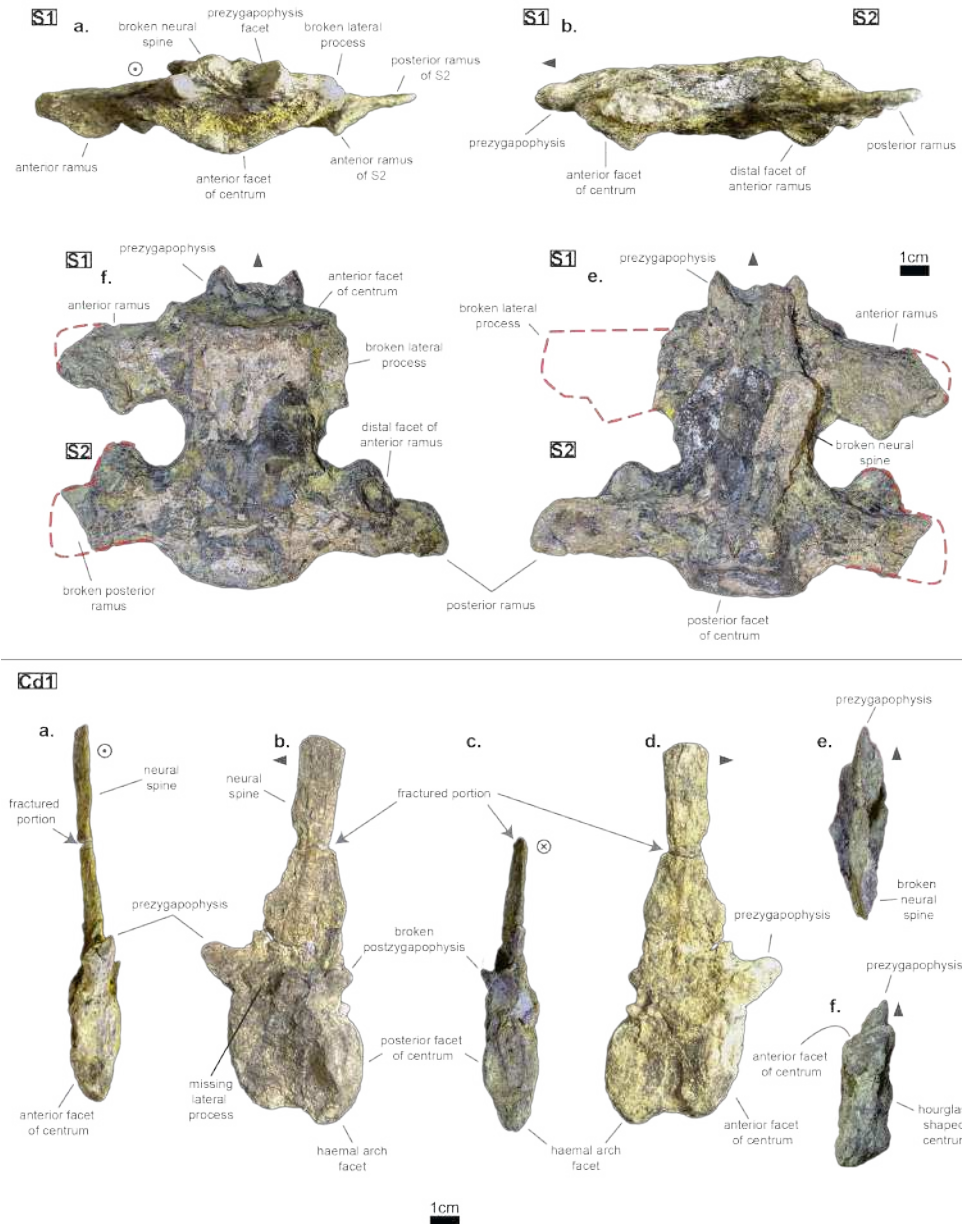


Figure 9. Sacrals and caudal of *Cerrejonisuchus improcerus* UF/IGM 31. **a.** anterior view; **b.** left lateral view; **c.** posterior view; **d.** right lateral view; **e.** dorsal view; **f.** ventral view. Grey arrow points towards anterior.

710 the caudal vertebrae of *C. improcerus* has a 71.2mm long neural for a 24.85mm long anterior facet, which
 711 gives a ratio value close to the anterior thoracics (see table 15) not unlike the hyposaurine dyrosaurids.
 712 Hence, it shows that basal dyrosaurids [Young et al., 2016] had already developed a massive tail. The
 713 neural spine of Cd1 also has its posterior and anterior surfaces parallel, giving it a vertical look, with
 714 a humped distal extremity like hyposaurine dyrosaurids (*i.e.* *Hyposaurus rogersii* NJSM 23368 and
 715 holotype of *Congosaurus bequaerti*; *pers. obs.*). Cd1 resembles the 9th caudal of *Congosaurus* (MRAC
 716 1892) with the swollen base of its neural rapidly slimming down distally, coupled with its relative vertical
 717 orientation. For this reason, the caudal of *Cerrejonisuchus* must have belonged somewhere around the
 718 10th position.

719

720 On the lateral sides of Cd1, around the base of the neural arch, are circular scars indicating the
 721 former position of the lateral process as in modern crocodylians [de Souza, 2018]. The lateral process
 722 usually fades away posteriorly along the caudal vertebra as seen in crocodylians (such as *Crocodylus*
 723 *porosus* Aquarium-Museum Liège R.G.294 or *Mecistops cataphractus* RBINS 18374; *pers. obs.*) or in
 724 *Congosaurus bequaerti* (Holotype, MRAC 1852 & 1879; *pers. obs.*).

725 There aren't any evidence of a hypophene structure preserved on this caudal.

726

	Aa	Ap	Ba	Bp	C	D	E	E/Aa(%)
UF/IGM 31 Cd1	24.85	31.72	-	-	34.32	90	71.21	286.56

Table 15. Table depicting each caudal vertebrae (ordered) and some measurements (part 1). 'A' represents the maximal height of the centrum (dorso-ventrally); 'B' represents the maximal width of the centrum (laterally); 'C' represents the anterior-posterior length of the centrum; 'D' represents the angle (whole number) that the neural forms with the horizontal. When the neural possesses a corner, the two angles are separated by a point; 'E' represents the height of the neural spine; and Hyp height represents the maximal height of the hypapophyse. The lower case letters 'a' and 'p' stand for 'anterior' and 'posterior' respectively

727

728 The facets of Cd1 are slightly larger dorsally than ventrally, and their outline resembles that of an
 729 apple. This type of shape is also found in the tail of other crocodyliformes such as thalattosuchians
 730 (*e.g.* *Metriorhynchus morelli* SMNS 10116 4th caudal; *pers. obs.*), hyposaurine dyrosaurids (*e.g.*
 731 *Congosaurus bequaerti* holotype, caudal numbered MRAC 1837; *pers. obs.*); or crocodylians (*e.g.*
 732 *Mecistops cataphractus* RBINS 18374 5th caudal; *pers. obs.*).

733 In this portion of the skeleton, the centrum is longer (anteroposteriorly) than it is high or wide. This
 734 feature is rather common among crocodyliforms, *e.g.*: *Mecistops cataphractus* (RBINS 18374; *pers.*
 735 *obs.*); *Terminonaris browni* (AMNH FARB 5844; *pers. obs.*); *Hyposaurus rogersii* (AMNH FARB 2390,
 736 NJSM 12293; *pers. obs.*); *Congosaurus bequaerti* (holotype, vertebrae numbered MRAC 1846; *pers.*
 737 *obs.*); or even in *Machimosaurus buffetauti* (SMNS 91415; *pers. obs.*).

738 4.9 Results

739 4.10 Ribs

740 The cervical ribs of *Cerrejonisuchus improcerus* (UF/IGM 31) are all still attached to the four cervical verte-
741ebra. Only the cervical C2 possesses the complete pair. The cervical ribs bear the typical crocodyliform
742shape in resembling a T in dorsal and ventral view, with the anterior portion shorter than the posterior one.
743

744 *Cerrejonisuchus improcerus* UF/IGM 31 only possesses two thoracic ribs, which belonged to a middle
745portion of the rib-cage. The thoracic ribs of UF/IGM 31 differ from those of *Congosaurus bequaerti*
746and *Hyposaurus rogersii* (NJSM 23368) in being relatively more convexe. In doing such, they appear to
747contrast with both the bracing systems observed in hyposaurine dyrosaurids and modern crocodylians.
748Indeed, the ribs of *Cerrejonisuchus improcerus* show a bending further distally than in hyposaurines,
749almost situated at the mid length of the bone which gives the bone an arched aspect (see fig. 10). The
750whole lateral outline of the rib is convex whereas in *Congosaurus bequaerti* (e.g. mid-thoracic rib MRAC
7511743 from the rib straightens distally after the bending. Indeed, in *Cerrejonisuchus* (UF/IGM 31) the
752concavity of the rib does not appear to change before and after the bending as opposed to *Crocodylus*
753*porosus* (Aquarium-Museum Liège R.G.294) or *Congosaurus bequaerti* (MRAC 1743) [Schwarz et al.,
7542009]. In the thoracic region, we hypothesized little to no dorsal deviation of the lateral process bearing the
755thoracic ribs. For these reasons, the bracing of the trunk of *Cerrejonisuchus* appears more cylindrical (see
756fig. 11) than in *Crocodylus porosus* (Aquarium-Museum Liège R.G.294), and also less elevated dorsally
757than in hyposaurine dyrosaurids [Schwarz et al., 2009]. It appears more similar to *Anteophtalmosuchus*
758*hooleyi* [Martin et al., 2016].
759

760 Compared to *Cerrejonisuchus improcerus* (UF/IGM 31), the thoracic ribs of *Anthracosuchus balrogus*
761(UF/IGM 67) are short and wide, with a shallower concavity. The ribs of *Anthracosuchus balrogus*
762(UF/IGM 67) also possess an enlarged distal extremity which would have been connected to a sternum
763of some kind. This difference stems from the absolute position of the ribs in the axial skeleton. Indeed,
764the ribs of *Anthracosuchus balrogus* (UF/IGM 67) ribs are more anterior than those of *Cerrejonisuchus*
765*improcerus* (UF/IGM 31) thanks to the presence of a neck on both the *capitulum* and *tuberculum*.
766

767 5 APPENDICULAR SKELETON ANATOMY

768 5.1 Humerus

769 The humerus of *Cerrejonisuchus improcerus* (UF/IGM 31, see fig. 12) is similar to those of *Hyposaurus*
770*rogersii* (NJSM 23368; *pers. obs.*) and *Congosaurus bequaerti* (MRAC 1813; *pers. obs.*) by presenting a
771straight shaft, and lacking the proximal torsion characteristic of crocodylians (e.g. *Mecistops cataphractus*;
772see also Stein et al. [2012]). The humerus of *Cerrejonisuchus improcerus* measures 146.8mm which
773accounts for 38.03% of the total skull length (i.e. snout tip to posterior-most portion of the quadrate) and
774for 83.41% of the femur's length (a similar ratio has been observed among terrestrial crocodyliforms
775such as *Tarsomordeo winkleri* [Adams, 2019]). This number (83.41%) falls under those observed for
776both *Congosaurus bequaerti* (MRAC 1813 & 1815 ; *pers. obs.*) and *Hyposaurus rogersii* (NJSM 23368,
777*pers. obs.*) with 96.32% and 94.47%, respectively. *Cerrejonisuchus improcerus* possessed a humerus
778shorter both proportionally and globally compared to the hyposaurine dyrosaurids (*Congosaurus bequaerti*
779MRAC 1813 reached 288.73mm and *Hyposaurus rogersii* NJSM 23368 is 188mm long, *pers. obs.*), which
780does not fit with the diagnostic limit of 90% set by Jouve et al. [2006] for Dyrosauridae. Instead, this trait
781(i.e. humerus attaining 90% of the femur's length) could become mainly indicative of derived dyrosaurids
782within Dyrosauridae, or could be lowered to 80% to include the basal *Cerrejonisuchus improcerus*.
783Unfortunately, the stylopodia were not completely recovered for the other two basal dyrosaurids (i.e.:
784*Anthracosuchus balrogus* & *Acherontisuchus guajiraensis*) from the same locality [Hastings et al., 2011,
7852014].

786 However, the 90% ratio of Jouve et al. [2006] can hardly be used as a diagnostic character of Dy-
787rosauridae within Crocodyliformes since many crocodylians also go beyond this limit, notably: *Alligator*
788*mississippiensis* (86-94%), *Alligator sinensis* (82-90%), *Caiman yacare* (76-94%), *Caiman crocodilus*
789(80-90%), *Crocodylus acutus* (89-96%), *Crocodylus moreletii* (90-96%), *Crocodylus palustris* (87-94%),
790*Crocodylus porosus* (89-92%), *Tomistoma schlegelii* (81-93%) [Iijima et al., 2018]. The wide range of
791number for some species bear witness to a sound intraspecific variation which is almost impossible to

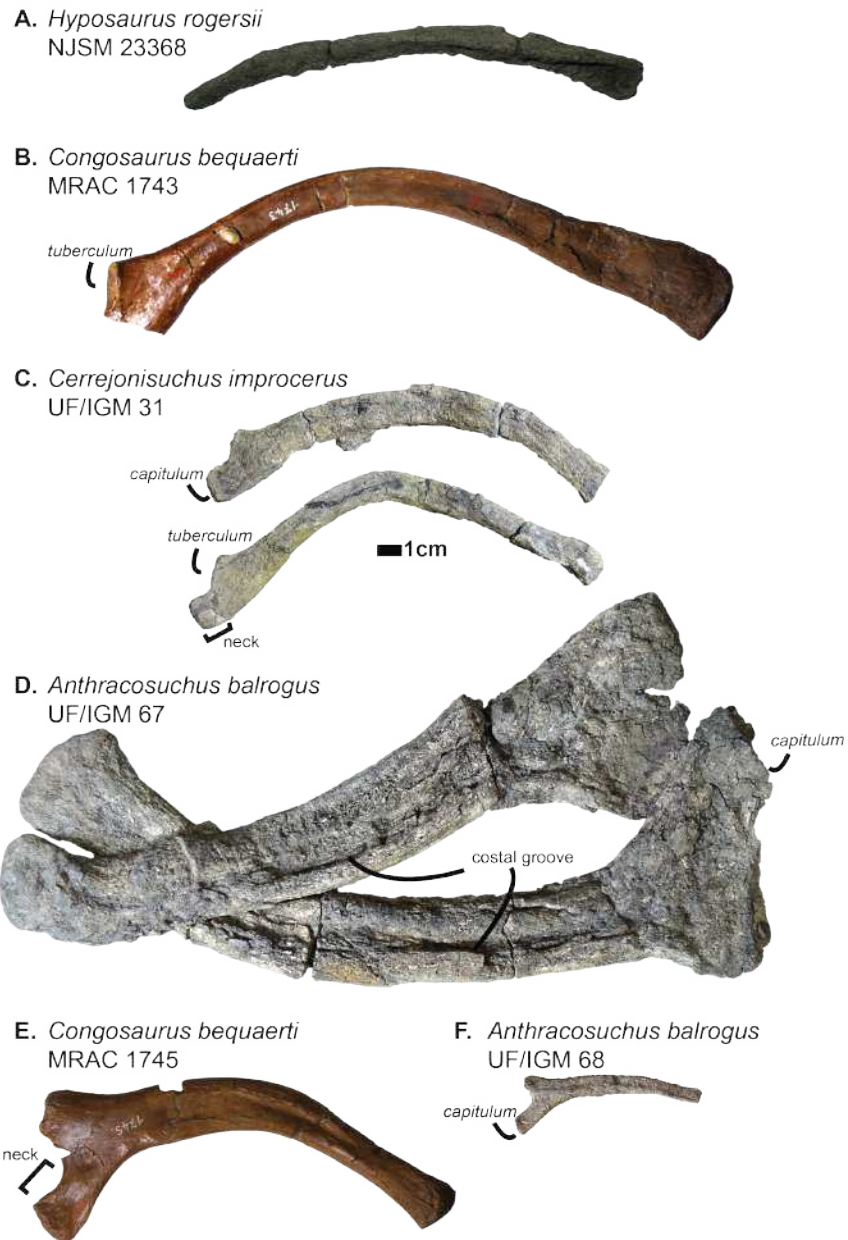


Figure 10. Scaled dyrosaurid thoracic ribs. Scale bar represents 1 cm. **A-C:** middle thoracic ribs, **D-F:** anterior thoracic ribs. **A:** *Hyposaurus rogersii* NJSM 23368; **B:** *Congosaurus bequaerti* MRAC 1743; **C:** *Cerrejonisuchus improcerus* UF/IGM 31; **D:** *Anthracosuchus balrogus* UF/IGM 67; **E:** *Congosaurus bequaerti* MRAC 1745; **F:** *Anthracosuchus balrogus* UF/IGM 68. Picture of *Hyposaurus rogersii* courtesy of Wayne Callahan.

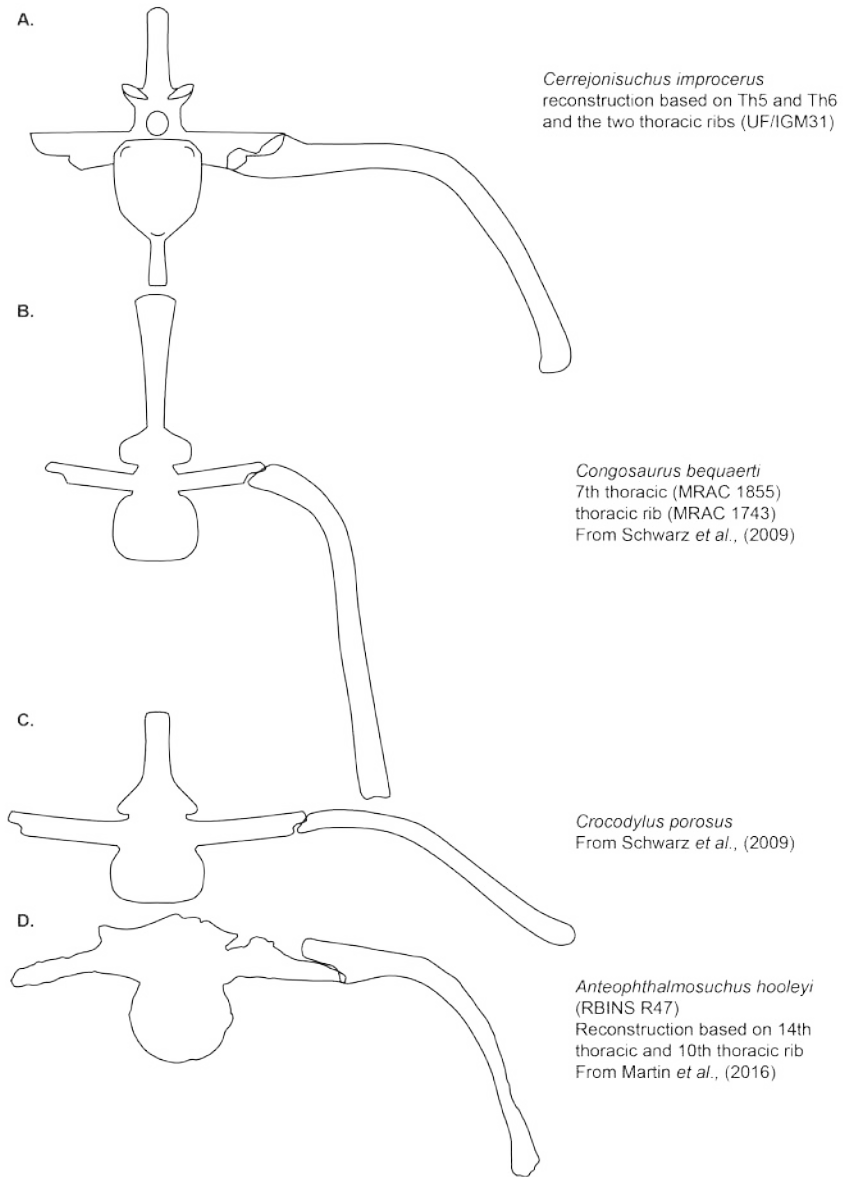


Figure 11. Test bracing (hypothetical reconstruction) of the trunk of *Cerrejonisuchus improcerus* based on the thoracic vertebrae UF/IGM 31 Th5 and Th6 and the two thoracic ribs. Comparison with reconstruction of the crocodylian, hyposaurine trunk bracing from Schwarz *et al.* [2009], and reconstruction of the goniopholid trunk bracing from Martin *et al.* [2016]. **A:** *Cerrejonisuchus improcerus*; **B:** *Congosaurus bequaerti*; **C:** *Crocodylus porosus*; **D:** *Anteophthalmosuchus hooleyi*.

792 take into account for fossil species.

793

794 *Cerrejonisuchus improcerus* is missing manus and pes, therefore the total limb length is restricted
 795 to the zeugopodium and stylopodium sum. Following this, the total forelimb and hindlimb lengths of
 796 *Cerrejonisuchus* reach 274.15 mm (right ulna and left humerus) and 327.96 mm (right tibia and left femur)
 797 respectively. This sound difference in length between the limbs of *Cerrejonisuchus* highly contrasts with
 798 the hyposaurine dyrosaurids, where forelimb and hindlimb are similarly proportioned [Denton et al., 1997]
 799 (e.g. *Hyposaurus rogersii* NJSM 23368 forelimb reaches 91.45% of hindlimb).

800

801 At its mid-length, the shaft presents an oval section whose greatest axis is parallel to the anterior-
 802 posterior direction; its measurements are: 20.33mm for the greatest axis vs 16.14mm for the minor axis.
 803 The deltopectoral process was located more anteriorly than in *Mecistops cataphractus* (for which it is
 804 more ventrally positioned). Unfortunately, the actual deltopectoral process is broken off and only its
 805 outline remains, which stretches up to 44mm which is almost 30% of the humerus' total length.

806

807 The humerus is also dorsoventrally flattened, as it can be easily seen from the squeezed distal condyles.
 808 In dorsal view, the overall shape of the bone is upright: its anterior surface forms roughly a straight line
 809 (since the deltopectoral crest is broken) while its posterior surface is slightly concave (which may appear
 810 accentuated by the flattened distal extremity). There is no proximal torsion of the humerus as in modern
 811 crocodylians [Stein et al., 2012]. In anterior view, the shaft is also upright with a slight sigmoid shape.
 812 This is a condition also observed in *Hyposaurus rogersii* (NJSM 23368, pers. obs.) and *Congosaurus*
 813 *bequaerti* (MRAC 1813; pers. obs.) meaning that the flattening of the bone has potentially little influence
 814 on the shape. However, there are other specimens of crocodyliforms where this sigmoid shape is even
 815 more accentuated in anterior and dorsal view, such as *Crocodylus rhombifer* (AMNH FARB 16697; pers.
 816 obs.), or *Hyposaurus rogersii* (AMNH FARB 2202; pers. obs.).

817

818 The anterior epicondyle (or AEC) of *Cerrejonisuchus improcerus* is partially broken in the anterior
 819 and ventral directions, but its distal outline is preserved and can be observed in dorsal view. In distal
 820 view, the anterior epicondyle greatly exceeds the size of the posterior epicondyle (or PEC), exactly like
 821 in *Congosaurus bequaerti* (MRAC 1813; pers. obs.). In *Hyposaurus rogersii* (NJSM 23368, YPM
 822 VP.000985; pers. obs.), this difference is present as well but is less marked so that both epicondyles may
 823 appear similar. In some crocodylians and crocodyliforms, there is practically no differences between the
 824 condyles as for example in: *Crocodylus niloticus* (NHMW 30900; pers. obs.), *Alligator sinensis* (NHMW
 825 37966; pers. obs.) or *Osteolaemus tetraspis* (NHMW 39338:2; pers. obs.) for the crocodylians (all of
 826 which are found in different environments); or in *Terminonaris browni* (AMNH FARB 5844; pers. obs.).
 827 There are, however, counterexamples such as *Caiman crocodilus* (NHMW 31137; pers. obs.), *Crocodylus*
 828 *rhombifer* (AMNH FARB 16697; pers. obs.) or *Mecistops cataphractus* (RBINS 18374; pers. obs.).

829

830 In dorsal view, the length of both epicondyle is almost the same with the PEC extending slightly
 831 more distally. This is also a feature observed on both *Hyposaurus rogersii* (NJSM 23368, pers. obs.)
 832 and *Congosaurus bequaerti* (MRAC 1813; pers. obs.). These differences in both epicondyles certainly
 833 influenced the positioning and the RO of the zeugopodia, but unfortunately *Cerrejonisuchus improcerus*
 834 is here missing the radius to further test this hypothesis (just like *Congosaurus bequaerti*, holotype
 835 pers. obs.). Besides, the ulna makes most of the elbow articulation as observed from crocodylians (e.g.
 836 *Mecistops cataphractus* RBINS 11839), and thus the modification of the proximal end of this bone could
 837 actually be the main influence over the humeral epicondyle shapes.

837

838 In dorsal view, *Cerrejonisuchus improcerus* shows a wider proximal end (encompassing all three
 839 tuberosities) than the distal one (with respectively 44.11mm and 28.33mm), whereas in *Congosaurus*
 840 *bequaerti* (MRAC 1813; pers. obs.) and *Hyposaurus rogersii* (NJSM 23368, pers. obs.) both distal
 841 and proximal ends are of similar width. The proximal end of those humeri (i.e. the aforementioned *C.*
 842 *improcerus*, *C. bequaerti* MRAC 1813 and *H. rogersii* NJSM 23368, YPM VP.000985; pers. obs.) are
 843 composed of three tuberosities which are observable on the dorsal side of the articulation. On their ventral
 844 side, the proximal articulation is however concave, thus giving the look of an arrowhead in proximal view
 845 like many other crocodyliforms (e.g. *Alligator sinensis* NMW 37966; *Dacosaurus maximus* SMNS 8203
 846 or *Terminonaris browni* AMNH FARB 5844; pers. obs.).



Figure 12. Left humerus and right ulna of *Cerrejonisuchus improcerus* UF/IGM 31. a. anterior view; b. posterior view; c. proximal view; d. distal view; e. dorsal view; f. ventral view. Grey arrow points towards anterior.

847 Still in anterior view, the anterior capitular tuberosity (*i.e.* ACT) and the dorsal capitular tuberosity (*i.e.*
 848 DCT) of *Cerrejonisuchus improcerus* both have their peak anteriorly oriented, while that of the posterior
 849 capitular tuberosity (*i.e.* PCT) is strictly posterior. The DCT is mainly responsible for the articulation of
 850 the humerus with the scapular girdle, and for this reason it is the biggest of the three tuberosities. The
 851 DCT is of similar dimensions (regarding the other tuberosities) in other crocodyliforms, as for example in
 852 *Alligator sinensis* (NMW 37966; *pers. obs.*) or in *Terminonaris browni* (AMNH FARB 5844; *pers. obs.*).
 853 It is however much more protruding in *Hyposaurus rogersii* (AMNH FARB 2202, 19205 ; *pers. obs.*),
 854 *Congosaurus bequaerti* (MRAC 1813; *pers. obs.*) or in some other crocodyliforms such as *Crocodylus*
 855 *niloticus* (NHMW 30900; *pers. obs.*) or *Osteolaemus tetraspis* (NHMW 39338:2; *pers. obs.*).

856 The PCT is also protruding posteriorly, thus exaggerating the convex shape of the posterior surface of
 857 the bone. Conversely, the ACT does not really protrude anteriorly and is undoubtedly the smallest of the
 858 three proximal capitular tuberosities.

859 5.2 Ulna

860 The only preserved ulna of *Cerrejonisuchus improcerus* (see fig. 12) unfortunately belongs to the opposite
 861 member of the only preserved humerus: it is a right ulna. It is recognizable thanks to the posteroventral
 862 facet of the proximal extremity which meets with a portion of the radius. The total length of the ulna
 863 measures 127.35mm, which is almost as long as the left humerus (thus the ulna accounts for 86.75% of
 864 the humerus). This proportional length could be a more terrestrial feature, similarly to what is observed
 865 among Crocodylia [Iijima et al., 2018]. The ulna of both *Congosaurus bequaerti* (MRAC 1816; *pers. obs.*)
 866 and *Hyposaurus rogersii* (NJSM 23368, *pers. obs.*) are proportionally shorter than that of *Cerrejonisuchus*
 867 as they respectively reach 74.1% and 73.9% of their corresponding humerus.

868 The ulna of *Cerrejonisuchus improcerus* is dorsoventrally flattened and is thus the thickest in the
 869 anterodorsal plane. The proximal extremity is 29.25mm wide (dorsoventrally) and 11.59mm thick in the
 870 perpendicular direction. Its distal extremity reaches 14.85mm in the anteroposterior plane, and is 2.95mm
 871 thick dorsoventrally. It is difficult to address the degree of flattening of the bone, but since the proximal
 872 extremity shows a subtriangular shape it is more likely that the ulna of *Cerrejonisuchus improcerus*
 873 resembled those of *Congosaurus bequaerti* (MRAC 1816; *pers. obs.*) and *Hyposaurus rogersii* (NJSM
 874 23368, *pers. obs.*): *i.e.* the ulna must have been relatively flat distally but thicker proximally. It is a trait
 875 which appears to be shared among some crocodyliforms at least (*e.g.* *Mecistops cataphractus* RBINS
 876 18374, *Alligator sinensis* NMW 37966, *Osteolaemus tetraspis* NMW 39338:2; *pers. obs.*) although
 877 thalattosuchians do not seem to show this feature (*e.g.* *Platysuchus multiscrobiculatus* SMNS 9930; *pers.*
 878 *obs.*). Yet, it is likely that the ulna of *Cerrejonisuchus improcerus* may have not been as expanded in the
 879 dorsoventral plane as the derived dyrosaurids [Schwarz et al., 2009] or modern crocodylians as mentioned
 880 above.

882 In anterior view, the ulna takes an atypical sigmoid shape where the shaft is protruding anteriorly at
 883 more-or-less one-third of the distal extremity. Indeed, this shape is unlike those of *Congosaurus bequaerti*
 884 (MRAC 1816; *pers. obs.*) and *Hyposaurus rogersii* (NJSM 23368, *pers. obs.*) where the ulna possesses a
 885 rather straight shaft (*i.e.* anterior and posterior surfaces not undulating), with a slight and general dorsally
 886 curved trend (more emphasized at the proximal extremity).

887 Yet, a similar sigmoid shape to *C. improcerus* can be found in other crocodyliforms, such as the
 888 goniopholid *Anteophtalmosuchus* [Martin et al., 2016], the baurusuchid *Pissarrachampsia sera* [Godoy
 889 et al., 2016] or the teleosaurid *Steneosaurus bollensis* (SMNS 9428, 15712a; *pers. obs.*) but with a lesser
 890 intensity. Still, it does not appear as a common shape among dyrosaurids (*i.e.* *C. bequaerti* MRAC 1816;
 891 *Hyposaurus rogersii* NJSM 23368; *pers. obs.*) or crocodylians (*e.g.* *Mecistops cataphractus* RBINS
 892 18374, *Alligator sinensis* NMW 37966, *Osteolaemus tetraspis* NMW 39338:2; *pers. obs.*).

894 As mentioned earlier, the proximal articulation of the ulna takes the overall shape of a triangle. In
 895 ventral view, the proximal condyle almost looks like a heart whose lower part (*i.e.* the area encompassing
 896 the pointed tip) which met with the radius is well developed as in the baurusuchid *Pissarrachampsia*
 897 *sera* [Godoy et al., 2016] or in the crocodylian *Mecistops cataphractus* (RBINS 18374; *pers. obs.*).
 898 This surface is not as expanded in *Hyposaurus rogersii* (NJSM 23368, *pers. obs.*), and is even less in
 899 *Congosaurus bequaerti* (MRAC 1816; *pers. obs.*) in which most of the proximal articulation of the ulna
 900 was likely reserved to meet the humerus.

901 The anterior and posterior protuberances, which make the top two rounded tips of the heart in ventral
 902 view, also show a dorsal depression between them that can be observed easily in proximal view. In dorsal
 903 view though, the depression does not expand much, which could or could not be a consequence of the
 904 flattening. Besides *Hyposaurus rogersii* (NJSM 23368, *pers. obs.*) does not show any cavity on any
 905 side of its ulna, while *Congosaurus bequaerti* (MRAC 1816; *pers. obs.*) bears an important hollow area
 906 similar to *C. improcerus* on its dorsal side.

907 5.3 Femur

908 The right femur of *Cerrejonisuchus improcerus* has not been recovered.
 909 The left femur of *Cerrejonisuchus improcerus* (see fig. 13) displays the typical sigmoid silhouette
 910 [Romer, 1923] found in many other crocodyliforms (*e.g.* *Hyposaurus rogersii* NJSM 23368, *Cerrejon-*
 911 *isuchus improcerus* MRAC 1815 & 1817, *Pelagosaurus typus* SMNS 80065, *pers. obs.*; *Wahasuchus*
 912 *egyptensis* [Saber et al., 2018], *Pissarrachampsia sera* [Godoy et al., 2016], *Mecistops cataphractus*
 913 RBINS 18374). This S-shape is mostly apparent in dorsal and ventral view since the bone is flattened
 914 dorsoventrally. It is therefore difficult to assess the degree of curvature in anterior or posterior view, yet a
 915 slight V-shape can be observed. This kind of shape is also found on both femora of *Hyposaurus rogersii*
 916 (NJSM 23368), and is accentuated by both the size of the fourth trochanter on the ventral side of the bone,
 917 and the corresponding dorsal surface which forms a slight depression.

918 The femur of *Cerrejonisuchus improcerus* shows a strong sigmoid shape compared to *Congosaurus*
 919 *bequaerti* (MRAC 1815 & 1817), but is similar to *Hyposaurus rogersii* (NJSM 23368). However, it is not
 920 as pronounced as it is for *Acherontisuchus guajiraensis* (UF/IGM 39), another al dyrosaurid from the
 921 same locality [Hastings et al., 2011]. Indeed, both extremities of the femur of *guajiraensis* (UF/IGM
 922 39) are protruding further away from the shaft than those of *C. improcerus* (UF/IGM 31). Yet both femora
 923 (from *i.e.* *C. improcerus* UF/IGM 31 & *A. guajiraensis* UF/IGM 39) are dorsoventrally flattened, which
 924 proves that the compaction had little influence over the general shape of the bone (it only emphasized it).
 925

926 In lateral (dorsal) view, the proximal head of the femur of *C. improcerus* shows a strongly rounded
 927 (convexe) outline, with a moderately impressive anterior protrusion which is here emphasized thanks to
 928 the presence of an anterior underlying depression (which is also partially responsible for highlighting the
 929 'V-shape' in anterior view). In anteroposterior view, the femoral head does not have a convex outline (like
 930 *H. rogersii* NJSM 23368 or *Hyposaurus sp.* DGM 803-R [de Souza, 2018], or *A. guajiraensis* (UF/IGM
 931 39) lesser extend) nor flat one (like *C. bequaerti* MRAC 1815 & 1817), but has the shape of a sheared
 932 og which appears unique to *Cerrejonisuchus improcerus* (UF/IGM 31). It is not known if there was
 933 a deep cavity on the ilium to meet with the femur's requirements, but such a rounded shape must have
 934 positively impacted the anterodorsal range of motion of the bone at the hip. However, regardless of the
 935 diagenetic flattening, the femoral head is not as smoothly curved dorsoventrally and may have inhibited
 936 some dorsal extension compared to a hypothetical perfectly round head. Comparatively, the femoral
 937 heads of *H. rogersii* (AMNH FARB 19204, 2202, NJSM 23368) and more importantly *A. guajiraensis*
 938 (UF/GM 39) show a strong anterior protrusion. This can however be partially explained through a more
 939 intensely sigmoid shape of the bone (*i.e.* the posterior surface of the femur is convexe for *H. rogersii*
 940 and *A. guajiraensis*, whereas it is straight for *C. improcerus*). A fragmentary femur (DGM 803-R) from
 941 the Upper Cretaceous of New Jersey referred to *Hyposaurus* [de Souza et al., 2019] also possesses a
 942 major anterior protrusion whose intensity is situated between *H. rogersii* (AMNH FARB 19204, 2202,
 943 NJSM 23368) and *A. guajiraensis* (UF/IGM 39), so that intraspecific variations cannot be ruled out to
 944 explain this phenomenon as well. Just like *H. rogersii*, *C. bequaerti* represents another pole: its femora
 945 (MRAC 1815 & 1817) show an even lesser protruding femoral head than *C. improcerus* (UF/IGM 31)
 946 along with a lesser sigmoidal shaft (altogether giving the look of a straighter femur for *C. bequaerti*).

947 An example of a wide, convex and strongly protruding femoral head can be found within *Crocodylus*
 948 *rhombifer* (AMNH FARB 16710), which also happens to be the most terrestrial modern crocodylian.
 949

950 The distal capitula of the femur indeed appear, as they are not complete, strongly asymmetrical:
 951 the posterior capitulum is greater (in length and width) than the anterior one (base used as reference),
 952 but also extends more distally (which is a trait one would expect from a sprawling animal, [Nyakatura
 953 et al., 2019]). Both capitula are well curved distally into a half-circle (of about 18mm each in height),
 954 which gives room for an extended range of motion with the tibia. *Cerrejonisuchus improcerus* could,

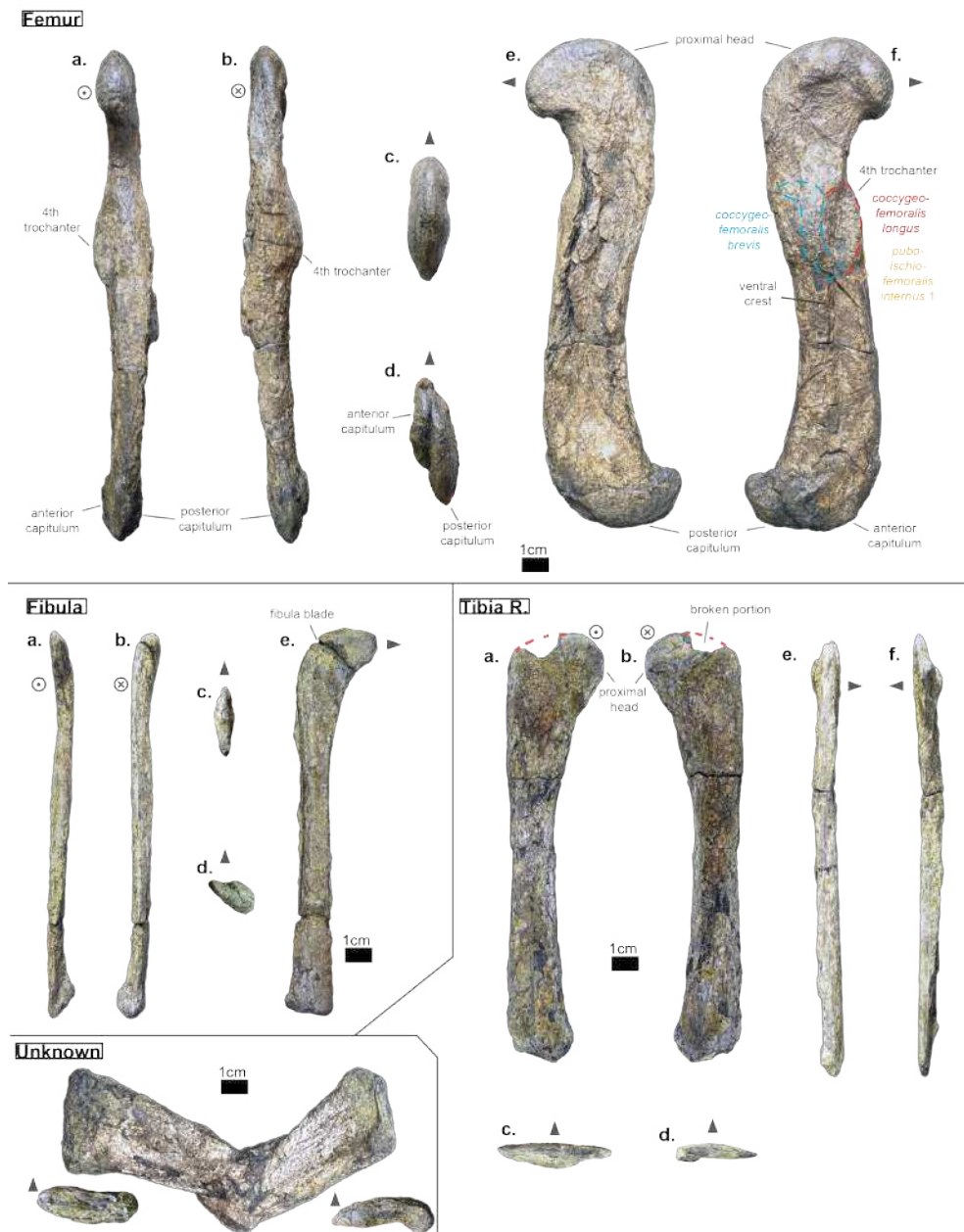


Figure 13. Left femur, left fibula and right tibia of *Cerrejonisuchus improcerus* UF/IGM 31. Mysterious bone featured in the bottom left corner. a. anterior view; b. posterior view; c. proximal view; d. distal view; e. dorsal view; f. ventral view. Grey arrow points towards anterior.

955 theoretically, rely on this articulation for effective land trips. Likewise, *Congosaurus bequaerti* (MRAC
 956 1817) and *Hyposaurus rogersii* (NJSM 23368) possess high and rounded distal capitula. However in
 957 *Congosaurus* the anterior capitulum is longer but thinner than the posterior one, and in *Hyposaurus* the
 958 posterior capitulum is actually shorter than the anterior one, but wider. Strangely, *Crocodylus rhombifer*
 959 (AMNH FARB 16710) shows a distribution similar to *C. improcerus* between its capitula (*i.e.* large
 960 posterior capitulum, short anterior one). Unfortunately, the femur of *Acherontisuchus guajiraensis* is
 961 missing the anterior capitulum. Another major feature of *C. improcerus* (UF/IGM 31) is the absence of a
 962 well defined intercapitular fossa separating the capitula dorsally while showing a clear sulcus running
 963 all the way dorsoventrally between the capitula. Even though the bone is broken in this area (*i.e.* the
 964 dorsal-most part of the distal articular surface is missing), there are no evidence on the surface of the femur
 965 indicating a deep dorsal indentation of the articular surface. Therefore, the trochlea of *C. improcerus*
 966 may have been slightly dorsally positioned, which is a trait found namely in *Hyposaurus rogersii* (YPM
 967 VP.000753, holotype of previous *H. natator* as proposed by Troxell [1925] but now a junior synonym of
 968 *H. rogersii* according to Parris [1986]; NJSM 23368) or *Pissarrachampsia sera* [Godoy et al., 2016]. There
 969 are other crocodyliforms who have their trochlea more centrally positioned, and thus show well developed
 970 dorsal and ventral intercapitular fossa *e.g.*: *Crocodylus rhombifer* AMNH FARB 16710; *Cerrejonisuchus*
 971 *improcerus* MRAC 1815; *Mecistops cataphractus* (RBINS 18374).

972
 973 The femur of *Cerrejonisuchus improcerus* measures 176mm long (distal-proximal length), which
 974 accounts for almost 120% of the humerus' length. The hyposaurine dyrosaurids possess comparatively
 975 a greater femur: those of *Congosaurus bequaerti* (MRAC 1817 & 1815; *pers. obs.* plus Jouve and
 976 Schwarz [2004]) reach about 299mm while that of *Hyposaurus rogersii* (NJSM 23368) measures 200mm,
 977 thus respectively representing 103.9% and 106.3% of their own humerus' length (which is less than
 978 *Cerrejonisuchus improcerus*). *Acherontisuchus guajiraensis* (UF/IGM 39) [Hastings et al., 2011], an
 979 other basal dyrosaurid from the same formation as *C. improcerus* (Cerrejón Formation) shows a femur
 980 of intermediate size, yet far greater than *C. improcerus*, with 248mm in length. It appears evident that
 981 *Cerrejonisuchus improcerus* was a relatively small-bodied dyrosaurid, but seemingly less aquatic than
 982 *Acherontisuchus guajiraensis* according to Hastings et al. [2011].

983
 984 Like *H. rogersii* (NJSM 23368), *C. bequaerti* (MRAC 1817) and *Acherontisuchus guajiraensis*
 985 (UF/IGM 39), the fourth trochanter of *C. improcerus* is mainly located on the ventral side of the bone. It is
 986 a rather well developed feature among dyrosaurids: the base area of the structure reaches about 422mm²
 987 for *C. improcerus* (UF/IGM 31), 692mm² for *A. guajiraensis* (UF/IGM 39), 251mm² for *H. rogersii*
 988 (NJSM 23368), and 1077mm² for *C. bequaerti* (MRAC 1815). Both the basal and the hyposaurine
 989 dyrosaurids show a depression anterior to the fourth trochanter, the paratrochanteric fossa, which either
 990 hints for a more developed *m. caudofemoralis* [Romer, 1923, Schwarz et al., 2009] (which who takes
 991 roots in the fossa), or a more developed *pubo-ischio-femoralis internus* [Romer, 1923], or both altogether
 992 sharing the fossa. *Congosaurus bequaerti* possesses by far the largest fossa (about 615.8mm²), but
 993 *Cerrejonisuchus improcerus* shows the longest one proportionally to the total length of the femur (see
 994 table 16).

995 5.4 Tibia

996 The bone referred to as the left tibia is too altered to bear any representative structures. This bone greatly
 997 differs from the right tibia both in shape and size of the proximal and distal extremities; the shaft of this
 998 bone is also much thicker than that of the right tibia. For these reasons, we believe it may not belong to
 999 *Cerrejonisuchus improcerus* (UF/IGM 31). ~~It is figured on fig. 13.~~

1000
 1001 The right tibia of *Cerrejonisuchus improcerus* extends as far as 151.96 mm in length, which is about
 1002 86.3% of the femur's length. The tibia of *Hyposaurus rogersii* (NJSM 23368) measures 158 mm which is
 1003 79% of the femur's length. The right tibia of *Congosaurus bequaerti* (MRAC 1808 & 1818) is unfortu-
 1004 nately incomplete, yet the tibia would have measured in between 240mm and 250mm which corresponds
 1005 to 80% and 83.3% respectively (a ratio close to *H. rogersii*). Therefore *Cerrejonisuchus improcerus*
 1006 possessed a rather long tibia compared to its femur, making it higher on its legs proportionally to its size.

1007
 1008 The overall shape of the tibia of *Cerrejonisuchus improcerus* resembles that of *Congosaurus bequaerti*

Species	Paratrochanteric area (mm ²)	Area trochanter/ paratrochanteric fossa	Femur length/ area fossa (mm ⁻¹)	Length femur / paratrochanteric fossa
<i>C. bequaerti</i> (MRAC 1815)	615.8	1077/615.8 = 1.748	299/615.8 = 0.48	299/37.41 = 7.99
<i>C. improcerus</i> (UF/IGM31)	169	422/169 = 2.49	176/169 = 1.04	176/25.32 = 6.95
<i>A. guajiraensis</i> (UF/IGM 39)	144.13	692/144.13 = 4.8	248/144 = 1.72	248/28.41 = 8.729
<i>H. rogersii</i> (NJSM 23368)	132.3	251/132.3 = 1.89	200/132.3 = 1.51	200/20.34 = 9.83

Table 16. Table showing ratios related to the 4th trochanter and the paratrochanteric fossa of several dyrosaurids.

(MRAC 1808 & 1818), *Hyposaurus rogersii* (NJSM 23368) and *Mecistop. cataphractus* (RBINS 18374): the shaft is straight and slender, the proximal extremity is wide, and the distal extremity splits into two asymmetrical condyles. The strongest identifying feature certainly is the combination of a flat anterodorsal surface and a concave posteroventral one, both creating a wide proximal extremity. The posterior portion of the proximal articular surface slightly extends towards the shaft: this is where it partially contacts the fibula proximally. The anterior portion of the proximal extremity is unfortunately partially broken off, but the articular surface is still not apparent on that side. Indeed, the proximal articular surface of the tibia is not flat but slightly tilted posteriorly. As the bone is strongly flattened anteroposteriorly, the actual shape of the proximal articulation is altered but still reflects the tuberosities on which the articulation with the femur took place.

The distal extremity of the bone splits into two uneven condyles where the posterior condyle extends more distally than the anterior condyle. Thus, the anterior condyle has its articular surface distally oriented while the posterior condyle is mainly posteriorly facing to meet with the corresponding surface of the fibula (which is therefore anteriorly facing).

5.5 Fibula

The fibula of *Cerrejonisuchus improcerus* measures 140.94 mm which is almost as long as the tibia (see fig. 13). This is unexpected as both bones are to display similar sizes if they are to be connected to the podial elements. The global shape of the fibula resembles that of an upside-down hockey stick: a long straight shaft plus a wide and flat proximal extremity reminding of a spatula. This last element is highly unusual as none of the fibulae of *H. rogersii* (NJSM 23368) are known to flare out so intensely (*C. bequaerti* MRAC 1814 is missing the proximal extremity). The diagenetic flattening of the bone can at best only be partially responsible. Besides the spatula-proximal end, the fibula of *C. improcerus* is vaguely similar to that of *H. rogersii* (NJSM 23368) and even to those of modern crocodylians (e.g. *M. cataphractus* RBINS 18374; *C. porosus* Aquarium-Museum Liège R.G.294; *C. niloticus* NMW 31137) in possessing a thin proximal end along with a wide distal end (whose orientations always differ slightly). The distal extremity of *C. improcerus* fibula is triangular in section, with a small portion of the articular surface extending towards the shaft in anterior view to meet with the distal part of the tibia.

5.6 Pubis

Both left and right pubic bones are preserved (see fig. 14). They possess an overall shape moderately unusual among crocodyliforms, like some thalattosuchians (e.g. *Suchodus cultridens* NHM VP R3804, *Platysuchus multiscrobiculatus* SMNS 9930), crocodylians (e.g. *Caiman crocodylus* NHMW 30900). Yet, there are some crocodyliforms like *Steneosaurus bollensis* SMNS 9428 that show a more similar shape to *Cerrejonisuchus improcerus*.

The pubis of *Cerrejonisuchus improcerus* (UF/IGM 31) also takes the shape of a distorted spatula since its distal extremity is rectangular and not triangular like *Caiman crocodylus* (NHMW 30900) or *Hyposaurus rogersii* (NJSM 23368). There are no gradual expansion of the shaft, which is rather elongated





Figure 14. Left and right pubis of *Cerrejonisuchus improcerus* UF/IGM 31. Right pubis is partially broken and located on the right side of the line. a. anterior view; b. posterior view; c. proximal view; d. distal view; e. medial view; f. lateral view. Grey arrow points towards anterior.

1046 and makes up for a little more than half the total length of the bone. The shaft is yet comparatively shorter
 1047 than in *Hyposaurus rogersii* (NJSM 23368). While the anterior part of the shaft is straight, the posterior
 1048 part is concave thus creating a ~~protuberant~~ peak at its intersection with the distal outline. Indeed, the
 1049 distal part of the pubis has anterior and posterior outlines exhibiting similar curvature: posterior outline is
 1050 convex and anterior one is concave. There is here a short and convex anteroventral surface ~~which~~
 1051 both anterior and posterior outlines, thus giving a rectangular look to the distal portion of the bone.

1052 On the lateral side of the bone, there is a shallow notch near the proximal end of the shaft which was
 1053 probably the attachment site for the *pubo-ischio-femoralis externus 1*. This muscle also covered most the
 1054 distal part on both sides [Romer, 1923].

1055 6 THE SKUL

1056 The s  of UF/IGM 31 (see fig. SI 5 in Supplementary Information), while not totally complete, strongly
 1057 resembles  that of the holotype UF/IGM 29 which is figured and extensively described in Hastings et al.
 1058 [2010]. ~~Still,~~ here the dorsal skull length of UF/IGM 31 reaches 386 mm from the tip of the snout
 1059 (premaxillae) to the quadrate, making it a ~~bigger~~ specimen than the holotype UF/IGM 29 [Hastings et al.,
 1060 2010], which is 299.5 mm long.
 1061

1062 7 SYSTEMATIC PALEONTOLOGY

1063 CROCODYLOMORPHA Walker, 1970

1064 CROCODYLIFORMES Hay, 1930

1065 MESOEUCROCODYLIA Whetstone and Whybrow, 1983

1066 DYROSAURIDAE de Stefano, 1903

1067 *Cerrejonisuchus improcerus* Hastings, 2010

1068 **Type species:** *Cerrejonisuchus improcerus* [Hastings et al., 2010]

1069 **Range:** Middle to late Paleocene of Colombia [Hastings et al., 2010]

1070 **Emended diagnosis:**

1071 We expanded the craniodental diagnosis of Hastings et al. [2010] with postcranial characters.

1072 *Cerrejonisuchus improcerus* (UF/IGM 31) shows these autapomorphic characters:

- 1073 - Each maxillary possesses 11 teeth, and 8 of those are anterior to the orbits [Hastings et al., 2010];
- 1074 - Fibula with extended proximal fibula blade, greatly protruding from the shaft;
- 1075 - Pubis with elongated, rectangular distal portion (rather than triangular in many crocodyliforms);
- 1076 - Ulna presenting double concavity (usually single concavity in crocodyliforms);
- 1077 - Proximal head of femur is round in dorsoventral views (whereas it is elliptic in hyposaurine; de Souza
 1078 et al. [2019]) and takes the shape of a Lancet arch in anteroposterior views;
- 1079 - Odontoid has an elliptic shape, with the greatest axis laterally oriented. Its height over width ratio is
 1080 much smaller than hyposaurine dyrosaurids with about 0.6 (*contra* 0.8 for *H. rogersii* and *C. bequaerti*);
- 1081
- 1082

1083 *Cerrejonisuchus improcerus* (UF/IGM 31) shows these unique combinations of characters:

- 1084 - Among Dyrosauridae, snout is the shortest with about 54-59% of the dorsal skull length [Hastings et al.,
 1085 2010];
- 1086 - Among Dyrosauridae, only one to possess a wide interfenestral bar which has a square shape in cross-
 1087 section with *Chenanisuchus* [Hastings et al., 2010];
- 1088 - Among Dyrosauridae, only one to possess a reduced fourth premaxillary tooth with *Phosphatosaurus*
 1089 (and possibly *Arambourgisuchus*) [Hastings et al., 2010];
- 1090 - In dorsal view, lacks a ‘festooned’ lateral margin of the snout thus differing from *Phosphatosaurus* and
 1091 *Sokotosuchus* among Dyrosauridae [Hastings et al., 2010];
- 1092 - Possesses a medio-laterally straight posterodorsal margin of the parietal, thus differing from *Hyposaurus*,
 1093 *Rhabdognathus*, *Atlantosuchus*, and *Guarinisuchus* among Dyrosauridae [Hastings et al., 2010];
- 1094 - Possesses well-developed occipital tuberosities, thus differing from *Chenanisuchus* and *Sokotosuchus*
 1095 among Dyrosauridae [Hastings et al., 2010];
- 1096

- 1097 - Skull is ornamented continuously across dorsal and lateral surfaces with no interruption across sutures,
 1098 and in addition the orbits are medially and dorsally placed all of which differ from *Chenanisuchus*
 1099 among Dyrosauridae. The position of the orbits most closely approximates that of *Dyrosaurus* among
 1100 Dyrosauridae [Hastings et al., 2010];
- 1101 - Teeth possess strait anterior carinae rather than twisted, thus differing from *Hyposaurus rogersii* among
 1102 Dyrosauridae [Hastings et al., 2010];
- 1103 - Among Dyrosauridae, long zeugopodia in relation to stylopodia (zeugopodia attaining >85% of the
 1104 length of the stylopodia), especially for the ulna as the opposed to 74% for *H. rogersii* and *C. bequaerti*);
 1105 - Short humerus shaft with wide proximal head but poorly developed proximal tuberosities (none of the
 1106 three tuberosities stand out);
- 1107 - Among Dyrosauridae, humerus proximodistal length attaining less than 90% of the femoral proximodistal
 1108 length (this value is >90% in all dyrosaurids for which this feature is known; Jouve et al. [2006]);
- 1109 - Among Dyrosauridae, the mesiolateral length of the lateral process (parapophyseal and diapophyseal
 1110 processes) in middle thoracics is the greatest in relation to the diameters of the centrum facets (>100%);
 1111 - The humerus possesses an extremely reduced posterior epicondyle;
- 1112 - Among Dyrosauridae, thoracic ribs are short and strongly arched;
- 1113 - Among Dyrosauridae, lumbar vertebra possess a ventral keel (shared with *Hyposaurus rogersii* and
 1114 *Congosaurus bequaerti*).

1115 8 MORPHOSPACE OCCUPATION

1116 Dyrosauridae, Crocodylia, and Thalattosuchia are dissimilar, occupying clearly separated areas of the
 1117 morphospace (see fig. 15). Even though some taxa share similar lifestyles, the three clades are clearly
 1118 separated along the first axis of the PCoA (which accounts for 23.9% of the relative eigenvalue) meaning
 1119 that this axis appears strongly influenced by the phylogenetic signal. While this was expected for
 1120 thalattosuchians, our results indicate that dyrosaurids also have a distinctive postcranial anatomy.

1121 The phylogenetic influence is less prominent along the second axis (which accounts for 14.2% of the
 1122 relative eigenvalue): Crocodylia and Dyrosauridae are still distinct from one another but are enclosed
 1123 within the range of Thalattosuchia. More precisely, dyrosaurids occupy the same range as metriorhyn-
 1124 choids (plus *Lemmysuchus obtusidens*) and thus cannot be simply discriminated; the hypothesis of existing
 1125 convergence between those two clades cannot be entirely ruled out and need to be further investigated.
 1126 For example, *Hyposaurus* has been considered to venture in the open-sea similarly to metriorhynchids,
 1127 while being able to easily wander over land [Buffetaut, 1978a, Denton et al., 1997]. In more recent
 1128 studies though, the hyposaurine lifestyle (including *Congosaurus*) was regarded as more similar to that of
 1129 teleosauroids [Schwarz et al., 2006, 2009] suggesting them as ambush predators instead of pursuit predator.

1130
 1131 The wide range of Thalattosuchia is essentially due to the Toarcian (late Early Jurassic) teleosauroid
 1132 *Platysuchus multiscrobiculatus* which is clearly separated from other thalattosuchians along the second
 1133 axis (see fig. 15). The other teleosauroid of the dataset, the Callovian *Lemmysuchus obtusidens* [Andrews,
 1134 1909, Johnson et al., 2017] is rather close to the metriorhynchoids but without being included in their
 1135 convex hull. This gap in morphospace occupation between *Platysuchus multiscrobiculatus* and *Lemmy-
 1136 suchus obtusidens* supports the idea proposed by Foffa et al. [2019] in which Teleosauroidea must be
 1137 split in two subclades: ‘T-subclade’ and ‘S-subclade’, grouping *Mycterosuchus nasutus*, *Aelodon priscus*,
 1138 *Bathysuchus megarhinus*, *Teleosaurus cadomensis*, *Platysuchus multiscrobiculatus*, ‘*Steneosaurus*’ *bre-
 1139 vior* plus a Chinese teleosauroid; and ‘*Steneosaurus*’ *bollensis*, ‘*Steneosaurus*’ *leedsii*, ‘*Steneosaurus*’
 1140 *larteti*, ‘*Steneosaurus*’ *herberti*, *Steneosaurus edwardsi*, *Lemmysuchus obtusidens*, *Machimosaurus buffe-
 1141 tauti*, *Machimosaurus mosae*, *Machimosaurus rex* and *Machimosaurus hugii* respectively [Foffa et al.,
 1142 2019].

1143 This chasm between *Platysuchus multiscrobiculatus* and *Lemmysuchus obtusidens* in the morphospace
 1144 also backs the results of Johnson et al. [2020], where *Platysuchus* is retrieved among Teleosauridae
 1145 (‘Family-T’) whereas *Lemmysuchus* is found within the new family Machimosauridae (‘Family-M’).
 1146

1147 At any rate, these preliminary results for thalattosuchians suggest the existence of an expected disparity
 1148 in the postcranial anatomy of teleosauroids. When Pierce et al. [2009] studied thalattosuchian skull dispar-
 1149 ity using geometric morphometrics, their results showed the opposite trend. The wide space occupation of
 1150 Thalattosuchia is not completely unexpected as thalattosuchians comprise highly differing morphologies

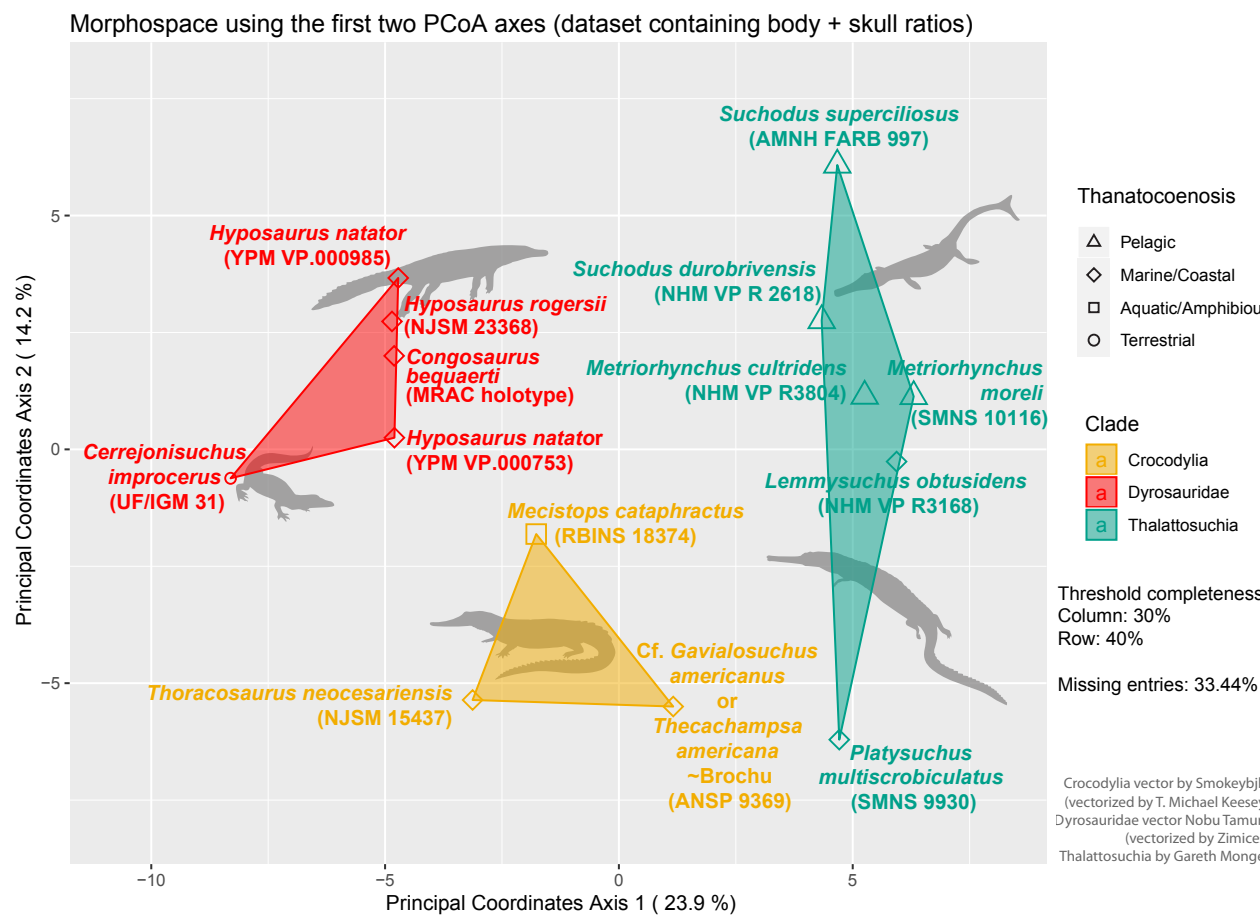


Figure 15. Morphospace representing dissimilarity between Dyrosauridae, Crocodylia and Thalattosuchia using the first two PCoA axes, and with the complete (skull+body) ratio dataset. Polygons demarcate families while colored symbols illustrate lifestyles.

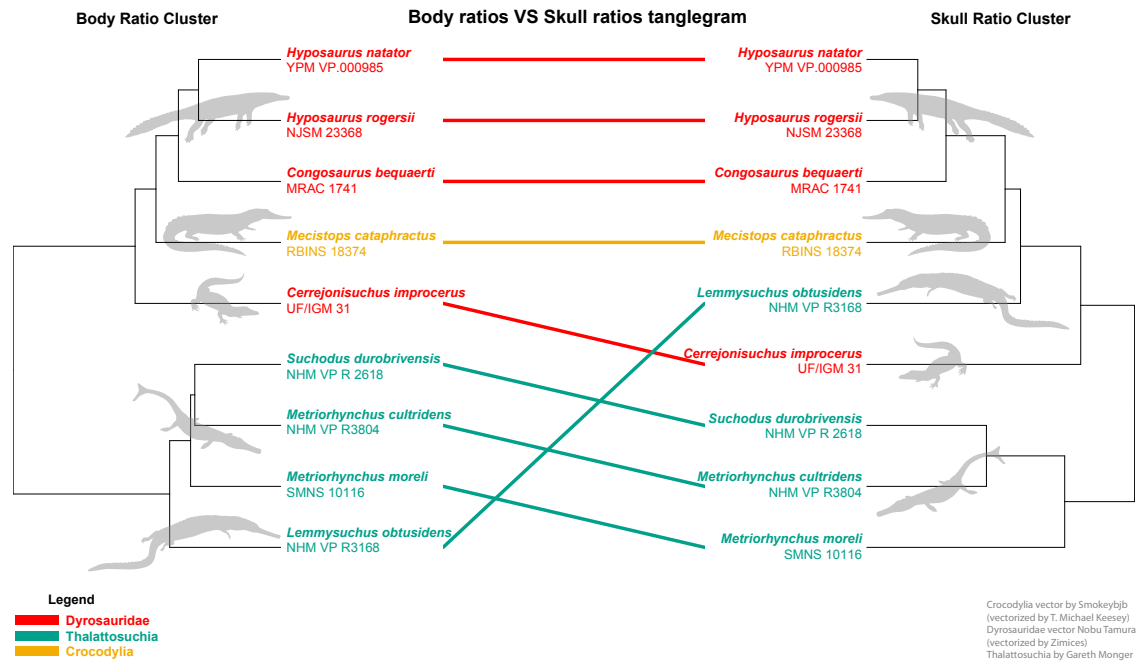


Figure 16. Tanglegram between the postcranial based cluster tree (left) and the cranial based cluster tree (right). Radically differing evolutionary histories are obtained for Dyrosauridae, Crocodylia, and Thalattosuchia.

1151 between and even within metriorhynchoids and teleosauroids due to highly different lifestyles [Buffetaut,
 1152 1981, Fernández and Gasparini, 2008, Young et al., 2010, Johnson et al., 2017, Wilberg et al., 2019].

1153

1154 Within Dyrosauridae, there is a clear demarcation between *Cerrejonisuchus* and all the other dy-
 1155 rosaurids.

1156

1157 Crocodylia is almost as dissimilar to Dyrosauridae than to Thalattosuchia, therefore it appears obvious
 1158 that modern crocodylians cannot account for extinct lineages, at least not entirely [Pierce et al., 2009].

1159 Within Crocodylia, a horizontal fronto-orbital (understand only depending on axis 2) can be traced isolating
 1160 *Mecistops* from *Gavialosuchus/Thecachamps* and *Thoracosaurus* which would either reflect phylogeny
 1161 (similarly to Thalattosuchia) between Crocodyloidae and Gavialoidea, a lifestyle demarcation, or a combi-
 1162 nation of both. In this case, phylogenetic and ecological signals are indistinguishable.

1163

1164 There seems to be no modularity between the skull and body ratio based datasets as the tanglegram
 1165 from fig. 16 reveals no major differences between both cluster dendrograms. Both postcranial and cranial
 1166 signals appear consistent. Though, the postcranial cluster more correctly reflects the phylogeny, thus
 1167 indicating that dyrosaurids do possess a distinctive postcranial anatomy.

1168 9 DISCUSSION

1169 9.1 Regionalization of the vertebral column in *Cerrejonisuchus* and *Congosaurus*

1170 Like Molnar et al. [2014], we took the assumption that mechanical constraints observed on modern
 1171 crocodylians apply to extinct forms. In *Congosaurus* and *Cerrejonisuchus*, the peak values of pre- and
 1172 postzygapophysis areas (see fig. 2 and fig. 4) are shifted more anteriorly along the axial skeleton than
 1173 it is for *Mecistops* (see fig. 3). The exact same phenomenon is observed with the zygapophysis angles
 1174 of *Congosaurus* and *Hyposaurus* (see fig. SI 3 in Supplementary). Therefore, it seems that the region-
 1175 alization of the vertebral column of *Cerrejonisuchus*, and hyposaurine dyrosaurids was different from
 1176 *Mecistops* and presumably other crocodylians. A rise in zygapophysis area could pinpoint increased
 1177 stiffness in those portions of the axial skeleton, as observed for *Crocodylus niloticus* [Molnar et al., 2014].
 1178 Besides, the increase in zygapophysis area in *Congosaurus bequaerti*, which would inhibits flexion in any
 1179 orientation, is positively correlated to a decrease in the inclination (in relation to the coronal plane) of

1180 the said zygapophysis, presumably resulting in a greater mediolateral, but not dorsoventral, flexibility
 1181 [Molnar et al., 2014]. In *Crocodylus niloticus*, vertically oriented zygapophyses (*i.e.* a high inclination
 1182 angle) are known to enable greater dorsoventral flexion [Molnar et al., 2014]. In parallel, as observed
 1183 for *Hyposaurus*, the high inclination angle of the zygapophyseal facets with the coronal plane would
 1184 inhibit increased lateral flexion, but not vertical flexion [Langston, 1995, Denton et al., 1997]. Yet, in
 1185 *Congosaurus* the mediolaterally stiffest portion of the cervicothoracic region appears limited to the last
 1186 cervicals (C8-C9, see fig. SI 3 in Supplementary Information), and does not encompass the anterior
 1187 thoracics as for *Hyposaurus* (see also [Langston, 1995]). Based on thoracics only, *Cerrejonisuchus* seems
 1188 to follow the same trend as *Congosaurus*. Conversely, there is no variation in the neck of *Mecistops*. This
 1189 suggests the existence of difference in flexibility among hyposaurine taxa, with *Hyposaurus* presumably
 1190 possessing more flexibility at the base of its neck. To sum up, the stiffness in the neck of dyrosaurids
 1191 increases posteriorly in all direction, which probably prevented them from performing the dorsoventral
 1192 shaking of modern crocodylians during prey capture [Grigg and Kirshner, 2015]. As the dorsal bending
 1193 was more restricted than the lateral one, dyrosaurids probably used lateral shaking of the head instead,
 1194 which corroborates the suggestion of Schwarz et al. [2009]

1196 In parallel, the osteodermal shield of hyposaurine dyrosaurids is known to have limited the dorsal
 1197 flexibility (but not the ventral and mediolateral flexibility) of the trunk anteriorly, while the posterior
 1198 portion was less restricted [Schwarz et al., 2006]. This dorsoventral stiffness, and mediolateral flexibility,
 1199 is also reflected in the low angles of the zygapophyses in the anterior portion of the thoracic region
 1200 of *Cerrejonisuchus*, *Congosaurus*, and *Hyposaurus* (Th1 through Th4, see fig. SI 3 in Supplementary
 1201 Information). Following this, the zygapophyseal angles increase posteriorly enabling more dorsoventral
 1202 flexibility but less mediolateral one. The high inclination angle of the zygapophyseal facets with the coronal
 1203 plane at the lumbosacral region of *Congosaurus* reflects an increased mediolateral stiffness in that region
 1204 too.

1206 In crocodylians, the height of neural spine is positively correlated to stiffness in lateral direction, along
 1207 with centrum width, and centrum length [Molnar et al., 2014]. All dyrosaurids show two major peaks in
 1208 the relative length of the neural spine: in the posteriormost cervicals and anteriormost caudals (see fig. SI
 1209 4). In contrast, the neural spines of *Mecistops* remain relatively constant, with a peak present in the first
 1210 thoracics. Thus, there is an anterior shift of the region containing the highest neural spine in Dyrosauridae
 1211 compared to Crocodylia, as it was the case for pre- and postzygapophysis areas. *Congosaurus* strongly
 1212 stands out from the other dyrosaurids by possessing the greatest amplitude and steepest increase, but also
 1213 the largest absolute values. The greater length of the neural spines locally create epaxial muscles with
 1214 high-oval sagittal sections [Schwarz et al., 2009], and limit the mediolateral bendings of the vertebral
 1215 column. In the case of dyrosaurids, the large size attained by the neural spine also limited dorsal bending
 1216 of the vertebral column. Both peaks of pre- and postzygapophysis areas and neural spine length are
 1217 positively correlated in the cervical region, meaning the base of the neck in dyrosaurids was strongly stiff
 1218 in the mediolateral direction compared to its surroundings.

1220 The variation of the inclination of the neural spine throughout the vertebral column follows the same
 1221 general trend in Hyposaurines, *Cerrejonisuchus*, and *Mecistops*: differences between *Mecistops* and
 1222 dyrosaurids are found in the neck, the last thoracics, and the first caudals where the neural spine is more
 1223 erected for dyrosaurids. These variations hint once more at the existence of distinct regionalizations
 1224 between the axial skeleton of Dyrosauridae and Crocodylia. *Hyposaurus rogersii* stands out with its less
 1225 constrained cervical and lumbar regions compared to other dyrosaurids and *Mecistops*. Yet, all display
 1226 a drop in flexibility among the first thoracics, with dyrosaurids showing a steeper decline compared to
 1227 *Mecistops*. This area possesses the lowest neural spine angle across all specimens, and corresponds to
 1228 the attachment of the pelvic girdle. This induced joint stiffness mirrors that of the sacral region, and
 1229 is necessary to weld in place the bony girdle (and muscle mass). Moreover, increased rigidity in this
 1230 very region probably helped sustain the vertebral column (*i.e.* prevent lateral undulation) during episodes
 1231 requiring the active use of forelimb for locomotion, to reallocate ground force responses similarly to
 1232 the lumbosacral region. In dyrosaurids, and more specifically in hyposaurine (*a.k.a.* where it has been
 1233 actually studied), the anterior portion of the trunk is encased in a rigid osteodermal shield which provided
 1234 both (dorsoventral) stiffness and broad support [Schwarz et al., 2009]. The low neural spine angle in this

1235 case reinforces the stiffness of the anterior portion of the trunk and base of the neck in dyrosaurids. In the
1236 meantime, the overall high inclination angle of the neural spine in dyrosaurids allows more flexibility to
1237 the vertebral column in all bending directions.

1238
1239 The mediolateral width of the centrum (see fig. SI 5 in Supplementary Information) is more or less
1240 constant throughout the cervical and thoracic region of *Mecistops*, shows a small peak at the sacral region,
1241 and slowly decreases throughout the caudals. A different relationship is observed for *Congosaurus*,
1242 *Hyposaurus*, and *Cerrejonisuchus*: while the width of the centrum remains constant throughout the
1243 thoracic region (with a peak at the lumbosacral transition), it shows an intense increase in the cervical
1244 region, and a strong decrease in the caudal region. The intensity of the width variation strongly differs
1245 from *Mecistops* for all dyrosaurids, and is the highest for *Congosaurus*. Since an increase in centrum
1246 width increases mediolateral stiffness [Molnar et al., 2014], dyrosaurids show stiffer trunk and more
1247 flexible neck and tail in the mediolateral direction.

1248
1249 The strong distinctive feature of dyrosaurids compared to crocodylians, is their long cervical centra and
1250 short caudal centra (see fig. SI 7). The exact length of the centra of *Cerrejonisuchus* is unknown and may
1251 vary from what has been collected on the seemingly less compressed vertebra. In parallel, *Hyposaurus*
1252 clearly differs from *Congosaurus* by showing a less regionalized axial skeleton, lesser amplitudes of
1253 variation of centrum lengths. *Hyposaurus* shows relatively small peaks at each transition of the vertebral
1254 column. The greater variation in centrum length of *Congosaurus* implies changing stiffness in localized
1255 portions of the vertebral column.

1256
1257 Regarding the intervertebral joints of dyrosaurids, the whole trunk constitutes the stiffest part of
1258 the axial skeleton. Indeed, the mediolateral rigidity reaches its maximum throughout the trunk with a
1259 peak at the lumbosacral region. The dorsoventral stiffness is the highest in the anterior portion of the
1260 thoracic region where it starts a constant decreasing trend posteriorly. As mentioned earlier, the anterior
1261 portion of the trunk is also bearing the rigid osteodermal shield, all of which make this portion the stiffest
1262 among thoracics. This dorsoventral stiffness probably enabled greater skull length [Molnar et al., 2014]
1263 in dyrosaurids compared to crocodylians. A second peak in stiffness in all directions is centered at the
1264 lumbosacral region. The lumbosacral peak in stiffness in all directions is more evident in dyrosaurids
1265 compared to *Mecistops*; a more rigid pelvic region can be useful for terrestrial locomotion (belly run,
1266 high walk, gallop, etc...) to hold in place the lumbosacral region (so it can move along in the dorsoventral
1267 plane instead of undulating laterally), and absorb shocks (and transmit them anteriorly) induced by both
1268 the movements of the limbs and the large tail [Molnar et al., 2014]. Similarly, increased stiffness in the
1269 scapular region was probably useful during episodes of terrestrial locomotion, at least to counter forces
1270 produced by the forelimb propulsion. A high stiffness in all direction at pelvic region also helps support
1271 large tails [Molnar et al., 2014], which is the case for dyrosaurids.

1272
1273 In crocodylians, the height of centrum is positively correlated to stiffness in dorsoventral direction
1274 [Molnar et al., 2014]. The variation of centrum height (see fig. SI 6) closely mirrors the variation of
1275 centrum width (see fig. SI 5) throughout the axial skeleton. In dyrosaurids, there is an important variation
1276 of height throughout the neck and the tail as opposed to the crocodylian *Mecistops*. This implies a greater
1277 gradient of stiffness in the dorsoventral plane between the base and extremity of the neck and tail. The
1278 intervertebral joints of the anterior portion of the neck were more flexible dorsoventrally than the base,
1279 and the posteriormost extremity of the tail was similarly more flexible.

1280
1281 The stiffness of the tail also decreases posteriorly in all direction except for the long and inclined neural
1282 spines of the last caudal. These observations are consistent with the hypothesis of a steering utility for the
1283 posteriormost portion of the tail [Schwarz et al., 2009]. *Congosaurus* possessed a relatively tight tail in the
1284 mediolateral spectrum of flexion due to the high inclination angle of the zygapophyseal facets (even greater
1285 than the cervicals see fig. SI 3 in Supplementary Information), with a more flexible base contrasting
1286 with *Mecistops*. Indeed, after a small depression at the lumbocaudal junction, the zygapophyseal angles
1287 drastically increase posteriorly with a small depression around the middle of the tail. Yet, the drop in area
1288 of the zygapophyseal facets at the extremity of the tail of *Congosaurus* and *Mecistops* indicates a loss of
1289 stiffness at the end of the tail which led Schwarz et al. [2009] to suggest a steering utility, like modern

1290 crocodylians, for the extremity of the tail of hyposaurine dyrosaurids. Indeed, a vertical orientation of the
 1291 prezygapophysis is considered to enable greater dorsoventral flexibility than mediolateral [Molnar et al.,
 1292 2014], which means that the base of the tail was potentially less stiff mediolaterally than its extremity.
 1293 Besides, in crocodylians, the height of the neural spine is known to inhibit mediolateral flexion as well
 1294 [Molnar et al., 2014], and *Congosaurus* displays high neural spines throughout its tail. The osteological
 1295 observations actually suffice [Molnar et al., 2014] to indicate that *Congosaurus* had a laterally stiff but
 1296 powerful tail. This corroborates with the conclusion obtained from muscular reconstruction [Schwarz
 1297 et al., 2009]. As more intense force needs to be allocated to a tight vertebral column to bend it, it leads to
 1298 higher undulatory frequency, and thus a faster swimming speed [Molnar et al., 2014]. This observation
 1299 supports the interpretations of Schwarz et al. [2006, 2009], as a tail propelled method (or a paraxial and
 1300 hybrid swimming for younger individuals [Schwarz et al., 2009]) was most probably a predominant form
 1301 of swimming for *Congosaurus* (which is also proposed for *Hyposaurus* [Denton et al., 1997]).

1302
 1303 The evolution of the neural canal throughout the axial skeleton of *Congosaurus* closely mirrors that
 1304 of *Mecistops*, which is correlated to the position of the girdles. Yet, the cervicothoracic transition is
 1305 smoother in *Congosaurus* than *Mecistops* since the cervicals of *Congosaurus* start off with greater area
 1306 values for their neural canal. This could possibly reflect a greater irrigation of the head for *Congosaurus*
 1307 than modern crocodylians require, which goes along the hypothesis of a heavy head for longirostrine
 1308 dyrosaurids [Buffetaut, 1979, Storrs, 1986].

1309
 1310 In conclusion, dyrosaurids possessed a relatively flexible neck in the mediolateral plane, with the
 1311 posteriormost part being stiffer. The anterior portion of the trunk was stiff, mainly due to the interlocked
 1312 osteodermal shields [Schwarz et al., 2009], but also due to wide centra and high neural spines which
 1313 limited lateral and dorsal bendings. The lumbosacral region and the anteriormost caudals were stiff as
 1314 well which helped support the large tail. The tail in overall was rigid, but showed an increase in flexibility
 1315 posteriorly in the mediolateral plane.

1316 9.2 The ecomorphology and possible lifestyle of *Cerrejonisuchus*

1317 The homodont dentition of *Cerrejonisuchus* [Hastings et al., 2010] with labiolingually-compressed teeth,
 1318 along with the presence of crenulations on the lingual side of the tooth are features that mostly resemble
 1319 the dentition of terrestrial, meat-eating crocodyliforms (e.g. *Sebecosuchia*, *Mekosuchinae*) [Turner and
 1320 Calvo, 2005]. A relatively elevated skull is usually associated with those traits [Turner and Calvo, 2005],
 1321 which is not the case with *Cerrejonisuchus*. The dentition of *Cerrejonisuchus* could represent yet another
 1322 terrestrial feature adding on to the list of terrestrial evidence for this taxon based on the postcranial skeleton.

1323
 1324 The convex mid-thoracic ribs of *Cerrejonisuchus* differ from both the high oval ribs of hyposaurines
 1325 [Schwarz et al., 2009], and reclining ones of crocodylians (see fig. 10 and fig. 11), giving *Cerrejonisuchus*
 1326 a more cylindrical trunk in transverse section, halfway between the high and low oval bracing systems
 1327 of hyposaurines and crocodylians respectively [Schwarz et al., 2009]. In this way, the trunk of *Cerre-*
 1328 *jonisuchus* must have been more similar to that of the pholidosaurid *Anteophthalmosuchus* [Martin et al.,
 1329 2016](see fig. 11). Bodies with high oblong transverse sections, like those of hyposaurine, are often found
 1330 in aquatic taxa not thriving within/limited to a specific water tier [Motani, 2001, O'Keefe et al., 2011],
 1331 which would dismiss *Cerrejonisuchus* from this lifestyle.

1332
 1333 The appendicular skeleton of *Cerrejonisuchus* contrasts with that of hyposaurine dyrosaurids in having
 1334 similarly proportioned zeugopodia and stylopodia within each limb (hyposaurines have relatively shorter
 1335 zeugopodia [Denton et al. [1997], Schwarz et al. [2009], Wilberg et al. [2019]). In marine thalattosuchians,
 1336 the zeugopodial elements tend to be extremely reduced, this condition is also found in the most aquatic
 1337 crocodylian *Gavialis*. Indeed, *Gavialis* possesses the shortest ulna for its humerus and shows dispropor-
 1338 tionate ulna and tibia, which are considered to reduce its terrestrial locomotor capacity [Iijima et al., 2018].
 1339 Therefore, we regard the relatively elongated zeugopodia of *Cerrejonisuchus* as suggestive of frequent
 1340 terrestrial locomotion.

1341
 1342 Another feature of *Cerrejonisuchus* is the presence of disproportioned limbs where the forelimb only
 1343 reaches 83% of the length of the hindlimb (*contra* 91.45% for *H. rogersii* NJSM 23368). Baurusuchids,

1344 such as *Stratiotosuchus maxhechti* show a similar relationship where the total length of the forelimb
 1345 (excluding the manus and pes) corresponds to 80% of that of the hindlimb, but those crocodyliforms were
 1346 bipedal [Riff and Kellner, 2011]. The difference of limb proportion of *Cerrejonisuchus* contrasts rather
 1347 sharply with the similarly sized limbs of hyposaurine [Denton et al., 1997], and must have provoked a
 1348 relative imbalance in the posture of *Cerrejonisuchus*. Supposing the thoracolumbar region reached at
 1349 least 400mm in length, the vertebral column must have inclined by an angle of 5.7° to 7.6° between the
 1350 scapular and thoracic girdle. Asymmetrical gaits are well-known in terrestrial crocodyliforms [Parrish,
 1351 1987, Adams, 2019], but *Cerrejonisuchus* certainly did not bear a parasagittal posture as the orientation
 1352 and position of the femoral condyles and 4th trochanter make it impossible for a vertically positioned
 1353 femur. Following this, the difference of length between the limbs of *Cerrejonisuchus*, and the short
 1354 absolute size of the limbs likely rendered the crocodylian ‘high walk’ difficult to sustain over extended
 1355 distances, similarly to adult crocodylians [Grigg and Kirshner, 2015]. Furthermore, the high neural spines
 1356 and the interlocked osteodermal shield of dyrosaurids likely prevented them from performing the gallop
 1357 as seen in mostly small bodied crocodylians [Grigg and Kirshner, 2015]. In addition, the large tail of
 1358 dyrosaurids presumably shifted the center of gravity more posteriorly compared to modern crocodylians
 1359 in elevated postures like the ‘high walk’ [Grigg and Kirshner, 2015], and induced extra weight on the
 1360 pelvic area and hind limbs. Consequently, the hind limb would constitute the main propulsive force
 1361 for this type of gait, and require to generate important work while the pelvic area would need to be
 1362 sufficiently supported to redistribute ground forces. The small size of *Cerrejonisuchus* probably played
 1363 a key role in a more terrestrial lifestyle, as large dyrosaurid individuals likely lost the ability to employ
 1364 terrestrial locomotion with their mass increasing [Schwarz et al., 2009]. The elongated zeugopodia of
 1365 *Cerrejonisuchus* probably enabled it to move more easily on land compared to *Gavialis* [Iijima et al.,
 1366 2018] or hyposaurine dyrosaurids, making *Cerrejonisuchus* one of the most terrestrial dyrosaurids while
 1367 likely retaining a sprawling posture [Molnar et al., 2015].

1368
 1369 Similarly to mekosuchines, the dyrosaurid humerus differs from that of crocodylians in possessing
 1370 a straight shaft as well as a more anteriorly positioned and oriented deltopectoral crest (e.g. *Kambara*
 1371 [Stein et al., 2012]). The goniopholid *Anteophthalmosuchus* further differs from those in possessing a
 1372 deltopectoral crest closer to the anterior margin of the shaft than to the ventral midline of the bone, along
 1373 with the proximal torsion of crocodylians [Martin et al., 2016]. The anterior position and orientation of
 1374 the deltopectoral crest increase the strength of the lever-force of adductor muscles [Stein et al., 2012],
 1375 enabling greater propulsive effort from the fore limbs which is notably useful for terrestrial locomotion or
 1376 hybrid swimming.

1377 9.3 The distinctive postcranial anatomy of dyrosaurids

1378 Previous works on Dyrosauridae almost exclusively focused on the skulls and mandibles, claiming
 1379 the postcrania (and sometimes the basicranium [Buffetaut, 1976]) were undiagnostic because constant
 1380 throughout the clade [Buffetaut, 1976, 1978b, Parris, 1986, Storrs, 1986, Norell and Storrs, 1989, Denton
 1381 et al., 1997]. However, our thorough osteological investigation of *Cerrejonisuchus* has underlined several
 1382 unique postcranial traits which are summed up in the emended diagnosis of *Cerrejonisuchus*. There is also
 1383 postcranial osteological evidence that differentiate *Hyposaurus*, *Cerrejonisuchus*, and *Congosaurus* from
 1384 one another and from other crocodyliforms, notably the shape of the femoral head (see also de Souza et al.
 1385 [2019]), the shape of the lateral process of cervicals and thoracics, the zeugopodial ratio to stylopodia,
 1386 the overall shape of the humerus (including torsion of the shaft, size and shape of proximal and distal
 1387 condyles). Dyrosaurids have diagnostic postcranial remains, and this distinction is also reflected in our
 1388 multivariate analyses using morphological ratios. On our main PCoA (see fig. 15), which is based on
 1389 a dataset mixing cranial (15%) and postcranial (85%) ratios, dyrosaurids occupy a distinct portion of
 1390 the morphospace. In parallel, our tanglegram revealed that postcranial data also seem somewhat more
 1391 conservative, with a slightly better match with phylogeny than the cranial-restricted cluster dendrogram
 1392 (see fig. 16). Yet, both signals of the tanglegram emanating from cranial and postcranial data are consistent,
 1393 reinforcing the conjecture of the existing distinctive cranial and postcranial anatomy of Dyrosauridae.

1394
 1395 The multivariate analyses of our extensive dataset on postcranial plus cranial data revealed the presence
 1396 of a demarcation between *Cerrejonisuchus* and all other dyrosaurids (see morphospaces fig. 15, fig. SI 1,
 1397 and fig. SI 2 from Supplementary Information). On both the main PCoA (see fig. 15), and the Dyrosaurid

1398 restricted PCoA (see fig. SI 2 in Supplementary Information), *Cerrejonisuchus* lies on distinct area of the
 1399 morphospaces, apart from the hyposaurine dyrosaurids. This supports our suggestion that *Cerrejonisuchus*
 1400 occupies a niche that is distinct from that of hyposaurines, leading to a basal dyrosaurid - hyposaurine
 1401 dichotomy overlapped by freshwater/terrestrial - marine dichotomy. Moreover, this result further backs the
 1402 hypothesis of an early shift to marine lifestyle within Dyrosauridae [Wilberg et al., 2019]. If we restrict the
 1403 dataset to Dyrosauridae (fig. SI 1 and SI 2 in Supplementary Information), the distribution of dyrosaurids
 1404 adheres to the Dyrosauridae phylogeny with basal dyrosaurids (i.e. *Anthracosuchus* and *Cerrejonisuchus*)
 1405 occupying distinct position from derived ones (i.e. *Hyposaurus*, *Dyrosaurus* and *Congosaurus*). Yet,
 1406 our analysis of craniodental morphological data (fig. SI 1 in Supplementary Information) splits the
 1407 Hyposaurine cluster of Schwarz et al. [2009], and places *Congosaurus* close to *Dyrosaurus* instead,
 1408 which complies with the results of Jouve and Jalil [2020]. The postcranial-restricted PCoA (fig. SI 2 in
 1409 Supplementary Information) also sets *Congosaurus* outside of the *Hyposaurus* collection while lacking
 1410 other crucial specimens like *Dyrosaurus*. Hence, the postcranial anatomy of Dyrosauridae and other
 1411 crocodyliforms seems to reflect accurately their phylogenetical relationships, while craniodental data
 1412 appears more volatile (see Wilberg et al. [2019], Jouve and Jalil [2020]).
 1413

1414 Our investigation of the bivariate distribution of the morphological ratios from the main analysis
 1415 (see script 'Script_parameters.r' in Supplementary Information) revealed the importance of the shape
 1416 of the femur as a discriminating feature between clades Crocodylia, Thalattosuchia and Dyrosauridae.
 1417 More precisely, it is the degree of curvature and the location of this curve along the proximodistal axis
 1418 of the bone that appear decisive in compartmenting the different clades, along with the proximodistal
 1419 length of the femur and the thickness of the bone at the 4th trochanter. These differences reflect its
 1420 distinct modes of locomotion. Thalattosuchia, Dyrosauridae, and Crocodylia are known to have thrived in
 1421 different environments, sometimes overlapping, and have colonized distinct ecological niches leading
 1422 to particularities echoed in femoral differences. Indeed, the shape of the femur, just like the skull and
 1423 mandible, is a mixture of inherited and newly evolved morphologies, thus reworking phylogenetic and
 1424 functional signals.

1425 10 CONCLUSIONS

1426 *Cerrejonisuchus improcerus* possesses numerous postcranial morphological traits that differ from other
 1427 dyrosaurids and crocodyliforms. Those traits, notably a fibula with an extended proximal fibula blade,
 1428 a pubis with an elongated and rectangular distal portion, an ulna presenting a double concavity, and an
 1429 elliptic-shaped odontoid, form a new set of features that expands the diagnosis of this taxon, which was
 1430 previously limited to craniodental features. We reveal *Cerrejonisuchus improcerus* is also characterized
 1431 by a suite of traits that strongly suggest a terrestrial - semi-aquatic lifestyle for this small-sized dyrosaurid:
 1432 comparatively long zeugopodia (zeugopodia attaining > 85% of the length of the stylopodia), a short
 1433 humerus (less than 90% of the femoral proximodistal length), an anteriorly positioned deltopectoral
 1434 crest, a large lateral process in thoracics, and short and strongly arched thoracic ribs. Finally, our
 1435 osteological analyses of *Cerrejonisuchus improcerus* and hyposaurine also hint at a new distinctive
 1436 feature of Dyrosauridae that requires further investigation among the other taxa: the presence of ventral
 1437 keels on the posterior cervicals and lumbar. *Cerrejonisuchus* and hyposaurine dyrosaurids possess
 1438 distinct regions along the axial skeleton, which can be identified following the variation of vertebral
 1439 features. These regions, and the distribution of rigid and flexible areas are not always located in the
 1440 same position of the axial skeleton, and often differ from what is observed for the modern crocodylian
 1441 *Mecistops cataphractus*. This suggests the existence of different regionalization and flexibility between
 1442 axial skeletons of Dyrosauridae and Crocodylia. We also highlight features in hyposaurine dyrosaurids
 1443 that are shared with modern crocodylians, such as reduced zeugopodia (proportionally to corresponding
 1444 stylopodia) and similarly sized stylopodia. Those traits may also hint at less terrestrial habits among
 1445 hyposaurine dyrosaurids. Multivariate analysis of our extensive morphological dataset describing the
 1446 anatomy of exemplar dyrosaurids, thalattosuchians, and crocodylians reveals that dyrosaurids possess
 1447 a distinctive postcranial anatomy among crocodyliforms, indicating that the latter cannot be used as
 1448 functional surrogate for the former.

11 ACKNOWLEDGMENTS

We ~~would like to~~ thank all the museum staff for smoothly granting us the access of the dyrosaurid collections.

We thank Dr. Jonathan Bloch, Dr. Richard Hulbert, and the rest of the staff at the Florida Museum (Florida Museum, Gainesville, USA); Dr. David Parris and Dr. Dana Ehret (New Jersey State Museum, Trenton, USA); Dr. Daniel Brinkman (Yale Peabody Museum, New Haven, USA); Dr. Mark Norell and Dr. Carl Mehling (American Museum of Natural History, New York, USA); Dr. Ned Gilmore (Academy of Natural Sciences of Drexel University, Philadelphia, USA); Dr. Susannah Maidment (Natural History Museum, London, UK) for the help and care.

We thank Wayne Callahan for sharing his personal data on the NJSM 23368 specimen, as well as Dr. Rodrigo Pellegrini for the cast humeri and femora of the NJSM 23368 specimen.

REVIEWERS

REFERENCE

- T. L. Adams. Small terrestrial crocodyliform from the Lower Cretaceous (late Aptian) of central Texas and its implications on the paleoecology of the Proctor Lake Dinosaur locality. *Journal of Vertebrate Paleontology*, 39(3):1–15, 2019. ISSN 19372809. doi: 10.1080/02724634.2019.1623226. URL <https://doi.org/10.1080/02724634.2019.1623226>.
- T. L. Adams, M. J. Polcyn, O. Mateus, D. A. Winkler, and L. L. Jacobs. First occurrence of the long-snouted crocodyliform *Terminonaris* (Pholidosauridae) from the Woodbine Formation (Cenomanian) of Texas. *Journal of Vertebrate Paleontology*, 31(3):712–716, 2011. ISSN 02724634. doi: 10.1080/02724634.2011.572938.
- M. J. Anderson. A new method for non-parametric multivariate analysis of variance. *Austral Ecology*, 26(1):32–46, 2001.
- C. W. Andrews. XXXVIII - on some new Steosaurs from the Oxford Clay of Peterborough. *Annals and Magazine of Natural History*, 3:299–308, 1909.
- C. W. Andrews. *A descriptive catalogue of the marine reptiles of the Oxford Clay. Part II*. Order the the Trustees of the British Museum, London, 1913.
- J. A. Barbosa, A. W. A. Kellner, and M. S. S. Viana. New dyrosaurid crocodylomorph and evidences for faunal turnover at the K-P transition in Brazil. *Proceedings of the Royal Society B: Biological Sciences*, 275(1641):1385–1391, 2008. ISSN 14712970. doi: 10.1098/rspb.2008.0110.
- A. Bell and L. M. Chiappe. A species-level phylogeny of the Cretaceous Hesperornithiformes (Aves: Ornithuromorpha): implications for body size evolution amongst the earliest diving birds. *Journal of Systematic Palaeontology*, 14(3):239–251, 2015. ISSN 14780941. doi: 10.1080/14772019.2015.1036141. URL <http://dx.doi.org/10.1080/14772019.2015.1036141>.
- R. B. J. Benson and P. S. Druckenmiller. Faunal turnover of marine tetrapods during the Jurassic-Cretaceous transition. *Biological Reviews*, 89:1–23, 2014.
- M. Bronzati, F. C. Montefeltro, and M. C. Langer. A species-level supertree of Crocodyliformes. *Historical Biology: An International Journal of Paleobiology*, pages 1–9, 2012. ISSN 08912963. doi: 10.1080/08912963.2012.662680.
- M. Bronzati, F. C. Montefeltro, and M. C. Langer. Diversification events and the effects of mass extinctions on Crocodyliformes evolutionary history. *Royal Society Open Science*, 2:140385, 2015.
- E. Buffetaut. Une nouvelle définition de la famille des dyrosauridae de Stefano, 1903 (Crocodylia, Mesosuchia) et ses conséquences : inclusion des genres *Hyposaurus* et *Sokotosuchus* dans les Dyrosauridae. *Geobios*, 3(9):333–336, 1976.

- 1496 E. Buffetaut. Crocodylian remains from the Eocene of Pakistan. *Neues Jahrbuch für Geologie und*
1497 *Paläontologie - Abhandlungen*, 156(2):262–283, 1978a.
- 1498 E. Buffetaut. Les Dyrosauridae (Crocodylia, Mesosuchia) des phosphates de l’Eocène inférieur de Tunisie
1499 : *Dyrosaurus*, *Rhabdognatus*, *Phospliatosaurus*. *Géologie Méditerranéenne*, 5(2):237–255, 1978b.
1500 ISSN 0397-2844. doi: 10.3406/geolm.1978.1046.
- 1501 E. Buffetaut. A dyrosaurid (Crocodylia, Mesosuchia) from the Upper Eocene of Burma. *Neues Jahrbuch*
1502 *für Geologie und Paläontologie - Abhandlungen für Geologie und Paläontologie. Monatshefte*, (5):
1503 273–281, 1978c.
- 1504 E. Buffetaut. *Sokotosuchus ianwilsoni* and the evolution of the dyrosaurid crocodylians. *The Nigerian*
1505 *Field, Monograph*, 1:31–41, 1979.
- 1506 E. Buffetaut. Radiation évolutive, paléoécologie et biogéographie des crocodyliens méso-suchiens. *Mémoire*
1507 *de la Société Géologique de France*, 142:88, 1981.
- 1508 W. Callahan, R. Pellegrini, J. P. Schein, D. C. Parris, and J. D. McCauley. A nearly complete specimen of
1509 *Hyposaurus rogersii* (Crocodylomorpha, Dyrosauridae) from the Late Cretaceous-Early Paleogene of
1510 New Jersey, 2015.
- 1511 K. Carpenter. *Thoracosaurus neocesariensis* (De Kay, 1842) (Crocodylia: Crocodylidae) from the Late
1512 Cretaceous Ripley Formation of Mississippi. *Mississippi Geology*, 4:10, 1983. ISSN 1098-6596. doi:
1513 10.1017/CBO9781107415324.004.
- 1514 R. G. de Souza. Comments on the Serial Homology and Homologues of Vertebral Lateral Projections in
1515 Crocodylia (Eusuchia). *Anatomical Record*, 301:1203–1215, 2018. ISSN 19328494. doi: 10.1002/ar.
1516 23802.
- 1517 R. G. de Souza, B. M. Hörmanseder, R. G. Figueiredo, and D. d. A. Campos. Description of new
1518 dyrosaurid specimens from the Late Cretaceous-Early Paleogene of New Jersey, United States, and
1519 comments on *Hyposaurus* systematics. *Historical Biology*, 00(00):1–17, 2019. ISSN 10292381.
1520 doi: 10.1080/08912963.2019.1593403. URL [https://doi.org/10.1080/08912963.2019.](https://doi.org/10.1080/08912963.2019.1593403)
1521 1593403.
- 1522 A. de Vries. Package ‘ggdendro’: Create Dendrograms and Tree Diagrams Using ‘ggplot2’. 2016. URL
1523 <https://cran.r-project.org/web/packages/ggdendro/ggdendro.pdf>.
- 1524 R. K. Denton, J. L. Dobie, and D. C. Parris. The marine crocodylian *Hyposaurus* in North America.
1525 *Ancient Marine Reptiles*, pages 375–397, 1997. doi: 10.1016/b978-012155210-7/50020-x.
- 1526 G. di Stefano. Nuovi rettili degli strati a fosfato della Tunisia. *Bollettino delle Società Geologica Italiana*,
1527 22:51–80, 1903.
- 1528 S. W. Evers, P. M. Barrett, and R. B. J. Benson. Anatomy of *Rhinochelys pulchriceps* (Protostegidae) and
1529 marine adaptation during the early evolution of chelonoids. *PeerJ*, 7, 2019.
- 1530 M. Fernández and Z. Gasparini. Salt glands in the Jurassic metriorhynchid *Geosaurus*: Implications
1531 for the evolution of osmoregulation in Mesozoic marine crocodyliforms. *Naturwissenschaften*, 95(1):
1532 79–84, 2008. ISSN 00281042. doi: 10.1007/s00114-007-0296-1.
- 1533 V. Fischer, N. Bardet, R. B. J. Benson, M. S. Arkhangelsky, and M. Friedman. Extinction of fish-shaped
1534 marine reptiles associated with reduced evolutionary rates and global environmental volatility. *Nature*
1535 *communications*, 7:1–11, 2016.
- 1536 D. Foffa, M. M. Johnson, M. T. Young, L. Stee, and S. L. Brusatte. Revision of the late jurassic deep-water
1537 teleosauroid crocodylomorph *Teleosaurus megarhinus* Hulke, 1871 and evidence of pelagic adaptations
1538 in Teleosauroidea. *PeerJ*, 2019(4):1–38, 2019. ISSN 21678359. doi: 10.7717/peerj.6646.
- 1539 E. Fraas. Die Meer-Krocodylier (Thalattosuchia) des oberen Jura unter specieller Berücksichtigung von
1540 *Dacosaurus* und *Geosaurus*. *Palaeontographica*, 49:1–72, 1902.

- 1541 T. Galili. dendextend: an R package for visualizing, adjusting, and comparing trees of hierarchical
1542 clustering. *Bioinformatics*, 31(22):3718–20, 2015.
- 1543 P. L. Godoy, M. Bronzati, E. Eltink, J. C. d. A. Marsola, G. M. Cidade, M. C. Langer, and F. C.
1544 Montefeltro. Postcranial anatomy of *Pissarrachampsia sera* (Crocodyliformes, Baurusuchidae) from the
1545 Late Cretaceous of Brazil: insights on lifestyle and phylogenetic significance. *PeerJ*, 4:1–56, may 2016.
1546 ISSN 2167-8359. doi: 10.7717/peerj.2075. URL <https://peerj.com/articles/2075>.
- 1547 S. Grenard. *Handbook of alligators and crocodiles*. Krieger Publishing Company, Melbourne, FL, United
1548 States, 1999.
- 1549 G. C. Grigg and D. Kirshner. *Biology and evolution of crocodylians*. Cornell University Press, 2015.
1550 ISBN 9780801454103.
- 1551 A. K. Hastings, J. I. Bloch, E. A. Cadena, and C. A. Jaramillo. A new small short-snouted dyrosaurid
1552 (Crocodylomorpha, Mesoeucrocodylia) from the Paleocene of Northeastern Colombia. *Journal of*
1553 *Vertebrate Paleontology*, 30(1):139–162, 2010.
- 1554 A. K. Hastings, J. I. Bloch, and C. A. Jaramillo. A new longirostrine dyrosaurid (Crocodylomorpha,
1555 Mesoeucrocodylia) from the Paleocene of north-eastern Colombia: biogeographic and behavioural
1556 implications for New-World Dyrosauridae. *Palaeontology*, 54(5):1095–1116, 2011. ISSN 00310239.
1557 doi: 10.1111/j.1475-4983.2011.01092.x.
- 1558 A. K. Hastings, J. I. Bloch, and C. Jaramillo. A new blunt-snouted dyrosaurid, *Anthracosuchus balrogus*
1559 gen. et sp. nov. (Crocodylomorpha, Mesoeucrocodylia), from the Palaeocene of Colombia. *Historical*
1560 *Biology*, pages 1–23, 2014.
- 1561 M. Iijima, T. Kubo, and Y. Kobayashi. Comparative limb proportions reveal differential locomotor
1562 morphofunctions of alligatoroids and crocodyloids. *Royal Society Open Science*, 5:14, 2018.
- 1563 M. M. Johnson, M. T. Young, L. Steel, D. Foffa, A. S. Smith, S. Hua, P. Havlik, E. A. Howlett, and
1564 G. Dyke. Re-description of '*Steneosaurus*' *obtusidens* Andrews, 1909, an unusual macrophagous
1565 teleosaurid crocodylomorph from the Middle Jurassic of England. *Zoological Journal of the Linnean*
1566 *Society*, XX:1–34, 2017. ISSN 10963642. doi: 10.1093/zoolinnean/zlx035.
- 1567 M. M. Johnson, M. T. Young, and S. L. Brusatte. Re-description of two contemporaneous mesorostrine
1568 teleosauroids (Crocodylomorpha: Thalattosuchia) from the Bathonian of England and insights into
1569 the early evolution of Machimosaurini. *1. Zoological Journal of the Linnean Society*, 20:1–34,
1570 2019. ISSN 0024-4082. doi: 10.1093/zoolinnean/zlz037. URL [https://doi.org/10.1093/](https://doi.org/10.1093/zoolinnean/zlz037)
1571 [zoolinnean/zlz037](https://doi.org/10.1093/zoolinnean/zlz037).
- 1572 M. M. Johnson, M. T. Young, and S. L. Brusatte. The phylogenetics of Teleosauroidea (Crocodylomorpha,
1573 Thalattosuchia) and implications for their ecology and evolution. *PeerJ*, pages 1–157, 2020. doi:
1574 10.7717/peerj.9808.
- 1575 S. Jouve. Taxonomic revision of the dyrosaurid assemblage (Crocodyliformes: Mesoeucrocodylia) from
1576 the Paleocene of the Iullemeden Basin, West Africa. *Journal of Paleontology*, 81(1):163–175, 2007.
1577 ISSN 0022-3360. doi: 10.1666/0022-3360(2007)81[163:trotda]2.0.co;2.
- 1578 S. Jouve and N. E. Jalil. Paleocene resurrection of a crocodylomorph taxon: Biotic crises, climatic and
1579 sea level fluctuations. *Gondwana Research*, 85:1–18, 2020. ISSN 1342937X. doi: 10.1016/j.gr.2020.
1580 03.010.
- 1581 S. Jouve and D. Schwarz. *Congosaurus bequaerti*, a Paleocene dyrosaurid (Crocodyliformes; Mesoeu-
1582 crocodylia) from Landana (Angola). *Bulletin de l'Institut Royal des Sciences Naturelles de Belgique*,
1583 74:129–146, 2004.
- 1584 S. Jouve, B. Bouya, and M. Amaghazaz. A short-snouted dyrosaurid (Crocodyliformes, Mesoeucrocodylia)
1585 from the Paleocene of Morocco. *Palaeontology*, 48(2):359–369, 2005.

- 1586 S. Jouve, M. Iarochène, B. Bouya, and M. Amaghazaz. A new species of *Dyrosaurus* (Crocodylomorpha,
1587 Dyrosauridae) from the early Eocene of Morocco: phylogenetic implications. *Zoological Journal of*
1588 *the Linnean Society*, 148:603–656, 2006.
- 1589 W. J. Langston. Dyrosaurs (Crocodylia, Mesosuchia) from the Paleocene Umm Himar Formation,
1590 Kingdom of Saudi Arabia. *US. Geological Survey*, 2093:F1–F36, 1995.
- 1591 J. V. T. Lara. Florida vertebrate fossils *Thecachampsa americana*, 2012. URL <https://www.floridamuseum.ufl.edu/florida-vertebrate-fossils/species/thecachampsa-americana/>.
- 1594 J. E. Martin, M. Delfino, T. Smith, J. E. Martin, M. Delfino, and T. S. Osteology. Osteology and affinities of
1595 Dollo's goniopholidid (Mesoeucrocodylia) from the Early Cretaceous of Bernissart, Belgium. *Journal*
1596 *of Vertebrate Paleontology*, (e1222534-2):27, 2016. doi: 10.1080/02724634.2016.1222534.
- 1597 J. E. Martin, R. Sarr, and L. Hautier. A dyrosaurid from the Paleocene of Senegal. *Journal of Paleontology*,
1598 93(2):343–358, 2019. ISSN 00223360. doi: 10.1017/jpa.2018.77.
- 1599 J. L. Molnar, S. E. Pierce, and J. R. Hutchinson. An experimental and morphometric test of the relationship
1600 between vertebral morphology and joint stiffness in Nile crocodiles (*Crocodylus niloticus*). *Journal of*
1601 *Experimental Biology*, 217(5):758–768, 2014. ISSN 00220949. doi: 10.1242/jeb.089904.
- 1602 J. L. Molnar, S. E. Pierce, B.-A. S. Bhullar, A. H. Turner, and J. R. Hutchinson. Morphological and
1603 functional changes in the vertebral column with increasing aquatic adaptation in crocodylomorphs.
1604 *Royal Society Open Science*, 2, 2015.
- 1605 C. C. Mook. Notes on the postcranial skeleton in the Crocodylia. *Bulletin American Museum of Natural*
1606 *History*, 44:67–100, 1921. ISSN 0003-0090.
- 1607 D. J. Morgan, R. K. Denton, and R. E. Weems. Presence of a dyrosaurid neosuchian in the Sev-
1608 ern/Brightseat Formation of Maryland. *The Mosasaur The Journal of the Delaware Valley Paleontolog-*
1609 *ical Society*, 10:91–104, 2018.
- 1610 R. Motani. Estimating body mass from silhouettes: testing the assumption of elliptical body cross-sections.
1611 *Paleobiology*, 27(4):735–750, 2001. ISSN 0094-8373. doi: 10.1666/0094-8373(2001)027<0735:
1612 ebfst>2.0.co;2.
- 1613 M. A. Norell and G. Storrs. Catalogue and review of the fossil crocodylians in the Yale Peabody Museum.
1614 *Posti*, 203(January 2014):1–28, 1989.
- 1615 J. A. Nyakatura, K. Melo, T. Horvat, K. Karakasiliotis, V. R. Allen, A. Andikfar, E. Andrada, P. Arnold,
1616 J. Laustroer, J. R. Hutchinson, M. S. Fischer, and A. J. Ijspeert. Reverse-engineering the locomotion of
1617 a stem amniote. *Nature*, 565(7739):351–355, 2019. ISSN 14764687. doi: 10.1038/s41586-018-0851-2.
1618 URL <http://dx.doi.org/10.1038/s41586-018-0851-2>.
- 1619 F. R. O'Keefe, H. P. Street, B. C. Wilhelm, C. D. Richards, and H. Zhu. A new skeleton of the cryptoclidid
1620 plesiosaur *Tatenectes laramienseis* reveals a novel body shape among plesiosaurs. *Journal of Vertebrate*
1621 *Paleontology*, 31(2):330–339, 2011. ISSN 02724634. doi: 10.1080/02724634.2011.550365.
- 1622 J. Oksanen, F. G. Blanchet, M. Friendly, R. Kindt, P. Legendre, D. McGlinn, R. P. Minchin, R. B. O'Hara,
1623 G. L. Simpson, P. Solymos, M. H. H. Stevens, E. Szoecs, and H. Wagner. vegan: Community Ecology
1624 Package (2.5-4). 2019. URL <https://cran.r-project.org/package=vegan>.
- 1625 H. F. Osborn. *Teleorhinus browni*, a teleosaur in the Fort Benton. *Bulletin of the American Museum of*
1626 *Natural History*, 20:239–240, 1904.
- 1627 R. Owen. Notes on remains of fossil reptiles discovered by Prof. H. Rogers in Greensand formations of
1628 New Jersey. In *The Quarterly journal of the Geological Society of London. Volume 5*, pages 380–383.
1629 Geological Society of London, London, 1849.
- 1630 E. Paradis, J. Claude, and K. Strimmer. APE: analyses of phylogenetics and evolution in R language.
1631 *Bioinformatics*, 20(2):289–290, 2004.

- 1632 D. C. Parris. Biostratigraphy of the fossil crocodile *Hyposaurus* Owen from New Jersey. *Investigation,*
1633 *New Jersey State Museum*, 4:1–16, 1986.
- 1634 J. M. Parrish. The origin of crocodylian locomotion. *Paleobiology*, 13(4):396–414, 1987. ISSN 19385331.
1635 doi: 10.1017/S0094837300009003.
- 1636 S. E. Pierce, K. D. Angielczyk, and E. Rayfield. Morphospace occupation in thalattosuchian crocody-
1637 lomorphs: skull shape variation, species delineation and temporal patterns. *Palaeontology*, 52(5):
1638 1057–1097, 2009.
- 1639 W. Revelle. Package 'psych': Procedures for Psychological, Psychometric, and Personality Research.
1640 2019. URL <https://personality-project.org/r/psych-manual.pdf>.
- 1641 D. Riff and A. W. A. Kellner. Baurusuchid crocodyliforms as theropod mimics: Clues from the skull
1642 and appendicular morphology of *Stratiotosuchus maxhecti* (Upper Cretaceous of Brazil). *Zoological*
1643 *Journal of the Linnean Society*, 163(SUPPL. 1), 2011. ISSN 00244082. doi: 10.1111/j.1096-3642.
1644 2011.00713.x.
- 1645 A. S. Romer. Crocodylian pelvic muscles and their avian and reptilian homologues. *Bulletin American*
1646 *Museum of Natural History*, 48:533–552, 1923.
- 1647 A. S. Romer. *Osteology of the reptiles*. University of Chicago Press, Chicago, 1956.
- 1648 S. Saber, J. J. Sertich, H. M. Sallam, K. A. Ouda, P. M. O'Connor, and E. R. Seiffert. An enigmatic
1649 crocodyliform from the Upper Cretaceous Quseir Formation, central Egypt. *Cretaceous Research*, 90:
1650 174–184, 2018. ISSN 1095998X. doi: 10.1016/j.cretres.2018.04.004. URL [https://doi.org/](https://doi.org/10.1016/j.cretres.2018.04.004)
1651 [10.1016/j.cretres.2018.04.004](https://doi.org/10.1016/j.cretres.2018.04.004).
- 1652 K. A. O. Salih, D. C. Evans, R. Bussert, N. Klein, M. Nafi, and J. Muller. First record of *Hyposaurus*
1653 (Dyrosauridae, Crocodyliformes) from the Upper Cretaceous Shendi Formation of Sudan. *Journal of*
1654 *Vertebrate Paleontology*, page 9, 2015. ISSN 19372809. doi: 10.1080/02724634.2016.1115408.
- 1655 D. Schwarz, E. Frey, and T. Martin. The postcranial skeleton of the Hyposaurinae (Dyrosauridae;
1656 Crocodyliformes). *Palaeontology*, 49(4):695–718, 2006.
- 1657 D. Schwarz, E. Frey, and T. Martin. Reconstruction of the Bracing System of the Trunk and Tail in
1658 Hyposaurine Dyrosaurids (Crocodylomorpha; Mesoeucrocodylia). *Journal of Vertebrate Paleontology*,
1659 29(2):453–472, 2009.
- 1660 R. Steel. *Handbuch der Palaoherpelologie Encyclopedia of Paleoherpetology Part 16 Crocodylia*. Gustav
1661 Fischer Verlag, Stuttgart, 1973. ISBN 3437301411.
- 1662 C. M. Stefanic and S. J. Nesbitt. The evolution and role of the hyosphene-hyantrum articulation in
1663 Archosauria: phylogeny, size and/or mechanics? *Royal Society Open Science*, 6:27, 2019.
- 1664 M. Stein, S. W. Salisbury, S. J. Hand, M. Archer, and H. Godthelp. Humeral morphology of the early
1665 Eocene mekosuchine crocodylian *Kambara* from the Tingamarra Local Fauna southeastern Queensland,
1666 Australia. *Alcheringa*, 36(4):473–486, 2012. ISSN 03115518. doi: 10.1080/03115518.2012.671697.
- 1667 G. W. Storrs. A dyrosaurid crocodile (Crocodylia: Mesosuchia) from the Paleocene of Pakistan. *Postilla*,
1668 (197):1–17, 1986.
- 1669 R. Suzuki and H. Shimodaira. Pvcust: An R package for assessing the uncertainty in hierarchical
1670 clustering. *Bioinformatics application note*, 22(12):1540–1542, 2006. ISSN 13674803. doi: 10.1093/
1671 bioinformatics/btl117.
- 1672 E. L. Troxell. *Hyposaurus*, a marine crocodylian. *American Journal of Science*, 9(54):489–514, 1925.
- 1673 E. Tschopp, O. Mateus, and R. B. J. Benson. A specimen-level phylogenetic analysis and taxonomic
1674 revision of Diplodocidae (Dinosauria, Sauropoda). *PeerJ*, 3, 2015.

- 1675 A. H. Turner and J. O. Calvo. A new sebecosuchian crocodyliform from the Late Cretaceous of Patagonia.
1676 *Journal of Vertebrate Paleontology*, 25(1):87–98, 2005. ISSN 19372809. doi: 10.1671/0272-4634(2005)
1677 025[0087:ANSCFT]2.0.CO;2.
- 1678 H. Wickham and K. Müller. Package 'DBI': R Database Interface. 2019. URL <https://cran.r-project.org/web/packages/DBI/DBI.pdf>.
- 1680 H. Wickham, W. Chang, L. Henry, T. Lin Pedersen, K. Takahashi, C. Wilke, K. Woo, H. Yutani, and
1681 D. Dunnington. Package 'ggplot2': Create Elegant Data Visualisations Using the Grammar of Graphics.
1682 2020. URL <https://cran.r-project.org/web/packages/ggplot2/ggplot2.pdf>.
- 1683 E. W. Wilberg, A. H. Turner, and C. A. Brochu. Evolutionary structure and timing of major habitat shifts
1684 in Crocodylomorpha. *Scientific reports*, 9(514):1–10, 2019. doi: 10.1038/s41598-018-36795-1.
- 1685 S. L. Wing, F. Herrera, C. A. Jaramillo, C. Gómez-Navarro, P. Wilf, and C. C. Labandeira. Late
1686 Paleocene fossils from the Cerrejón Formation, Colombia, are the earliest record of Neotropical
1687 rainforest. *Proceedings of the National Academy of Sciences of the United States of America*, 106(44):
1688 18627–18632, 2009.
- 1689 X.-C. Wu, A. P. Russell, and S. L. Cumbaa. *Terminonaris* (Archosauria: Crocodyliformes): new material
1690 from Saskatchewan, Canada, and comments on its phylogenetic relationships. *Journal of Vertebrate
1691 Paleontology*, 21(3):492–514, 2001. ISSN 0272-4634. doi: 10.1671/0272-4634(2001)021.
- 1692 J. Yans, M. Amaghazaz, B. Bouya, H. Cappetta, P. Iacumin, L. Kocsis, M. Mouflih, O. Selloum, S. Sen,
1693 J. Y. Storme, and E. Gheerbrant. First carbon isotope chemostratigraphy of the Ouled Abdoun
1694 phosphate Basin, Morocco; implications for dating and evolution of earliest African placental mammals.
1695 *Gondwana Research*, 25(1):257–269, 2014. ISSN 1342937X. doi: 10.1016/j.gr.2013.04.004.
- 1696 M. T. Young, S. L. Brusatte, M. Ruta, and M. B. de Andrade. The evolution of Metriorhynchoidea
1697 (Mesoeucrocodylia, Thalattosuchia): an integrated approach using geometric morphometrics, analysis
1698 of disparity, and biomechanics. *Zoological Journal of the Linnean Society*, 158:801–859, 2010.
- 1699 M. T. Young, A. K. Hastings, R. Allain, and T. J. Smith. Revision of the enigmatic crocodyliform
1700 *Elosuchus felixi* de Lapparent de Broin, 2002 from the Lower-Upper Cretaceous boundary of Niger :
1701 potential evidence for an early origin of the clade Dyrosauridae. *Zoological Journal of the Linnean
1702 Society*, (July):1–27, 2016. doi: 10.1111/zoj.12452.
- 1703 N. Zverkov and M. Jacobs. Revision of *Nannopterygius* (Ichthyosauria: Ophthalmosauridae): reappraisal
1704 of the 'inaccessible' holotype resolves a taxonomic tangle and reveals an obscure ophthalmosaurid
1705 lineage with a wide distribution. *Zoological Journal of the Linnean Society*, pages 1–48, 2020.